AD-A072 680 NAVAL POSTGRADUATE SCHOOL MONTEREY CA F/G 18/12
FEASIBILITY OF BREED/BURN FUEL CYCLES IN PEBBLE BED HTGR REACTO--ETC(U)
SEP 78 T S JENKS

UNCLASSIFIED NL

1 OF 2
AD
A072680

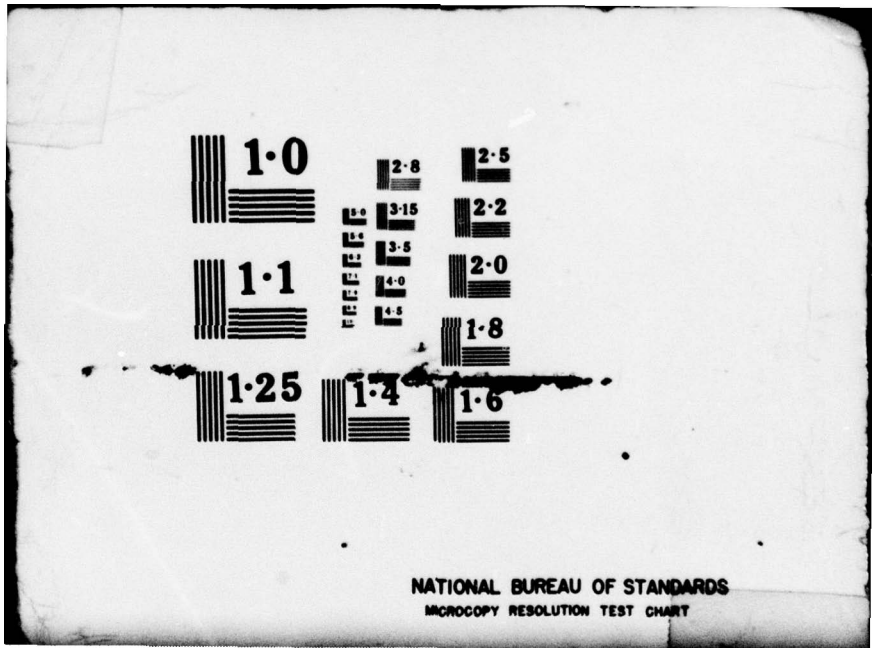
1·0
1·1
1·25
2·8
3·15
3·5
4·0
4·5
1·4
2·5
2·2
2·0
1·8
1·6
NATIONAL BUREAU OF STANDARDS
MICROCOPY RESOLUTION TEST CHART

SECURITY CLASSIFICATION OF THIS PAGE (When Data Entered)

REPORT DOCUMENTATION PAGE

READ INSTRUCTIONS BEFORE COMPLETING FORM

1. REPORT NUMBER
2. GOVT ACCESSION NO.
3. RECIPIENT'S CATALOG NUMBER

4. TITLE (and Subtitle)
FEASIBILITY OF BREED/BURN FUEL CYCLES IN PEBBLE BED HTGR REACTORS

5. TYPE OF REPORT & PERIOD COVERED
THESIS

6. PERFORMING ORG. REPORT NUMBER

7. AUTHOR(s)
JENCKS, TIMOTHY STORRS

8. CONTRACT OR GRANT NUMBER(s)

9. PERFORMING ORGANIZATION NAME AND ADDRESS
MASS. INST. OF TECHNOLOGY

10. PROGRAM ELEMENT, PROJECT, TASK AREA & WORK UNIT NUMBERS

11. CONTROLLING OFFICE NAME AND ADDRESS
Code 031
NAVAL POSTGRADUATE SCHOOL
MONTEREY, CALIFORNIA, 93940

12. REPORT DATE
SEP 78

13. NUMBER OF PAGES
178

14. MONITORING AGENCY NAME & ADDRESS(if different from Controlling Office)

15. SECURITY CLASS. (of this report)
UNCLASS

15a. DECLASSIFICATION/DOWNGRADING SCHEDULE

LEVEL II

16. DISTRIBUTION STATEMENT (of this Report)
APPROVED FOR PUBLIC RELEASE; DISTRIBUTION UNLIMITED

17. DISTRIBUTION STATEMENT (of the abstract entered in Block 20, if different from Report)

DDC RECEIVED AUG 14 1979 C

18. SUPPLEMENTARY NOTES

19. KEY WORDS (Continue on reverse side if necessary and identify by block number)
BREED/BURN FUEL CYCLES, PEBBLE BED HTGR REACTORS

20. ABSTRACT (Continue on reverse side if necessary and identify by block number)
SEE REVERSE

THIS DOCUMENT IS BEST QUALITY PRACTICABLE.
THE COPY FURNISHED TO DDC CONTAINED A
SIGNIFICANT NUMBER OF PAGES WHICH DO NOT
REPRODUCE LEGIBLY.

DD FORM 1 JAN 73 1473 (Page 1)
EDITION OF 1 NOV 65 IS OBSOLETE
S/N 0102-014-6601

UNCLASS
SECURITY CLASSIFICATION OF THIS PAGE (When Data Entered)

AD A072680

DDC FILE COPY

DISCLAIMER NOTICE

THIS DOCUMENT IS BEST QUALITY PRACTICABLE. THE COPY FURNISHED TO DDC CONTAINED A SIGNIFICANT NUMBER OF PAGES WHICH DO NOT REPRODUCE LEGIBLY.

ABSTRACT

The feasibility of the breed/burn fuel cycle concept, originally proposed for Pu239/U FBR applications, has been evaluated for use in a U233/Th fueled pebble bed HTGR. Because of its excellent neutron economy, its versatility with respect to fueling strategies and the high fuel burnup achievable as well as the ability to approach continuous fueling operation, the pebble bed HTGR was judged to be the best suited, of reactors currently of commercial interest, for implementation of the breed/burn fuel cycle in a thermal/epithermal system.

Three necessary (but not sufficient) criteria for successful system operation were defined: (1) achieving system criticality, $k_\infty \geq 1.0$; (2) achieving a breed zone fissile production rate such that the asymptotic enrichment attained in the breed zone and the end-of-life burnup in the burn zone (expressed in percent) are related by $\varepsilon_{ASY} \geq B_{EOL}$; and (3) accounting for zone-to-zone leakage by providing adequate excess reactivity, shown to require that $k_\infty \geq 1.5$.

State-of-the-art computation methods, PDQ-7/AMPX, were employed for the analysis of homogeneous breed/burn pebble bed HTGR regions. Breed zones achieved their highest asymptotic enrichment ($\sim$3.5%) for carbon-to-heavy metal atom ratios, C/HM = 110; when charged to the burn zone this maximized k_∞ ($\sim$1.3). Highly-moderated burn zones (C/HM = 450) were most able to attain high fuel burnups ($\sim$100,000 MWD/MTHM) while sustaining the highest possible values of k_∞. No combination of the compositions evaluated here ($110 \leq C/HM \geq 450$), however, were able to achieve the k_∞ ($k_\infty \geq 1.5$) required to overcome the effects of zone-to-zone leakage. For these compositions then, successful operation of a breed/burn system was not possible. Further study of reactor systems operating with very hard breed zone eipthermal spectra (C/HM < 110) should be undertaken if a feasible breed/burn system is to be pursued since it was found that asymptotic zone enrichment reaches a maximum in a spectrum between that typical of a hard-spectrum HTGR and soft-spectrum LMFBR.

Thesis Supervisor: Michael J. Driscoll
Title: Associate Professor of Nuclear Engineering

Thesis Supervisor: David D. Lanning
Title: Professor of Nuclear Engineering

(2)

Approved for public release;
distribution unlimited.

(6) FEASIBILITY OF BREED/BURN FUEL CYCLES IN PEBBLE BED HTGR REACTORS.

by

(10) TIMOTHY STORRS/JENKS

B.S.M.E., United States Naval Academy
(1977)

(12) 181 p.

SUBMITTED IN PARTIAL FULFILLMENT
OF THE REQUIREMENTS FOR
THE DEGREE OF

MASTER OF SCIENCE (9) Master's thesis,

at the

MASSACHUSETTS INSTITUTE OF TECHNOLOGY

(11) SEPTEMBER, 1978

Signature of Author ..... Timothy S. Jenks
Department of Nuclear Engineering

Certified by ..... Michael J. Driscoll
Thesis Supervisor

Certified by ..... D. D. Lanning
Thesis Supervisor

Accepted by .....
Chairman, Departmental Committee
on Graduate Students

FEASIBILITY OF BREED/BURN FUEL CYCLES IN PEBBLE BED HTGR REACTORS

by

TIMOTHY STORRS JENKS

Submitted to the Department of Nuclear Engineering on September 8, 1978 in partial fulfillment of the requirements for the Degree of Master of Science

ABSTRACT

The feasibility of the breed/burn fuel cycle concept, originally proposed for Pu239/U FBR applications, has been evaluated for use in a U233/Th fueled pebble bed HTGR. Because of its excellent neutron economy, its versatility with respect to fueling strategies and the high fuel burnup achievable as well as the ability to approach continuous fueling operation, the pebble bed HTGR was judged to be the best suited, of reactors currently of commercial interest, for implementation of the breed/burn fuel cycle in a thermal/epithermal system.

Three necessary (but not sufficient) criteria for successful system operation were defined: (1) achieving system criticality, $k_\infty \geq 1.0$; (2) achieving a breed zone fissile production rate such that the asymptotic enrichment attained in the breed zone and the end-of-life burnup in the burn zone (expressed in percent) are related by $\varepsilon_{ASY} \geq B_{EOL}$; and (3) accounting for zone-to-zone leakage by providing adequate excess reactivity, shown to require that $k_\infty \geq 1.5$.

State-of-the-art computation methods, PDQ-7/AMPX, were employed for the analysis of homogeneous breed/burn pebble bed HTGR regions. Breed zones achieved their highest asymptotic enrichment ($\sim$3.5%) for carbon-to-heavy metal atom ratios, C/HM = 110; when charged to the burn zone this maximized k_∞ ($\sim$1.3). Highly-moderated burn zones (C/HM $\simeq$ 450) were most able to attain high fuel burnups ($\sim$100,000 MWD/MTHM) while sustaining the highest possible values of k_∞. No combination of the compositions evaluated here ($110 \leq$ C/HM ≥ 450), however, were able to achieve the k_∞ ($k_\infty \geq 1.5$) required to overcome the effects of zone-to-zone leakage. For these compositions then,

successful operation of a breed/burn system was not possible. Further study of reactor systems operating with very hard breed zone eipthermal spectra (C/HM < 110) should be undertaken if a feasible breed/burn system is to be pursued since it was found that asymptotic zone enrichment reaches a maximum in a spectrum between that typical of a hard-spectrum HTGR and soft-spectrum LMFBR.

Thesis Supervisor: Michael J. Driscoll
Title: Associate Professor of Nuclear Engineering

Thesis Supervisor: David D. Lanning
Title: Professor of Nuclear Engineering

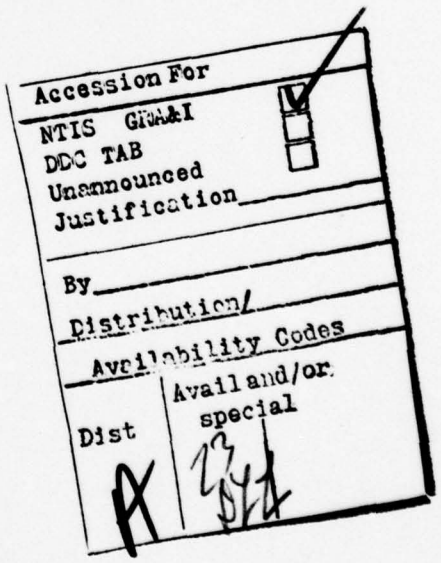

ACKNOWLEDGEMENTS

The author wishes to express his deep gratitude to his advisors, Professor Michael J. Driscoll and Professor David D. Lanning, for their invaluable advice and guidance throughout the course of this study.

In addition, special thanks are due to Dr. Edward K. Fujita for his patient direction in the preparation and use of computer codes, and Mr. Dale Lancaster for his able assistance in the development of the various analyses of this study.

The help of Dr. Brian A. Worley of Oak Ridge National Laboratory in computer depletion treatment and cross-section generation is greatly appreciated.

This thesis was completed while the author, serving on active duty in the United States Navy, attended M.I.T. on a Graduate School Endowed Tuition Scholarship, awarded through the M.I.T. Department of Nuclear Engineering.

Computer calculations described herein were performed at the M.I.T. Information Processing Center.

Ms. Gail Jacobson very ably handled the typing of this manuscript and Mr. Ray A. Rothrock skillfully prepared the tables and figures.

TABLE OF CONTENTS

	Page
Abstract	2
Acknowledgements	4
Table of Contents	5
List of Figures	8
List of Tables	9
CHAPTER I. INTRODUCTION	
1.1 Foreword	11
1.2 Background	14
1.3 Previous Work	18
1.4 Outline of Present Work	25
CHAPTER II. BREED/BURN OPERATION	
2.1 Introduction	27
2.2 Breed/Burn Potential for U233 Production	27
2.3 Factors Affecting the Breeding Ratio	28
2.4 Breed Zone U233 Conversion	32
2.5 Evaluation of Homogeneous Zone Characteristics	34
2.6 Variation in Neutron Spectra	41
2.7 System Criticality	55
2.8 Summary	61
CHAPTER III. COMPUTATIONAL METHODS	
3.1 Introduction	64

Table of Contents (continued)

		Page
3.2	System Model	64
3.3	Computer Codes	66
3.3.1	PDQ-7	66
3.3.2	AMPX	68
3.4	Computational Methods for Evaluation of Homogeneous Zone Parameters	69
3.5	Summary	74
CHAPTER IV.	BREED/BURN COMPUTATIONAL RESULTS	
4.1	Introduction	76
4.2	Variation of k_∞ with Fuel Burnup	76
4.3	Variation of ε^{23} with Fuel Burnup	84
4.4	Criticality with Zone Leakage	93
4.5	Summary	94
CHAPTER V.	SUMMARY, CONCLUSIONS AND RECOMMENDATIONS	
5.1	Introduction	96
5.2	Summary of Analysis	97
5.3	Conclusions	102
5.4	Recommendations for Future Work	103
APPENDIX A	ONE-GROUP CONSTANTS	106
APPENDIX B	TABULATION OF DATA USED IN CHAPTERS 2 AND 4	112
APPENDIX C	FOUR-GROUP CONSTANTS	119
APPENDIX D	COMPUTER CODE INPUT PARAMETERS	148

Table of Contents (continued)

	Page
D.1 Introduction	148
D.2 Nuclide Identification	148
D.3 Number Densities	148
D.3.1 Nomenclature	150
D.3.2 Material Properties	151
D.3.3 Calculation of Number Densities	155
D.4 Exposure Times	160
D.4.1 Nomenclature	160
D.4.2 Calculation of Exposure Times	161
D.5 Depletion Treatment	163
D.5.1 Depletion Chains	163
D.5.2 Nuclide Decay Constants	163
D.5.3 Fission Product Yields	163
D.5.4 Energy Release per Fission	163
D.5.5 Chi (Neutron Yield) Spectra	163
D.5.6 Neutron Flux	173
APPENDIX E REFERENCES	176

LIST OF FIGURES

Fig.		Page
1.1	Pebble Bed Htgr Breed/Burn System Schematic	21
2.1	Pebble Bed HTGR Fuel Element	37
2.2	Schematic Diagram Showing Potential Feasibility of Breed/Burn Systems	46
2.3	Asymptotic Fissile Enrichment Limits for U233 and Pu239 Spectra Using Sheaffer's Correlation	49
2.4	Asymptotic Enrichments for U233/Th Systems	54
3.1a	Representative Variation of k_∞ with Burnup (linear)	70
3.1b	Representative Variation of Enrichment with Burnup	70
4.1	k_∞ versus Fuel Burnup for C/HM = 110	78
4.2	k_∞ versus Fuel Burnup for C/HM = 250	79
4.3	k_∞ versus Fuel Burnup for C/HM = 325	80
4.4	k_∞ versus Fuel Burnup for C/HM = 450	81
4.5	Reactivity-Limited Burnup for Asymptotic Enrichment Loadings	86
4.6	U233 Enrichment versus Fuel Burnup for C/HM = 110	87
4.7	U233 Enrichment versus Fuel Burnup for C/HM = 250	88
4.8	U233 Enrichment versus Fuel Burnup for C/HM = 325	89
4.9	U233 Enrichment versus Fuel Burnup for C/HM = 450	90
4.10	$k_{\infty_{BOL}}$ versus C/HM Atom Ratio as a Function of BOL Enrichment	92
D.1	Sectional View of Fuel Ball	153

LIST OF TABLES

No.		Page
1.1	Spectrum-Averaged Neutron Yield per Fissile Absorption	24
2.1	Composition of Pebble Bed Feed Balls	38
2.2	Spectrum-Averaged Homogeneous Zone Parameters	40
2.3	Asymptotic Enrichments and Fissile η Values for Fast Spectra	48
2.4	Spectral Index and Asymptotic Enrichments for the U233/Th Pebble Bed HTGR	53
2.5	Asymptotic Fissile Enrichment Limits	56
2.6	Beginning-of-Life Infinite-Medium Multiplication Factors	58
2.7	k_∞ for Various Zone Combinations	59
4.1	Reactivity-Limited Burnup for Continuously-Fueled Burn Zones with $\varepsilon_{BOL_c} = \varepsilon_{ASY_{bz}}$	83
4.2	Comparison of Actual End-of-Cycle U233 Enrichments and Predicted Asymptotic Limits	85
5.1	Performance Parameters as a Function of Breed and Burn Zone Composition	101
A.1	Relative Groupwise Neutron Flux	107
A.2	One-Group Cross-Sections for C/HM = 110	108
A.3	One-Group Cross-Sections for C/HM = 250	109
A.4	One-Group Cross-Sections for C/HM = 325	110
A.5	One-Group Cross-Sections for C/HM = 450	110
B.1	Constants for Sheaffer Cross-Section Correlation	113
B.2	Neutron Cross-Sections for Fast Spectra	114
B.3	k_∞ as a Function of Fuel Burnup (from PDQ-7)	115

List of Tables (continued)

No.		Page
B.4	U233 Enrichment as a Function of Fuel Burnup (from PDQ-7)	116
B.5	Curve-Fit Coefficients for Linear k_∞ versus Burnup Correlation	117
B.6	Curve-Fit Coefficients for Linear Burnup Model	118
C.1	Four-Group Cross-Sections for C/HM = 110 (7 pages)	120
C.2	Four-Group Cross-Sections for C/HM = 250 (7 pages)	127
C.3	Four-Group Cross-Sections for C/HM = 325 (7 pages)	124
C.4	Four-Group Cross-Sections for C/HM = 450 (7 pages)	141
D.1	Nuclide Identification	149
D.2	Ball Material Properties	152
D.3	Packing Fraction of Grains in Meat	154
D.4	Initial Cell-Averaged Heavy Metal Number Densities	158
D.5	Initial Cell Number Densities	159
D.6	Exposure Times	162
D.7	Depletion Chains	164
D.8	Nuclide Decay Constants	168
D.9	Fission Product Yields	170
D.10	Energy Release per Fission	171
D.11	Chi (Neutron Yield) Spectra	172
D.12	Groupwise Relative Neutron Flux	174
D.13	Energy Groups	175

I. INTRODUCTION

1.1 Foreword

In the past the general public has understood the term "nuclear proliferation" in a restricted sense, referring almost exclusively to the widespread deployment of nuclear weapons throughout the world. The realization that a growing number of foreign countries are operating commercial nuclear powered electrical generating stations and the implied relationship between nuclear electric plants and weapons has resulted in a broader interpretation of proliferation. In the United States, this interpretation has achieved the status of official government policy and has led to both national and international reassessments, e.g. the Nonproliferation Alternative System Assessment Program (NASAP) and the International Fuel Cycle Evaluation (INFCE) efforts. The question of the safeguarding of sensitive nuclear materials has become a major area of emphasis in furthering the development and application of the nuclear fuel cycle for commercial electrical production.

Previously it was envisioned that light water reactors (LWR) would serve an interim role as precursors to fast breeder reactors (FBR). This status is testified to by the omission in most of the older long range systems studies of "advanced LWRs." Until such time as FBRs could become commercially feasible and sufficient fissile reserves could be bred to permit their widespread deployment, LWRs were to be the mainstay of commercial nuclear power.

Currently, however, the transition to a breeder economy is not envisioned for the United States, at least in the short term, so it is prudent to consider other options to meet the needs for a growing electrical generating capacity [N1]. Since the objectionable feature of the FBR is that it utilizes fertile uranium-238 (U238) to breed large amounts of fissile plutonium, new options must permit utilizing nuclear fuels in such a manner that the production of and/or commercial traffic in materials suitable for weapons applications is minimized at all levels.

The dilemma posed by this objective is highlighted by rising oil prices and limited and unevenly distributed national energy resources. Many nonnuclear weapons states, desiring to provide for their own growing energy needs, have opted to develop civilian nuclear power programs. In the United States, the lack of expansion of enrichment capacity or the commercial deployment of reprocessing and mixed oxide fabrication capability has increased the economic and commercial incentives for other countries to develop such capabilities independently [P1].

In view of the above considerations, development and evaluation of the commercial feasibility of schemes utilizing the nuclear fuel cycle in a manner so as to minimize proliferation risks, while providing suitable economic and commercial incentives for their widespread deployment, has become an important national and international objective. It is the purpose of the present thesis to evaluate one particular class of proliferation-resistent fueling schemes; here designated the "breed/burn"

concept. As will be discussed further, in its fullest development this scheme would allow charging only fertile material to a reactor after initial startup and dispatch of fully spent fuel to disposal rather than reprocessing and reuse.

1.2 Background

Throughout its history, commercial nuclear power in the United States has been subjected to several periods of changing emphasis. To the public utilities, short term fuel cycle costs have always been a most important consideration. While long-term trends are reviewed and evaluated, the utility always seeks to minimize the current costs of electricity to the consumer, hence causing the short-term economic considerations to dominate. Indeed, the very practice of present value discounting emphasizes the short-term.

National energy planning, on the other hand, is concerned with being able to insure the availability of adequate energy resources within reasonable economic limits for the very long-term. With specific application to the nuclear fuel cycle, although most quantities of high-cost fissile uranium in the earth's crust can conceivably be considered a source of energy, the cost of utilizing it is prohibitive. In this light, a more economically viable solution to the long-term energy supply problem is to produce most future fissile materials by irradiating fertile materials in the fuel elements of a nuclear reactor. However, to accomplish this without relying on the commercialization of the FBR, it becomes necessary to operate other types of reactors as near- or net-breeders.

Current pressurized water reactors (PWR) operate with conversion ratios on the order of 0.60 [D1] on the uranium-238 fuel cycle. High temperature gas-cooled reactors (HTGR), however, typically operate with thorium-232 (Th232) to uranium-233

(U233) conversion ratios of 0.76 [D1], based on optimization of near term economics. Conversion ratios of 0.84 are feasible and favored for ore conservation, however [D1], and even higher values are readily obtainable [L4,R2,S3]. Thus, we will focus on this inherently superior class of reactors in the present study. Most HTGRs built or designed to date utilize a highly enriched uranium/thorium (HEU/Th) fuel cycle which necessitates uranium-235 (U235) enrichments as high as 93%. Obviously, to meet nonproliferation objectives, alternatives to this fuel cycle must be evaluated.

The HTGR coated-particle fuel design allows a variety of alternative cycles, each having characteristic advantages and disadvantages in particular circumstances. Designing alternative fuel cycles that can use the same core layout, fuel zoning and fuel blocks as the HEU/Th cycle means that conversion from one fuel cycle to another can be accomplished in available plant designs merely by replacing fuel blocks in each segment with alternative cycle blocks during the course of the regular refueling sequence. Since the parameters of fissile-to-fertile and heavy metal-to-moderator atom ratios control the conversion ratio of the reactor system, the versatility of the HTGR makes it a logical choice for tailoring fuel loadings and burnups, based on changing economic and resource availability conditions.

Even more versatile and convenient for implementation of alternative fuel cycles among the advanced HTGRs is the pebble bed reactor [L4,T1]. The injection-molded spherical graphite fuel balls used to fuel this system can easily be fabricated

with any desired fissile or fertile fuel density, and immediately be introduced into the continuous refueling cycle.

Operating an HTGR as a near-to-net-breeder utilizing the thorium fuel cycle requires low power density operation with heavy thorium loadings. Since operating trends are dictated by short term energy costs, obtaining a maximum conversion ratio and better fuel utilization is not necessarily a desirable near term goal. In obtaining a higher conversion ratio, increasing the thorium loading in the core while decreasing the core power density and fuel residence time would incur offsetting economic penalties which in turn may or may not be balanced by the advantages of improved fuel utilization. The penalties would depend on projected economic conditions, the projected availability of uranium ore, costs for separative work, reprocessing and recycle, and transportation and disposal costs.

With increasing thorium loading, although an increase in the conversion ratio will be realized, a higher fissile inventory is also required. The resulting higher initial costs will be attractive if sufficient money is saved over the life of the reactor. This outcome is favored in an economic environment where large price increases are projected for fresh feed fuel.

Lowering the core power density in an HTGR will result in a larger core volume for a given thermal output. Hence, additional volume is available for fertile thorium loading, producing the same net result as previously described. Additionally, neutron utilization is improved due to a reduction in

losses to xenon-135 (Xe135) and protactinium-233 (Pa233) [K2]. The larger reactor volume will increase initial capital investment and will also change the required coolant pumping power of the system. Keeping the coolant temperature increase constant across the core while maintaining similar height-to-diameter ratios, the larger, low power density core will require a higher coolant mass flow for a given thermal output. Because the HTGR uses helium as its primary cooling medium, very high coolant mass flow rates require that a significant fraction of the plant power output be utilized in operating the coolant pumps. Therefore, a variation in the core power density that will increase the pumping requirements can add a sizeable financial burden to the overall operating costs.

In addition to the HEU/Th fuel cycle, the use of a uranium-233/thorium (U233/Th) cycle, a low-enriched uranium (LEU) cycle or various plutonium/uranium (Pu/U) or plutonium/uranium/thorium (Pu/U/Th) fuel cycles are also possible in the HTGR [B1,S3,T1]. For all of the options the reduced total uranium ore requirement achieved by increasing the conversion ratio requires accepting either a higher capital investment or higher operating costs in other areas.

The present work focuses primarily on the U233/Th cycle (because of its well known superiority in thermal and epithermal systems) and the possibility of its utilization in a system designed to accomplish most key nonproliferation objectives. Since U233 is required as the initial fissile loading in this cycle, the resource conservation is not direct,

but rather indirect. To provide the initial U233 loading, adequate fissile production in prebreeders, operating expressly for the production of U233 is required. To accomplish the objectives of nonproliferation effectiveness we will evaluate the feasibility of using the U233/Th cycle in either the internally recycled or the "Once-Through-Then-Out" (OTTO) modes in a pebble bed reactor system [T1].

In the projection of any long-term energy strategy, the extension of uranium resources must be considered as most important, even in view of the increasing relevance of the objectives of nonproliferation. The present work, however, will attempt only to evaluate the feasibility of a single scheme for effectively providing a viable solution to the proliferation problem of safeguarding sensitive nuclear reactor materials through all steps of the fuel cycle without regard to its long-term effects on either the utilization of resources or the economics of implementing such a scheme commercially. However, because breakeven breeding is necessary to fully achieve the nonproliferation objectives, long-term ore utilization should be quite efficient.

1.3 Previous Work

The use of the breed/burn concept was proposed by Fischer et al [F1] for implementation in a reactor operating with a hard spectrum core. Depleted uranium monocarbide feed fuel would be introduced to breed fissile plutonium, and after a period of residence in the hard spectrum the fuel, now slightly

enriched, would be moved to the more thermalized outer region of the fast core. Energy would be generated as the fuel burns to a design-dependent burnup limit while the fissile-to-fertile fuel ratio is reduced toward the equilibrium value for that neutron energy spectrum.

The present work extends the concept of the breed/burn cycle to assess the feasibility of its implementation in the thermal/epithermal spectrum of the HTGR. Nonproliferation objectives of reducing fissile enrichments can be realized in addition to the benefits of decoupling this type of reactor from breeders and the constraints related to reprocessing facilities. The exception, of course, is the need to obtain the initial startup core, here requiring a substantial U233 inventory.

The introduction of this fueling scheme into the pebble bed reactor system provides the ability to readily adjust the core neutron spectrum simply by varying the moderator-to-fuel (carbon-to-heavy metal) ratio. Additionally, core zoning (establishing separate breed and burn regions) can easily be accomplished in this application. A given ball, during its lifetime, would reside in two distinct regions. Radial zoning would make coolant temperature control difficult. Since the breed zone would operate at a lower power density than the burn zone, cold coolant bypass would degrade the bulk core exit temperature. Therefore, the core will be divided into axial zones, allowing it to be seen that for a fertile load ball, the "breed zone" can be defined as that region of the

reactor in which the fissile concentration of the ball is increasing. Similarly, the "burn zone" is that region in which the fissile concentration decreases. The desired breeding and burning effects can be accomplished by operating the breed zone in a predominantly epithermal spectrum. Thus, in its lifetime, a fertile-fueled ball would travel through both zones, entering the thermal burn zone (together with pure graphite balls necessary to attain the desired moderator-to-fuel ratio) after first passing through the breed zone (which contains only fueled balls). A schematic diagram of system operation is illustrated in Figure [1.1].

In successive passes through the breed zone, the concentration of U233 is built up to the maximum possible amount for the given spectrum. It is then cycled (with additional graphite-only balls) into the burn zone, again being recycled for successive passes until a design-limited burnup is attained. At this point the depleted balls are removed from the system for disposal.

Operating on this type of fuel cycle, the proposed reactor would allow very high burnups, and as a result, the total fissile enrichment of the discharged balls would be very low, particularly if the number of passes could be minimized, in which case discharge compositions approaching those of the OTTO cycle could be envisioned. If the reactor core can be adequately segregated so as to maintain distinct breed and burn regions, then the practicality of achieving the properties sought by Fischer et al can be evaluated.

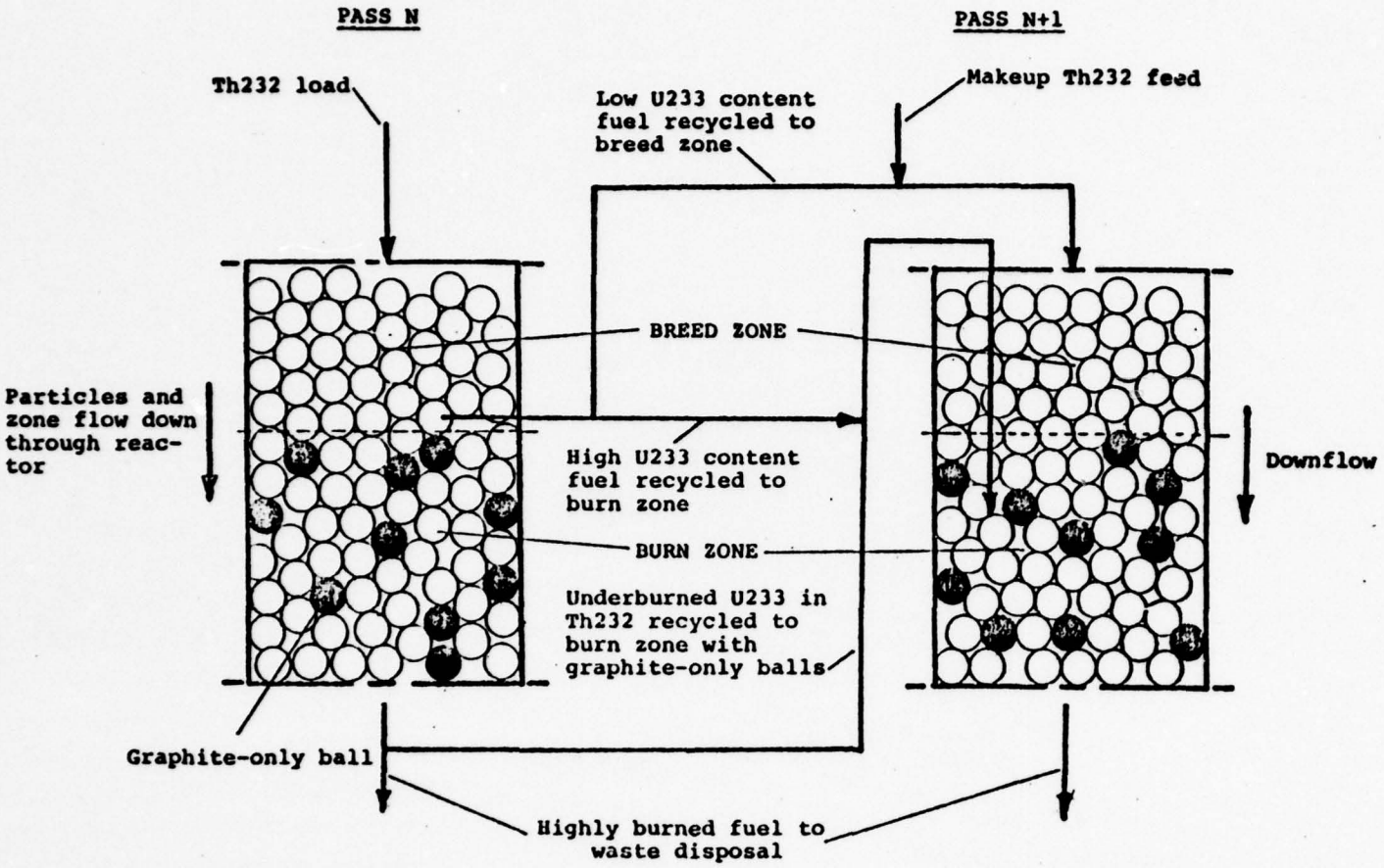

FIGURE 1.1: PEBBLE BED HTGR BREED/BURN SYSTEM SCHEMATIC

Work on HTGRs has been devoted mainly to the use of the HEU/Th fuel cycle, both in traditional graphite block-element reactors and pebble bed systems. Many alternative cycles, previously noted, have also been investigated more recently and in less detail, both from their ability to meet nonproliferation objectives as well as their respective roles in the extension of uranium resources. Current studies [D2,T1,V1] are focusing on the flexibility of the HTGR fuel cycle, which permits it to adapt to variations in fuel materials relatively efficiently. While favorable in many respects, this feature also makes it difficult to determine optimal strategies. This extra flexibility, relative to other reactor types, results from the particle loading system, which allows one to vary the fertile and fissile loadings almost independently and also to adjust the resonance shielding, not only by varying the size and loading of the fuel elements, but also by adjusting the dimensions of the individual fuel kernels [D1].

Utilizing this flexibility it is possible to operate HTGRs with conversion ratios slightly greater than unity [R2,S3]. But considering resources and economics, the high fissile inventories required and the resulting recycle losses have made fuel designs with conversion ratios on the order of 0.9 appear more promising [S3], because near this value, burnup and processing losses reach a minimum [D1].

Fuel cycle optimization in the HTGR has traditionally been most heavily concerned with minimizing fuel cycle cost. It is clear that this approach does not fully utilize the potential

in the HTGR for resource conservation through the use of the U233/Th fuel cycle. To obtain a breeding system with this cycle, if less than η-2 neutrons are lost to parasitic absorbers, then after one neutron is utilized in sustaining criticality, one additional neutron is available for absorption by the fertile thorium to produce, after β-decay, a new fissile U233 atom. The selection of the U233/Th cycle for this application is clear when the spectrum-averaged neutron yield per absorption, shown in Table [1.1], is considered for this reactor type. For various carbon-to-heavy metal atom ratios (N_C/N_{HM}) only fissile U233 has a value of η adequately high to allow breeding.

The high flexibility in the design of fuel elements and the reactor refueling scheme in the pebble bed HTGR has made its use as a thermal breeder possible [R2]. Using highly enriched U233 ((U233/U)$\simeq$ 0.9) produced in a prebreeder as feed fuel, thick radial blankets of thorium, high heavy metal loadings in the fuel elements and relatively low heavy metal burnups will allow the pebble bed system to be self-supporting; independent of uranium resources after the first core inventories have been built up. Such designs have been shown to achieve conversion ratios greater than 1.05 [R2].

Other studies [T1,V1], dealing more with nonproliferation and ore conservation strategies than with breeding potential have shown that proliferation resistance is best achieved in the low-enriched mixed oxide cycle (mixed uranium/thorium oxides with U235/U$\simeq$ 0.20). Reactor loading is restricted to

TABLE 1.1

SPECTRUM-AVERAGED NEUTRON YIELD

PER FISSILE ABSORPTION*

FISSILE	CARBON-TO-HEAVY METAL ATOM RATIO (N_C/N_{HM})†			
ISOTOPE	110	250	325	450
U233	2.209	2.240	2.246	2.253
U235	1.928	1.989	2.001	2.011
Pu239	1.775	1.788	1.791	1.794

* $\eta = \frac{\nu\sigma_f}{\sigma_a}$

† C/HM ratios correspond to spectrum averaged cross-section data given in Appendices B and D.

non-sensitive materials while 95% of the bred fissile plutonium is burned in situ [T1].

Resource conservation, however, is most favorable for OTTO cycles using highly-enriched U/Th mixed oxide ((U235/U) ≈ 0.93) fuels designed for burnups of 100 to 130 GWD/MTHM [T1].

From the above discussion, it can be seen that the wide latitude of compositions and fueling schemes available in the HTGR allow considerable breadth in designing strategies emphasizing objectives of proliferation resistance, fissile breeding potential, uranium resource conservation or fuel cycle economics. Each strategy has characteristic advantages and disadvantages, depending on the design criteria for the chosen fuel cycle. The breed/burn concept, when applied to the pebble bed HTGR system, combines the objectives of nonproliferation and fissile breeding. It is anticipated that the HTGR system can best provide the versatility needed to devise such a scheme for a thermal/epithermal system.

1.4 Outline of Present Work

The main body of this report consists of three chapters. Chapter 2 discusses the operation of the breed/burn fuel cycle in the pebble bed system and the relationship of the neutronic parameters of the two regions. Additionally, an evaluation is made of the potential of the pebble bed system for successful operation utilizing the breed/burn concept using one group models. Discussion is presented of the effects of spectrum hardening on the rate and amount of fissile breeding obtainable.

Chapter 3 describes the computational methods used for evaluation of the reactor system, nuclear data input, cross-section generation and the reactor model.

The results of the analysis are discussed in Chapter 4 with regard to reactor criticality, burnup limits and rates of fissile production as a function of composition. Possible modifications to the system are suggested.

Chapter 5 summarizes the analysis and reiterates the main conclusions. Recommendations are made for future work. Appendices containing supplementary information are also included.

II. BREED/BURN OPERATION

2.1 Introduction

The pebble bed HTGR is expected to provide the best available system for implementation of the breed/burn concept into a thermal/epithermal reactor because of it compositional flexibility and high burnup. In order to utilize the breed/burn fuel cycle in this system, the feasibility of operating it as a two-zone reactor will be investigate. Dividing the core axially will allow the two zones to exist in harmony with the flow-through fuel cycle, such that all fuel elements will move through both zones during successive passes through the core.

The purpose of this chapter is to consider the effects of various parameters on the rate of U233 production in the breed zone of such a system and to evaluate the potential for successful operation in the pebble bed HTGR. Possible modifications will be discussed to enhance system performance.

2.2 Breed/Burn Potential for U233 Production

The objective is to determine if, in fact, it is a feasible consideration to attempt using the breed/burn system in a pebble bed HTGR. For this analysis, the system considered will alternate breed and burn regions axially for the length of the reactor. The pebble bed HTGR is a very large, low power density system, and hence the net neutron leakage from the core is relatively low. By varying the composition

and geometry of each region, the respective neutronic characteristics of the zones can be altered, thereby changing the internal leakage between zones and hence changing the operating envelope of the entire system.

First, an analytical method will be used to evaluate the parameters having the greatest effect on the rate of fissile breeding, and then the entire system will be evaluated for its operational capabilities.

2.3 Factors Affecting the Breeding Ratio

The customary index of fissile breeding (here of U233 from neutron capture in fertile Th232) is represented by the breeding ratio, b, defined as:

$$b = \frac{\text{Rate of fissile production in the system}}{\text{Rate of fissile consumption in the system}}$$

or,

$$b = \frac{C_c^{02} + C_{bz}^{02}}{A_c^{23} + A_{bz}^{23}} \qquad (2.1)$$

where C = neutron capture rate in the species indicated,

A = neutron absorption rate in the species indicated,

c = burn zone

and bz = breed zone.

For simplicity in this analysis, the effects of only the most significant materials will be considered. While it is

realized that a rigorous approach which would include the production and depletion of protactinium and U235 and the depletion of Th232 could yield more precise conclusions, the factors controlling the rate of fissile U233 production can be examined adequately by this more simple analysis.

In each region a neutron balance can be written as:

Production = Losses + Absorption + Leakage

which, for the burn zone, is given by:

$$\bar{\nu}F_c^{23} + \bar{\nu}F_c^{02} = L_c + F_c^{23} + F_c^{02} + C_c^{23} + C_c^{02} + A_c^{P}. \qquad (2.2)$$

Similarly for the breed zone:

$$\bar{\nu}F_{bz}^{23} + \bar{\nu}F_{bz}^{02} + L_c = F_{bz}^{23} + F_{bz}^{02} + C_{bz}^{23} + C_{bz}^{02} + A_{bz}^{P} \qquad (2.3)$$

where

F = fission rate in the species indicated,

L = neutron leakage from the region indicated

and A^P = parasitic absorption.

Combining these terms the breeding ratio of the system can be expressed as:

$$b \approx \eta_s + \frac{(\bar{\nu} - 1)\, F_s^{02}}{A_s^{23}} - \frac{A_s^{P}}{A_s^{23}} - 1 \qquad (2.4)$$

where η_s = mean neutron yield per fissile absorption in the system

$$= \bar{\nu} \frac{F_s^{23}}{A_s^{23}} \tag{2.5}$$

and s = sum of indicated interactions in the breed and burn zones.

Similarly, the breeding ratios for the burn zone alone and the breed zone alone, respectively, are given by:

$$b_c \simeq \eta_c + \frac{(\bar{\nu} - 1)\, F_c^{02}}{A_s^{23}} - \frac{A_c^{P}}{A_s^{23}} - 1 \tag{2.6}$$

and

$$b_{bz} \simeq \eta_{bz} + \frac{(\bar{\nu} - 1)\, F_{bz}^{02}}{A_s^{23}} - \frac{A_{bz}^{P}}{A_s^{23}} - 1 \tag{2.7}$$

where

$$\eta_c = \frac{\bar{\nu}\, F_c^{23}}{A_s^{23}} \tag{2.8}$$

and

$$\eta_{bz} = \frac{\bar{\nu}\, F_{bz}^{23}}{A_s^{23}} . \tag{2.9}$$

Equations (2.4), (2.6) and (2.7) are composed of three main terms. The first term, η, dominates the expressions, and hence increasing η will increase the breeding ratio proportionately. This can be accomplished by hardening the core neutron spectrum through an increase in the concentration of the fertile and fissile species. That is, lowering the carbon-to-heavy metal (C/HM) atom ratio and thus decreasing the moderation results in a harder neutron spectrum.

The second term, $(\bar{\nu} - 1)\ F^{02}/A^{23}$, represents the gain in η due to fast fissioning of fertile material. Because of the small threshold fission cross-section of Th232 this term is relatively small.

The third term, A^{P}/A^{23}, represents the neutrons lost to parasitic absorption and leakage and hence is negative. Thus, the objective of increasing the amount of fissile breeding necessitates minimizing the amount of parasitic absorption and leakage losses. Fuel material absorption cross-sections and those of structural materials, therefore, become important design considerations. From this analysis we must conclude that in order to increase the breeding ratio in our system a hardened neutron spectrum is generally favored since it minimizes parasitic absorption and maximizes neutron yield, as will be shown in succeeding sections. Leakage losses may or may not be improved, however. The first design strategy clue is then to obtain as hard a spectrum as practical in both the breed and burn zones within other constraints. Because we want to be able to produce adequate masses of fissile material in the breed zone to fuel the burn zone, our attention focuses on the parameters of the breed zone. It is realized at this point, however, that the two zones will have significant coupling in their characteristics. That is, considering a given number of neutrons in the system, favoring neutron availability in one region will decrease the effectiveness of the other. If the breed zone is, under any conditions, unable to breed adequate masses of U233, then the neutron balance in the

burn zone will still be unable to effect satisfactory system operation. It is for this reason that the breed zone parameters will be examined in more detail.

2.4 Breed Zone U233 Conversion

To some degree, breeding of U233 will occur throughout the reactor. In applying the breed/burn concept to the pebble bed HTGR a criterion for successful operation has been set that adequate breeding in the breed zone alone can be achieved to provide sufficient total fissile mass to fuel the burn zone. Obviously, a simultaneous objective is to maintain system criticality for a reasonable cycle lifetime. Breeding of U233 in the entire system can be divided into two parts, corresponding to burn zone breeding and breeding in the breed zone.

For the burn zone:

$$b_c = \frac{\text{Rate of fissile production in the burn zone}}{\text{Rate of fissile consumption in the breed and burn zones}}$$

$$= \frac{C_c^{02}}{(A_c^{23} + A_{bz}^{23})}, \qquad (2.10)$$

while for the breed zone:

$$b_{bz} = \frac{\text{Rate of fissile production in the breed zone}}{\text{Rate of fissile consumption in the breed and burn zones}}$$

$$= \frac{C_{bz}^{02}}{(A_c^{23} + A_{bz}^{23})} . \qquad (2.11)$$

Solving Eq. (2.3) for the neutron capture rate in Th233 in the breed zone:

$$C_{bz}^{02} = \bar{\nu}F_{bz}^{23} + \bar{\nu}F_{bz}^{02} - F_{bz}^{23} - F_{bz}^{02} - C_{bz}^{23} - A_{bz}^{P} + L_c$$

$$= (\bar{\nu} - 1)(F_{bz}^{23} + F_{bz}^{02}) - C_{bz}^{23} - A_{bz}^{P} + L_c.$$

Using $F_{bz} = F_{bz}^{23} + F_{bz}^{02}$ and $A_{bz}^{PC} = C_{bz}^{23} + A_{bz}^{P}$,

we can write:

$$b_{bz} = \frac{(\bar{\nu} - 1)F_{bz} + L_c - A_{bz}^{PC}}{(A_c^{23} + A_{bz}^{23})} . \qquad (2.12)$$

Since the thermal power of an operating reactor is essentially constant, then $A_c^{23} + A_{bz}^{23}$, the total rate of fissile consumption in the reactor, can be treated as a fixed value. It can be seen then, that Eq. (2.12) expresses the dependence of the rate of U233 conversion in the breed zone on:

(a) the rate of neutron leakage from the burn region into the breed zone, $[L_c]$,

(b) the rate of neutron production in the breed zone, $[(\bar{\nu} - 1)\ F_{bz}]$ and

(c) the rate of neutron loss in the breed zone, $[A_{bz}^{PC}]$.

Losses due to parasitic absorption and leakage in the breed zone have the effect of cancelling the gains made by the production of neutrons in the zone. It is these factors that must be reduced while simultaneously increasing the rate of neutron production in the breed zone to secure high neutron

availability and improve the rate of U233 conversion.

Combining Eqs. (2.10) and (2.11) yields:

$$b_c + b_{bz} = \frac{C_c^{02} + C_{bz}^{02}}{A_c^{23} + A_{bz}^{23}} \qquad (2.13)$$

which, of course, is the system breeding ratio, expressed in Eq. (2.1). It is clear then, that the rate of breeding in the breed zone is increased only at the expense of breeding in the burn zone. The objective then becomes to optimize the total rate of U233 conversion for the system, under the constraints that criticality be maintained -- which will be made more difficult if the burn zone breeding ratio is small. Since this breed/burn concept is designed for application in commercial power plants, high burnups and good ore utilization are essential. Design parameters that will allow the production of U233 in the required quantities while achieving reasonable fuel element lifetimes and core power densities must, therefore be considered.

2.5 Evaluation of Homogeneous Zone Characteristics

Operation of the breed/burn fuel cycle for the pebble bed reactor system has been defined and its operation described in the preceding sections. To predict more precisely the characteristics of such a system, the parameters involved in breed/burn operation for homogeneous one-zone regions will be evaluated. This analysis should show, for a given composition, how a region would operate

without the coupling effects (leakage) of a zone of different composition on its boundaries.

Neutron economy in any reactor system is a function of the ambient neutron spectrum, axial and radial zoning of compositions, power level and system geometry. The rate of neutron leakage, being dependent on the size of the reactor, decreases with increasing core volume, holding other parameters constant. For this analysis, to provide the most ideal and hence a limiting-case representation of the feasibility of breed/burn operation, an infinite-medium model will be used. Pebble bed reactors, designed in cylindrical geometries, operate at low power densities (typically 5 w/cm^3 [W3]) and hence are inherently large systems. Reactors having thermal power outputs currently competitive commercially ($\sim$3000 MW_{th}) would therefore have core volumes on the order of 600 m^3, and in such cases would have neutron leakage fractions below 5% [W3]. Using an infinite system model for this analysis, therefore, is not an unreasonable approximation.

For layered zoning of the pebble bed system described in Chapter 1, both breed and burn zones will be treated here as uniform, separate regions. In this way, for a given spectrum, the best possible operating characteristics can be determined as there will be no coupling effects between regions which would perturb the spectrum in the vicinity of the boundary. As shown in the previous section, the breeding ratio for the system is simply the sum of the breeding ratios in the breed

and burn zones. Therefore, if one can determine the maximum amount of breeding possible in a homogenized region, this will approximate the system-averaged breeding ratio for a two-zone reactor in the ideal case.

The pebble bed HTGR utilizes injection-molded spherical graphite elements, illustrated in Fig. [2.1], fueled with pyrolytic carbon (PyC) and silicon carbide (SiC) coated ThO_2 and UO_2 microspheres. The balls themselves provide all of the fuel, moderator, structural material and coolant channels (free space between balls) necessary for the reactor. Therefore, in a clean core, the only materials present are those found in the newly fabricated feed balls, in addition to the helium coolant. As a function of the carbon-to-heavy metal atom ratio, the number densities of fertile feed ball materials are given in Table [2.1] (for calculation of number densities, refer to Appendix D).

Variation in the carbon-to-heavy metal atom ratio significantly alters the neutron spectrum in a given region due to the change in moderation. One-group constants for carbon-to-heavy metal atom ratios of 110, 250, 325 and 450 are given in Appendix A, collapsed from the AMPX-generated 4-group cross-sections given in Appendix C (the AMPX system is described in Chapter 3). To illustrate the effect of the carbon-to-heavy metal atom ratio on the neutron spectrum, the spectrum-averaged values for η^{23}, the rate of neutron production per fissile absorption, given by:

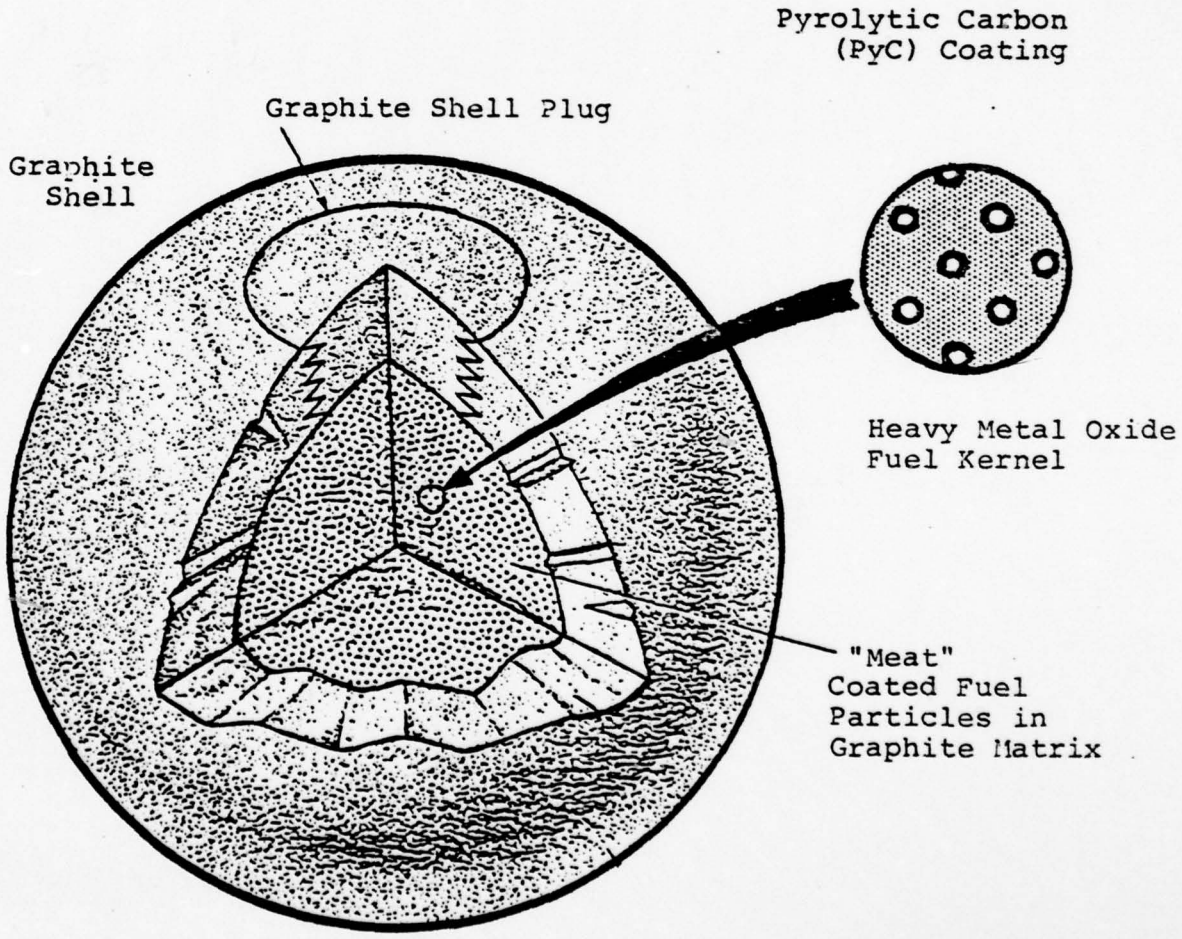

FIGURE 2.1: PEBBLE BED HTGR FUEL ELEMENT

TABLE 2.1

COMPOSITION* OF PEBBLE BED FEED BALLS

	C/HM ATOM RATIO			
NUCLIDE	110	250	325	450
Thorium	2.422E-4	1.041E-4	7.872E-5	5.702E-5
Oxygen	4.844E-4	2.083E-4	1.574E-4	1.140E-4
Carbon	2.666E-2	2.610E-2	2.600E-2	2.591E-2
Silicon	6.644E-4	2.857E-4	2.160E-4	1.564E-4

* Number densities in $b^{-1}cm^{-1}$.

$$\eta^{23} = \frac{\nu\sigma_f^{23}}{\sigma_a^{23}}, \qquad (2.14)$$

the microscopic fission cross-section for Th232, σ_f^{02}, and the microscopic neutron absorption cross-sections for the parasitic absorbers, σ_a^{carbon}, σ_a^{oxygen} and $\sigma_a^{silicon}$, are tabulated in Table [2.2].

It can be seen from these results that the preference for a hardened neutron spectrum is not immediately justified. The values given in Table [2.2] are those used in determining the breeding ratio of the system, expressed by Eq. (2.1). It is immediately apparent that increasing the carbon-to-heavy metal atom ratio from 110 to 450 increases η^{23}. This is opposed to our analysis in that an increase in η^{23} with added moderation would cause an increase in the breeding ratio. However, Table [2.2] also reveals decreases with a harder spectrum in the absorption cross-sections of the parasitic nuclides and an increase in the fission cross-section of Th232. These factors lead to increases in the breeding ratio with spectrum hardening. In fact, while η^{23} decreases $\sim$2% from C/HM = 450 to C/HM = 110, the macroscopic parasitic absorption cross-section ($\Sigma_a^C + \Sigma_a^O + \Sigma_a^{Si}$) decreases $\sim$36%, while the Th232 fission cross-section increases $\sim$72%. So although Eq. (2.1) is dominated by η^{23}, the much larger changes in Th232 fissioning and parasitic absorption could have the dominant effect on the breeding ratio. For these reasons it is important to more carefully consider the effects of the ambient spectrum on breed/burn operation.

TABLE 2.2

SPECTRUM-AVERAGED HOMOGENEOUS ZONE PARAMETERS

	C/HM ATOM RATIO			
PARAMETER	110	250	325	450
η^{23}	2.209	2.240	2.246	2.253
σ_f^{02}	8.097E-3	6.051E-3	5.446E-3	4.718E-3
σ_a^C	3.830E-4	7.095E-4	8.191E-4	9.507E-4
σ_a^O	5.306E-4	4.146E-4	3.811E-4	3.409E-4
σ_a^{Si}	1.358E-2	2.709E-2	3.160E-2	3.702E-2

Cross-sections in barns.

2.6 Variation in Neutron Spectra

The proposal by Fischer et al [F1] for implementation of the breed/burn fuel cycle in a hard spectrum core indicated that, with respect to breeding ratio, the best results would be obtained if the ambient spectrum was hardened as much as possible. In considering the pebble bed HTGR, our first indications verify Fischer's claims for the preference of the hardened spectrum. It has now become necessary to justify this claim more fully if it is to be used as a design objective for thermal reactor versions of the breed/burn concept.

Two criteria for successful operation of the breed/burn cycle have been established: (1) the ability to maintain system criticality, and (2) the ability to breed adequate fissile mass in the breed zone to fuel the burn zone. The second objective is solely a function of the breeding ratio in the breed zone. Maximizing the rate of U233 conversion by increasing the parameters in Eq. (2.1), as described in the previous section, makes it easier to achieve the second goal alone, if adequate exposure time can be provided by artificially satisfying the first objective. However, when the criteria for successful operation must be satisfied simultaneously, it is realized that the optimization of one parameter detracts from the ability to satisfy the other.

By this reasoning, Fischer et al, in achieving both breed/burn operation and the highest breeding ratio possible, might not be able to maintain criticality in their overall system. If this is the case, operating a breed/burn cycle

becomes a futile task. Then, not only must the factors involved in obtaining a high breeding ratio be considered, but also those factors affecting the criticality of the system.

Sheaffer et al [S1] have correlated microscopic cross-sections with the ambient neutron spectrum in fast reactors by defining a spectral index parameter, S, given by:

$$S = \frac{\nu\Sigma_f}{\nu\Sigma_f + \xi\Sigma_{tr}} \quad . \tag{2.15}$$

Physically, S is a measure of the average neutron energy in the core population. Cross-sections, as a function of S, are given by:

$$\sigma = \sigma_1 S^g \tag{2.16}$$

where σ_1 and g are constants appropriate for the indicated nuclide and cross-section (the constants σ_1 and g are tabulated in Appendix B, Table [B.1] for the materials used in this analysis). The correlation expressed by Eq. (2.16) was developed for application to fast reactor systems and has been verified (with very good accuracy) for values of S in the range 0.3 to 1.0 [S1] (corresponding to a wide range of fast reactor spectra, from oxide-fueled LMFBRs to metal-fueled GCFRs). Sheaffer's method can be used to evaluate breed/burn performance in FBR systems.

The ability of the system to breed fissile enrichments suitable to fuel its fast core must be investigated. In any breeding system, if it was assumed that the neutron flux could be maintained artificially, then the system would eventually achieve a conversion ratio of 1.00, at which time the rate of fertile neutron capture would exactly equal the rate of fissile destruction by neutron absorption. Thus, the system would maintain an asymptotic fissile enrichment limit which would be the maximum possible enrichment compatible with the ambient spectrum.

If the fertile capture rate is equal to the fissile absorption rate:

$$N\sigma_c \phi\Big|_{\text{fertile}} = N\sigma_a \phi\Big|_{\text{fissile}} . \tag{2.17}$$

Neglecting all heavy metals except the principal fertile and fissile species, the fissile enrichment, ε, can be defined as:

$$\varepsilon = \frac{N^{\text{fissile}}}{N^{\text{fissile}} + N^{\text{fertile}}} . \tag{2.18}$$

Combining Eqs. (2.17) and (2.18), an expression for the asymptotic fissile enrichment, ε_{ASY}, as a function of the cross-section ratio $\sigma_c{}^{\text{fertile}}/\sigma_a{}^{\text{fissile}}$ is:

$$\varepsilon_{ASY} = \frac{\sigma_c{}^{\text{fertile}}/\sigma_a{}^{\text{fissile}}}{1 + \left(\sigma_c{}^{\text{fertile}}/\sigma_a{}^{\text{fissile}}\right)} . \tag{2.19}$$

For a plutonium-239/uranium-238 system, Eq. (2.19) becomes:

$$\varepsilon_{ASY} = \frac{\sigma_c^{28}/\sigma_a^{49}}{1 + (\sigma_c^{28}/\sigma_a^{49})} \qquad (2.20)$$

and similarly for a U233/Th system:

$$\varepsilon_{ASY} = \frac{\sigma_c^{02}/\sigma_a^{23}}{1 + (\sigma_c^{02}/\sigma_z^{23})} \quad . \qquad (2.21)$$

With these approximations the practical end-of-life (EOL) fissile enrichment, ε_{EOL}, obtainable with high fuel burnup in a breed/burn system, can be roughly estimated.

Consider the following conceptual picture of breed/burn operation: pairs of physically identical fuel elements exist -- one in the breed zone and the other in the burn zone. The fissile enrichment in the breed zone at end-of-cycle must equal the fissile enrichment in the burn zone at the beginning-of-cycle if a "stand-alone" breed/burn cycle is to be feasible. For every fission in the burn zone element roughly one excess neutron is produced which can be used to produce fissile material in the breed zone element. Since both elements have very nearly equal heavy metal contents, the maximum percent fissile enrichment in the breed element is equal to the percent burnup in the burn zone. That is, for breed/burn operation (in %):

$$\varepsilon_{BOL_C} = \varepsilon_{EOL_{bz}} \simeq \frac{B_c[\text{MWD/MTHM}]}{10^4} \quad . \qquad (2.22)$$

The potential of different reactor types is as follows:

LWR: $\varepsilon_{BOL} \sim 3\%$; $B_{EOL} \sim 30{,}000$ MWD/MTHM = 3%

HTGR: $\varepsilon_{BOL} \sim 9\%$; $B_{EOL} \sim 120{,}000$ MWD/MTHM = 12%

LMFBR or GCFR: $\varepsilon_{BOL} \sim 15\%$; $B_{EOL} \sim 100{,}000$ MWD/MTHM = 10%.

This information is illustrated in Fig. [2.2], where it can be seen that the potentially feasible breed/burn systems would be those operating below the line, whereas those above the line would not be feasible. The circumstances indicated in Fig. [2.2] are, in fact, a large part of the motivation for investigating the HTGR as a breed/burn reactor in the present study.

Since the cross-sections of the fertile and fissile species vary with the ambient spectrum, Eq. (2.19) can be used to estimate the attainable asymptotic enrichment limit for any given system. This limit indicates for a reactor operating with the breed/burn fuel cycle, whether to harden or soften the ambient spectrum. A high asymptotic enrichment would imply that relatively short burnups would be required to achieve a desired enrichment value, whereas a low asymptotic limit would mean that if a beginning-of-life enrichment was required near the asymptotic value, then very high burnups would be essential to achieve that limit. This argument adds preference to those spectra whose asymptotic enrichment limits are as high as possible.

From Eq. (2.16), cross-sections can be determined for any given fast reactor spectrum (composition). For this analysis,

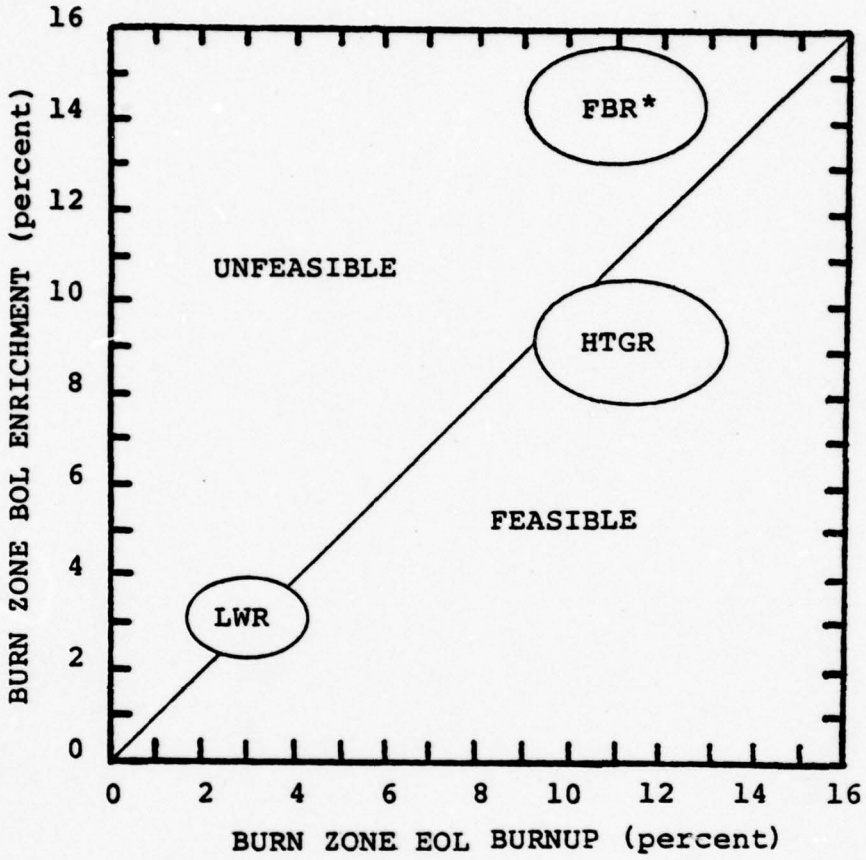

FIGURE 2.2: SCHEMATIC DIAGRAM SHOWING POTENTIAL FEASIBILITY OF BREED/BURN SYSTEMS

*Typical FBR with current burnup limits.

the following approximation is used:

$$\sigma_c^{\text{fertile}} \simeq \sigma_a^{\text{fertile}} \tag{2.23}$$

which, from Eq. (2.19), yields:

$$\varepsilon_{ASY} \simeq \frac{\sigma_a^{\text{fertile}}/\sigma_a^{\text{fissile}}}{1 + (\sigma_a^{\text{fertile}}/\sigma_a^{\text{fissile}})} \cdot \tag{2.24}$$

This approximation overestimates the value of ε_{ASY} and therefore yields a conservative upper limit for the asymptotic enrichment. Listed in Table [2.3] are values for ε_{ASY}, using Eq. (2.24), calculated for spectra varying from S = 0.3 to S = 1.0. Also tabulated are values for fissile η, given by:

$$\eta = \frac{\nu\sigma_f}{\sigma_a} \tag{2.25}$$

for the indicated fissile species. It is clear from the data in Table [2.3] that values for fissile η for both the Pu239/U and U233/Th systems increase with spectrum hardening, justifying the claim of Fischer et al that harder spectra will yield better breeding potential. This alone, however, does not justify the preference of the harder spectra for the breed/burn concept. In fact, because a balance must exist between fissile breeding and system criticality, the asymptotic fissile enrichments, illustrated in Fig. [2.3], indicate that the softer fast reactor spectra would be preferable. Operation

TABLE 2.3

ASYMPTOTIC ENRICHMENTS AND FISSILE η VALUES

FOR FAST SPECTRA*

S	ε^{23}_{ASY}	η^{23}	ε^{49}_{ASY}	η^{49}
0.3	0.1388	2.175	0.1480	2.308
0.4	0.1210	2.224	0.1368	2.415
0.5	0.1085	2.264	0.1286	2.502
0.6	0.09918	2.296	0.1223	2.574
0.7	0.09190	2.324	0.1172	2.638
0.8	0.08591	2.348	0.1128	2.694
0.9	0.08097	2.370	0.1091	2.744
1.0	0.07675	2.390	0.1059	2.790

*From Sheaffer et al [S1] correlation: cross-sections are listed in Table [B.2].

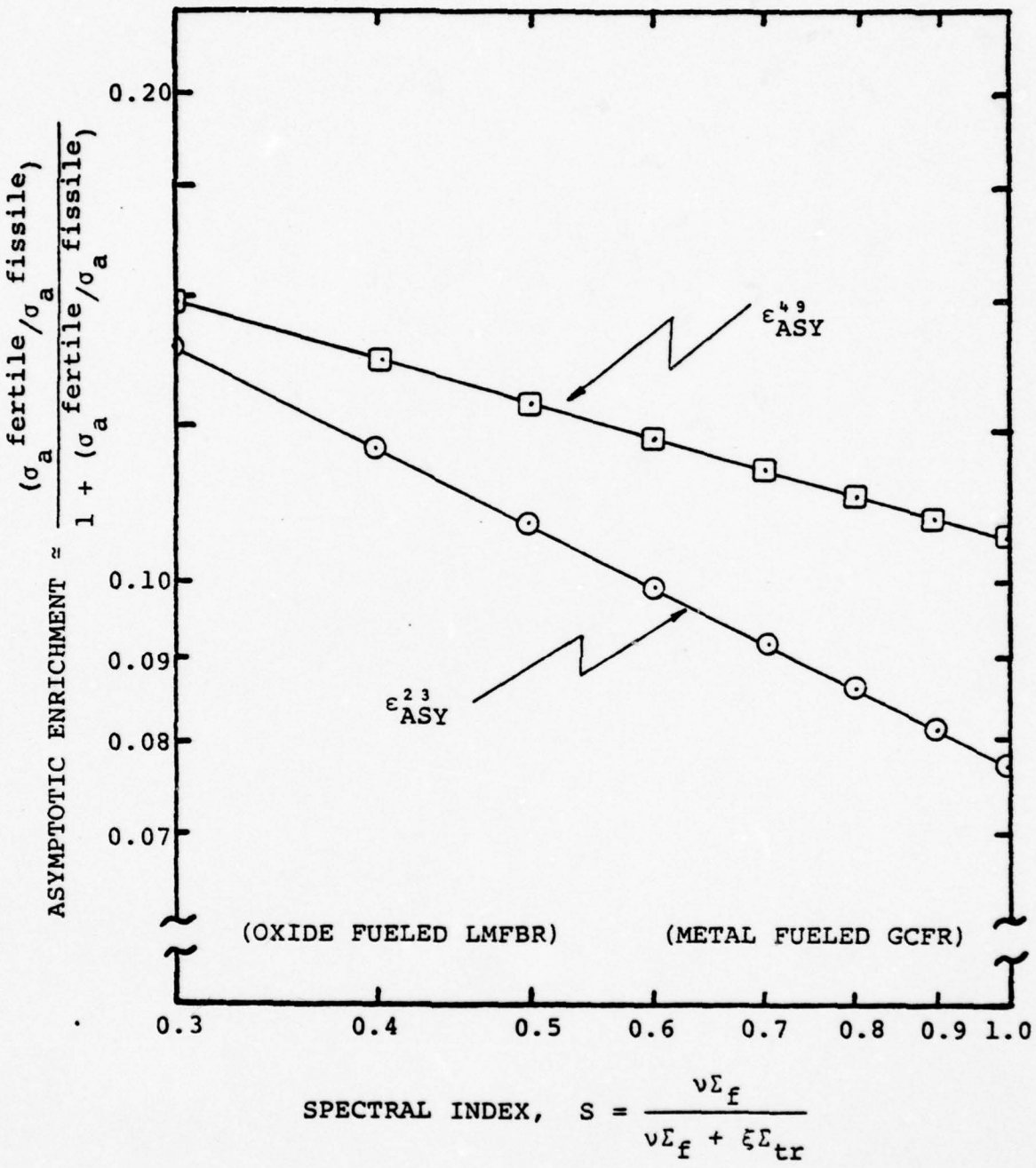

FIGURE 2.3: ASYMPTOTIC FISSILE ENRICHMENT LIMITS FOR U233 AND Pu239 SPECTRA USING SHEAFFER'S CORRELATION [S1]

can, in this case, achieve much higher fissile enrichments for a given burnup than can a system operating in a much harder spectrum. For a Pu239/U fueled system, the softer (S = 0.3) spectrum burnup (assuming a linear relation between burn zone and breed zone enrichments) would require an exposure time ∿ 32% less than the hard (S = 1.0) spectrum, while for the U233/Th system the same change in spectrum would reduce the exposure time by ∿ 48%.

These cases have indicated, contrary to the proposal of Fischer et al, that a softer spectrum is preferred for breed/burn operation in a fast reactor. A similar analysis can be performed to determine the more favorable operating conditions for the thermal/epithermal HTGR. Because Sheaffer's correlations were developed for fast reactor calculations they do not account for the high degree of resonance shielding in the fertile species for highly epithermal applications. Hence, the model is invalid for values of S < 0.3; the lowest values verified.

A similar spectral index can be derived for application in the U233/Th HTGR cases. In the expression for the resonance escape probability from classical continuous slowing theory, p, given by:

$$p = \exp\left[- \int_E \frac{\Sigma_a \, dE'}{E' \, \xi(\Sigma_a + \Sigma_s)} \right] , \qquad (2.26)$$

an effective Σ_a can be used to account for leakage by adding a "leakage cross-section":

$$\Sigma_a \rightarrow \Sigma_a + DB^2. \tag{2.27}$$

Then, accounting for criticality by applying the neutron balance:

$$\Sigma_a + DB^2 = \nu\Sigma_f \quad , \tag{2.28}$$

one gets:

$$p \approx \exp\left[- \int_E \frac{\nu\Sigma_f}{\xi(\nu\Sigma_f + \Sigma_s)} \cdot \frac{dE'}{E'} \right] . \tag{2.29}$$

Since $\Sigma_s \approx \Sigma_{tr}$, and recognizing that in the thermal / epithermal region $\nu\Sigma_f \ll \Sigma_{tr}$, a spectral index, S' can be defined by:

$$S' = \frac{\nu\Sigma_f}{\xi\Sigma_{tr}} . \tag{2.30}$$

Using this definition, the index can be redefined as:

$$S = \frac{S'}{1 + S'} \quad , \tag{2.31}$$

which yields the same form used by Sheaffer et al [S1], given by:

$$S = \frac{\nu\Sigma_f}{\nu\Sigma_f + \xi\Sigma_{tr}} . \tag{2.15}$$

From the computations to be discussed in Chapter 3, values used to calculate S were found for the pebble bed HTGR compositions used in the analysis of Section [2.5]. Table [2.4] lists values for ε_{ASY}, given by Eq. (2.21), with corresponding values of S as a function of the carbon-to-heavy metal atom ratio. In Fig. [2.4] the asymptotic enrichments, $\varepsilon_{ASY}{}^{23}$, are plotted versus the spectral index for both the U233/Th fast reactor cases and the pebble bed systems. It can be seen that in the thermal/epithermal region, spectral hardening is advantageous in increasing the asymptotic enrichment limit.

As shown previously, although the harder HTGR spectra lead to increasing values of fissile η, decreasing parasitic absorption rates and improved fertile fission rates combined with the benefit of higher asymptotic enrichment limits indicate a strong preference for the use of a hardened spectrum for successful thermal/epithermal breed/burn operation. This conclusion is contrary to that of fast reactors, where the softer spectra are preferred. The indication here is that an optimum breed zone ambient spectrum may be attainable in the regions between those considered in this analysis. The apparent maximum value for ε_{ASY}, shown in Fig. [2.4], clearly indicates this possibility. Hence, in order to maximize the effectiveness of the breed/burn concept it would be advisable to consider systems operating with neutron spectra in the area of maximum ε_{ASY} between a "soft" FBR and a "hard" HTGR.

TABLE 2.4

SPECTRAL INDEX AND ASYMPTOTIC ENRICHMENT LIMITS FOR THE U233/Th PEBBLE BED HTGR

	C/HM ATOM RATIO			
PARAMETER	110	250	325	450
S	0.0724	0.0583	0.0518	0.0438
ε_{ASY}	0.03526	0.02686	0.02497	0.02302

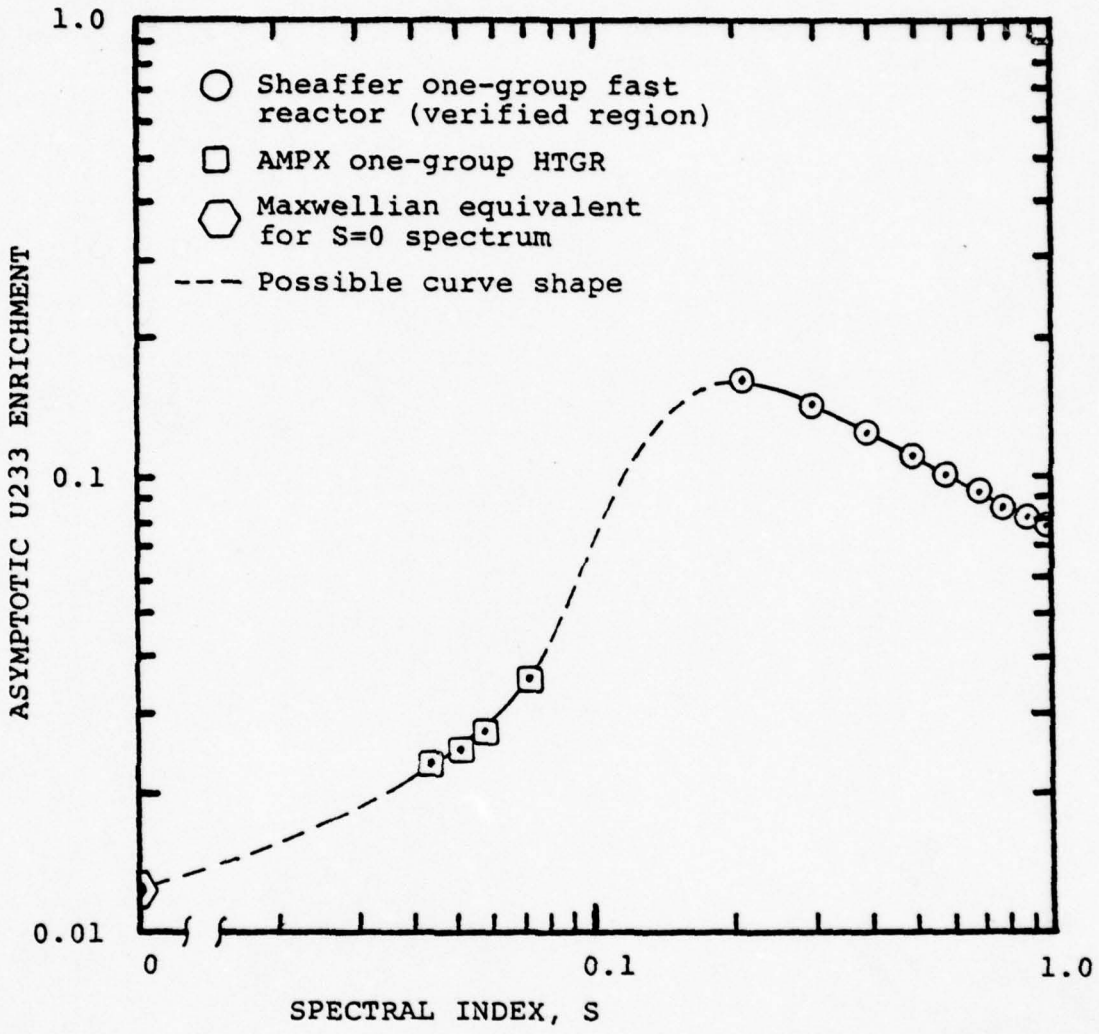

FIGURE 2.4: ASYMPTOTIC ENRICHMENTS FOR U233/Th SYSTEMS

2.7 System Criticality

In the previous section it was shown that in using a breed/burn fuel cycle in the pebble bed HTGR, it is advantageous to harden the breed zone neutron spectrum in order to increase the rate of fissile U233 production. The required burn zone burnup for each element necessary to achieve any given breed zone fissile enrichment can therefore be shortened, and hence, the number of passes through the breed zone required of each fuel ball can be minimized.

The fissile enrichments attainable for each composition can be approximated using Eq. (2.21), again utilizing the one-group constants given in Appendix A. As a function of the carbon-to-heavy metal atom ratio, these enrichments are listed in Table [2.5] along with the cross-section ratio, $\sigma_c{}^{02}/\sigma_a{}^{23}$. Using these values to approximate the beginning-of-life fissile enrichment for a clean core, the system criticality at the beginning of each cycle can be estimated. Applying a one-group model, the infinite-medium multiplication factor, k_∞ , can be estimated at the beginning-of-life as:

$$k_{\infty_{BOL}} \simeq \frac{\bar{\nu}\Sigma_f}{\Sigma_a} \tag{2.31}$$

and the BOL excess reactivity, ρ_{BOL} , is:

$$\rho_{BOL} = \frac{k_{\infty_{BOL}} - 1}{k_{\infty_{BOL}}} \quad . \tag{2.32}$$

TABLE 2.5

ASYMPTOTIC FISSILE ENRICHMENT LIMITS

	C/HM ATOM RATIO			
PARAMETER	110	250	325	450
$\frac{\sigma_c^{02}}{\sigma_a^{23}}$	0.03655	0.02760	0.02561	0.02357
ε_{ASY}(%)	3.526	2.686	2.497	2.302

Values for $k_{\infty_{BOL}}$ and ρ_{BOL} are given in Table [2.6].

It can be seen that in all cases, $k_{\infty_{BOL}} > 1.00$, indicating criticality at the start of the cycle. Using the amount of U233 bred, for example, in the region of C/HM = 110 to fuel the regions where C/HM = 250 or higher would yield an even greater value for $k_{\infty_{BOL}}$. For the four compositions considered, the values of $k_{\infty_{BOL}}$ obtained for various combinations of breed and burn zone carbon-to-heavy metal atom ratios are shown in Table [2.7]. The highest $k_{\infty_{BOL}}$ obtained is for that of a burn zone with C/HM = 450 being fueled by a breed zone where C/HM = 110. This combination has the softest burn zone spectrum operating with the hardest spectrum (and hence, highest ε_{ASY}) breed zone of those compositions evaluated.

Careful analysis is required in these cases to insure that a given breed zone would produce not only adequate fissile enrichment, but also sufficient total fissile mass to fuel the burn zone. From this analysis, the first order estimate leads to the conclusion that it is possible to breed enough fissile material in a breed zone, given adequate exposure time, to fuel and obtain criticality in a pebble bed breed/burn system. The amount of BOL excess reactivity is quite small, however, which indicates that it may not be possible to maintain criticality long enough to breed fissile enrichments near the asymptotic limits. One can adapt to this situation to some extent by using rapid fuel flow through the core, approaching continuous refueling in the limiting case, but of course this increases the complexity of operation.

TABLE 2.6

BEGINNING-OF-LIFE INFINITE-MEDIUM

MULTIPLICATION FACTORS

	C/HM ATOM RATIO (both zones)			
PARAMETER	110	250	325	450
$\bar{\nu}\Sigma_f$	1.435E-3	7.782E-4	6.163E-4	4.662E-4
Σ_a	1.293E-3	7.110E-4	5.695E-4	4.392E-4
$k_{\infty BOL}$	1.110	1.095	1.082	1.062
ρ_{BOL} (%)	9.91	8.64	7.60	5.78

TABLE 2.7

k_∞ FOR VARIOUS ZONE COMBINATIONS*

		BURN ZONE C/HM ATOM RATIO			
		110	250	325	450
BREED ZONE C/HM ATOM RATIO	110	1.110	1.256	1.286	1.313
	250	0.9515	1.095	1.125	1.152
	325	0.9103	1.052	1.082	1.109
	450	0.8654	1.005	1.035	1.062

* k_∞ in burn zone using asymptotic enrichments achievable in breed zone

The analysis of Section [2.6] can be refined further to consider some of the specific features of the breed/burn cycle. In the expression for k_∞ , given by Eq. (2.31), a "leakage cross-section" can be added to the absorption cross-section, so that:

$$k = \frac{\nu\Sigma_f}{\Sigma_a + \Sigma_L} \tag{2.33}$$

where, for example, one can use $\Sigma_L = DB^2$. The criterion for criticality, that $k \geq 1.00$, yields the necessity that:

$$k_\infty \geq 1 + \frac{\Sigma_L}{\Sigma_a} \tag{2.34}$$

or,

$$k_\infty - 1 \geq \frac{\Sigma_a{}^{23}}{\Sigma_a{}^{23} + \Sigma_a{}^{02} + \Sigma_a{}^{P}} \tag{2.35}$$

where $\Sigma_a{}^{P}$ refers to neutron absorption by the parasitic absorbers.

Therefore, Eq. (2.35) can be used to find that:

$$k_\infty - 1 \geq \frac{1}{1 + b_c + (\Sigma_f{}^{02}/\Sigma_a{}^{23}) + (\Sigma_a{}^{P}/\Sigma_a{}^{23})} \tag{2.36}$$

where b_c is the breeding ratio in the burn zone, approximated by:

$$b_c = \frac{\Sigma_c{}^{02}}{\Sigma_a{}^{23}} \ . \tag{2.37}$$

In Eq. (2.37), both $\Sigma_f^{02}/\Sigma_a^{23}$ and $\Sigma_a^{P}/\Sigma_a^{23}$ are small. The criticality limit becomes:

$$k_\infty \geq 1 + \frac{1}{1 + b_c} \quad . \tag{2.38}$$

In the burn zone, however, the maximum value of b_c is attained under EOL asymptotic conditions. In this case, $b_c = 1.0$, which therefore defines a lower limit for k_∞ of:

$$k_\infty \geq 1.5 \ , \tag{2.39}$$

which is now a third criteria for successful system operation. Thus, k_∞ for the burn zone must exceed 1.5 for a breed/burn cycle to be able to operate independent of additional external fissile sources.

Since the greatest value obtained for $k_{\infty_{BOL}}$, given in Table [2.7], was $k_\infty \sim 1.3$, we must conclude that for the pebble bed HTGR, stand-alone breed/burn operation does not appear possible.

2.8 Summary

In this chapter the parameters affecting successful breed/burn operation in the pebble bed HTGR have been examined. While preliminary evaluation suggested that spectral hardening would detract from system performance due to the decreasing values of fissile η, closer examination revealed that while η decreases slightly, parasitic absorption decreases significantly while

the fertile fission rate also increases substantially. In addition, harder spectra yield higher asymptotic enrichment values, thus making it easier to achieve acceptable fissile enrichments in the breed zone with reasonable burnups in the burn zone. The results also showed that highly thermalized systems are best for the burn zone because of their high k_∞ at a given load enrichment and low asymptotic (hence discharge) fissile enrichment. Of all reactors of current interest, it was found that the HTGR had the most favorable ratio of discharge burnup ro reload enrichment.

These observations, with respect to spectral hardening, were found to apply for thermal and epithermal systems only. In fact, for fast reactors it was found that the breed function of breed/burn cycles would be best carried out in softer spectra, such as those found in oxide-fueled LMFBRs -- or, indeed, even softer.

In examining system criticality, although it was found that a breed zone in a pebble bed reactor could fuel and achieve criticality ($k_\infty = 1.0$) in an infinite burn zone, the high BOL excess reactivity ($k_\infty \geq 1.5$) necessary for finite coupled zone (high burn and breed zone leakage) system operation could apparently not be achieved. Hence, operating such a system in the pebble bed HTGR would require some degree of fissile makeup to operate for any sustained period; either that or a substantially harder breed zone spectrum (yielding higher asymptotic enrichment and hence larger k_∞ in the burn

zone). An even higher carbon-to-heavy metal atom ratio in the burn zone could also be contemplated.

III. COMPUTATIONAL METHODS

3.1 Introduction

The analysis in the previous chapter led to the conclusion that in a pebble bed HTGR, it would probably not be possible to sustain a stand-alone breed/burn system. However, the one-group calculations performed could only indicate the gross features of system operation and were limited to either the beginning-of-life or the asymptotic limit of ultra-high burnup. The effects of fission product buildup, U235 and Pa233 production, Th232 depletion, fast fission, power density and group-wise changes in flux and cross-sections, all as functions of burnup, were neglected. When fully evaluated, the sum of the above effects can significantly alter the reactor performance characteristics as a function of time, which therefore necessitates a more precise evaluation.

Calculation of the performance characteristics of the proposed breed/burn system, using state-of-the-art computer programs, is described in this chapter. The system model, cross-section generation, nuclear data input, codes used and problem descriptions are described.

3.2 System Model

In the breed/burn fuel cycle, it is necessary for the reactor system to operate under "breakeven" breeding conditions. That is, as a minimum, one fissile atom must be produced in the breed zone for every one destroyed in the burn

zone. A first approximation can be used to evaluate this ability (i.e., by considering a homogeneous system) as was done in Chapter 2. The two-zone layered system, described in Chapter 1, will operate with a strong neutronic coupling between zones. The burn zone fission rate, and hence, power density, will be higher than that in the breed zone. Also, the total neutron flux in the burn zone should be higher, whereas groupwise flux will be shifted towards the faster groups in the breed zone, assuming that the carbon-to-heavy metal atom ratio in the breed zone is less than that of the burn zone.

A conservative overestimation of the performance of the system can be found, therefore, by homogenizing the two zones into a single region. If the conditions required for successful breed/burn operation can be met in the homogeneous region, then a more careful analysis is required to determine, when the reactor is modeled in a heterogeneous, axially-layered configuration, if satisfactory performance is still achieved.

In analyzing the heterogeneous two-zone system, the requirement for the breeding of adequate total mass in the breed zone to fuel the burn zone dictates size limitations on the two zones, contingent upon the number of passes through each zone required to achieve design burnup limits. That is, given the compositions of each zone, in a period of one cycle, the total fissile mass being bred in the breed and burn zones must equal the total mass destroyed in the burn zone for net breeding; for breed/burn operation the breed zone alone must provide the

burn zone fissile deficit. Therefore, calculations must be performed iterating between size options for the two zones. If the reactor is assumed to be infinite radially, then the calculations can be performed using an infinite slab model varying only the compositions and axial thicknesses of each zone.

The first analysis to be performed, however, utilizes a homogeneous zone as previously described. Unity albedo boundary conditions are used for all three dimensions, thus effecting an infinite reactor calculation. Again, an infinite slab treatment is appropriate. As will be described in Section [3.4], compositions (carbon-to-heavy metal atom ratios and fissile enrichments) will be varied to determine system characteristics.

3.3 Computer Codes

Analysis of the pebble bed HTGR breed/burn fuel cycle in the homogeneous system model described in the previous section required precise definition of nuclear data parameters for input into a code that would treat the one-dimensional diffusion-depletion problem accurately. In this section the computer codes used for this application and their respective input parameters are described.

3.3.1 PDQ-7

The PDQ-7 code [C1] was used in the present work for the calculation of the operating characteristics of the breed/burn system model. PDQ-7 can solve the diffusion and depletion

equations in up to three dimensions in rectangular, cylindrical, spherical or hexagonal geometry for up to five energy groups. Depletion calculations and management of the neutron cross-section data are handled by the HARMONY system [B2], which provides a flexible representation of the time-dependent depletion equations for any nuclide chain.

The PDQ-7 code solves the diffusion equation by discretizing the energy variable and finite differencing (central) the equation in space. For this application, only one-dimensional problems were treated, which the code solves by Gaussian elimination.

For all calculations, PDQ-7 requires that input parameters define the system geometry and energy groups with respective chi (fission neutron) spectra, as well as the complete representation of nuclide chains, decay constants, initial nuclide number densities and microscopic neutron cross-section data.

The problems described in Section [3.4] were all solved using four energy groups in an infinite slab system, with depletion parameters calculated for a static core arrangement, from the beginning-of-life to an end-of-cycle fuel burnup of 120,000 MWD/MTHM.

The depletion chain treatment followed 46 nuclides, for which the respective nuclide chains are detailed in Appendix [D.5]. Initial nuclide number densitites were calculated as a function of the carbon-to-heavy metal atom ratio and the beginning-of-life fissile enrichment, as described in Appendix

[D.3]. Beginning-of-life heavy metal number densities are given in Table [D.4] as a function of fissile enrichment, and all other initial concentrations are listed in Table [D.5].

Exposure times (in hours) used for the depletion increments were calculated for burnup intervals as detailed in Appendix [D.4]. All problems were treated for burnups to 120,000 MWD/MTHM.

Cross-section input for PDQ-7 was provided by calculations using the AMPX Code System [G2], as described in Section [3.3.2].

3.3.2 AMPX

The AMPX Code [G2] is a modular system (NITAWL and XSDRNPM codes) which evaluates 123 group cross-section data with resonance parameters to generate coupled multi-group neutron cross-sections. The reference ball design used for number density calculations is described in Appendix [D.3]. The reference cell-averaged ambient temperature was 900°C [W3].

AMPX calculations generated all cross-section data used in the present work, treating the 46 nuclides listed in Table [D.1]. For the depletion chains detailed in Table [D.7], appropriate nuclide decay constants, fission product yields, energy releases per fission, groupwise χ spectra and the resulting relative groupwise fluxes are given in Tables [D.8], [D.9], [D.10], [D.11] and [D.12], respectively, as functions of the carbon-to-heavy metal atom ratio. Energy group parameters are given in Table [D.13].

The four-group cross-section data generated by AMPX and used in PDQ-7 calculations is listed in Appendix C.

3.4 Computational Methods for Evaluation of Homogeneous Zone Parameters

As discussed in Chapter 2, evaluation of breed/burn operation in a homogeneous one-zone system requires computation of system criticality and fissile enrichment as a function of burnup. The performance characteristics of an arbitrary region can be bracketed through the evaluation of several reference examples.

Using the system model described in Section [3.2], the carbon-to-heavy metal atom ratio and the beginning-of-cycle fissile enrichments for the system were varied in a series of eigenvalue/depletion calculations. From the calculated information, the parameters necessary for an evaluation of the breed/burn system were obtained.

For a given burn zone composition, varying the initial fissile enrichment will yield a series of similar curves when k_∞ is plotted versus the fuel burnup, as illustrated in Fig. [3.1a]. Achieving a value of $k_\infty > 1.0$ will satisfy the first operating criterion: achieving system criticality. Then, a linear burnup model of the form:

$$B_{EOL_c} = a(\varepsilon_{BOL_c} - b)\ \frac{2n}{n+1} \qquad (3.1)$$

can be applied to the zone, where a and b are constants and n is the number of batch fuel loadings. For a continuously-fueled system, whose performance can be approached in a pebble bed reactor, $n \to \infty$ so that:

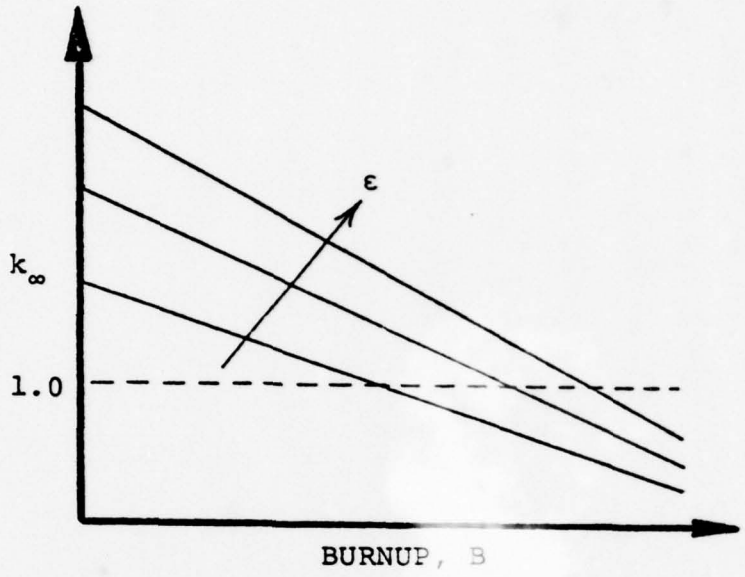

FIGURE 3.1a: REPRESENTATIVE VARIATION OF k_∞ WITH BURNUP (linear)

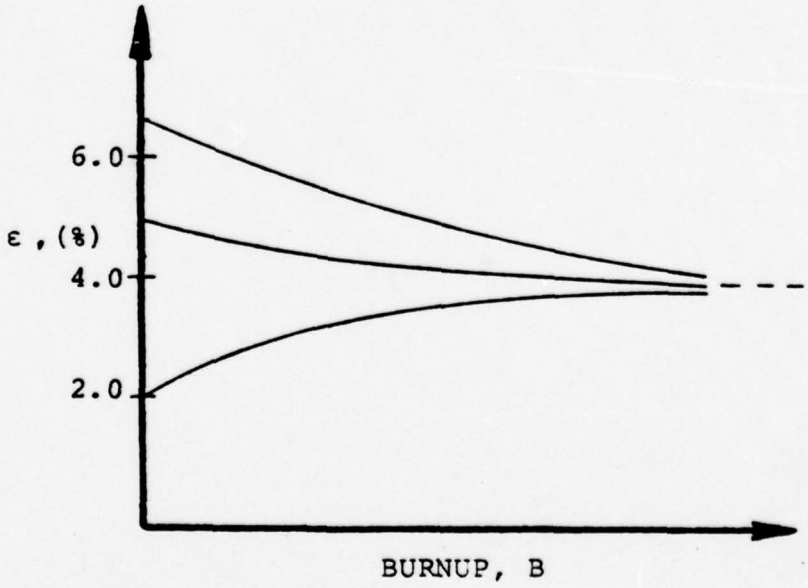

FIGURE 3.1b: REPRESENTATIVE VARIATION OF ENRICHMENT WITH BURNUP

$$B_{EOL_c} = 2a(\varepsilon_{BOL_c} - b) \quad . \tag{3.2}$$

The constants a and b can be calculated if batch depletion calculations are performed for two different initial enrichments; therefore, to achieve any design-limited end-of-life burnup for continuous burn zone refueling, Eq. (3.2) can be used to find the required ε_{BOL_c}. Hence, for a burn zone loaded with an initial fissile enrichment of ε_{ASY}, bred in a breed zone, the maximum obtainable end-of-cycle burnup can be calculated using Eq. (3.1) for either a batch load or for continuous refueling.

In its fullest development, the breed/burn cycle uses the heavy metal discharged from the breed zone at an enrichment ε_{ASY} as the fuel loaded into the burn zone at beginning-of-cycle, again at an enrichment ε_{ASY}. Therefore, the value of ε_{ASY} charged to the burn zone must be high enough to allow the next cycle to achieve an equivalent breed zone discharge enrichment. Several successive passes through the breed zone may be required for a given fuel ball to achieve a desired enrichment, but as a very rough approximation, assuming one fissile nucleus is bred (and preserved) in the breed zone for every fissile nucleus burned in the burn zone:

$$B_{EOL_{bz}}\ (\%) \geq \varepsilon_{BOL_c}\ (\%), \text{ or} \tag{3.3}$$

$$B_{EOL_{bz}}\ (\%) \geq \varepsilon_{ASY}\ (\%). \tag{3.4}$$

In evaluating this criterion, breed zone enrichments at breed zone end-of-cycle will be taken to be equal to the asymptotic values given in Table [2.5] as a function of the ambient spectrum.

Burn zone enrichments can be treated more explicitly. Because the PDQ-7 analysis takes into account the effects of U235 and Pa233 production, fission product buildup, Th232 depletion and parasitic absorption, all of which were neglected in the simplistic analysis of Chapter 2, the actual system operating characteristics may differ slightly from those predicted previously. Concentrations of all nuclides appearing in the depletion chains are calculated by PDQ-7 at each time increment. Using Eq. (2.18), the enrichment of a given burn zone as a function of burnup can be calculated. Operating at a constant power density to high fuel burnups will result in fissile enrichments being reduced to the spectrum-averaged equilibrium limits at end-of-cycle, as illustrated in Fig. [3.1b]. If the ambient spectrum in the breed zone is much harder than that in the burn zone, the equilibrium enrichment in the burn zone will be significantly less than the asymptotic limit achieved in the breed zone. Burning fuel elements in the burn zone to high burnups and hence to low fissile enrichments at end-of-life (for high carbon-to-heavy metal atom ratio compositions) is in keeping with the nonproliferation objectives of the breed/burn system. Very low end-of-life fissile enrichments thus allow spent fuel elements to be

discharged directly to waste disposal, in accordance with the system schematic in Fig. [1.1].

Zone compositions were evaluated using PDQ-7 in batch load depletion calculations, so the maximum burn zone burnups (achieved using continuous refueling) are twice that obtained by applying Eq. (3.1) (setting n = 1) to batch zone calculations.

In summary, the second criterion for successful operation, that adequate fissile material be bred in the breed zone to fuel the burn zone, is accomplished only if the breed zone end-of-life enrichment (here estimated as ε_{ASY}) is:

$$\varepsilon_{EOL_{bz}}\ (\%) \simeq \varepsilon_{ASY_{bz}}\ (\%) \geq B_{EOL_c}\ (\%) \quad . \tag{3.5}$$

This requirement, combined with the requirement for system criticality are necessary (but not sufficient) conditions for successful breed/burn operation. The third assessment criterion, that of zone leakage, must be examined.

Equation (2.39) defines the requirement that $k_\infty \geq 1.5$. This value applies only when the burn zone breeding ratio, b_c, is maximized, which occurs under end-of-life asymptotic conditions, or when $b_c = 1.0$. Since this condition (Eq. (2.39)) defines a minimum value for k_∞, only those combinations of breed and burn zone compositions for which the first two criteria for operation have been met and for which $k_{\infty_{BOL}} \geq 1.5$ will be considered as feasible possibilities.

Should all three criteria be met by any given candidate system, then a more detailed analysis examining system geometry in a two-zone heterogeneous configuration will be required.

For this analysis, PDQ-7 depletion calculations were carried out for beginning-of-life enrichments of 2.0%, 4.5% and 7.0% U233, for zone carbon-to-heavy metal atom ratios of 110, 250, 325 and 450. The analyses of k_∞ and ε_{ASY} as a function of the zone burnup, previously described, were performed to evaluate the operating characteristics of the breed/burn system. Depletion calculations were run for all compositions through fuel burnups of 120,000 MWD/MTHM. A summary of these results is given in Chapter 4.

3.5 Summary

Procedures used to analyze the characteristics of operating breed/burn fuel cycles in pebble bed HTGRs have been presented. A series of PDQ-7 eigenvalue/depletion runs were carried out on homogeneous one-zone systems to evaluate system performance, varying the parameters of the carbon-to-heavy metal atom ratio (composition) and the beginning-of-life fissile enrichment.

Successful system operation will be achieved only if three necessary (but not sufficient) conditions are met:

(a) achieving system criticality, $k_\infty \geq 1.0$,

(b) achieving a fissile production rate such that

$$\varepsilon_{ASY_{bz}}\ (\%) \geq B_{EOL_c}\ (\%),$$

and (c) accounting for zone leakage by providing adequate excess reactivity, $k_\infty \geq 1.5$.

Satisfying all three of these objectives simultaneously will allow the two-zone layered pebble bed system to operate on a stand-alone breed/burn fuel cycle (within the limits of the conservative approximations used in this analysis).

IV. BREED/BURN COMPUTATIONAL RESULTS

4.1 Introduction

The PDQ-7 runs made for analysis of breed/burn feasibility were detailed in Chapter 3. The results, to be described in this chapter, will characterize the operating parameters, consistent with core compositions and power densities as a function of burnup history necessary to assess the capability of the pebble bed HTGR system to achieve breed/burn operation. The analysis specifically addresses the three necessary (but not sufficient) criteria defined for successful breed/burn operation:

(a) system criticality, $k_\infty \geq 1.0$,

(b) rate of fissile production, B_{EOL_c} (%) $\leq \varepsilon_{ASY_{bz}}$ (%)

and (c) accounting for zone leakage, $k_\infty \geq 1.5$.

4.2 Variation of k_∞ with Fuel Burnup

Three depletion cases were treated for each homogeneous zone composition (carbon-to-heavy metal atom ratios of 110, 250, 325 and 450), corresponding to fissile enrichments at the beginning-of-cycle of 2.0%, 4.5% and 7.0%. For each case, the depletion time increments corresponded to fuel burnups of 2000, 6000, 30,000, 60,000 90,000 and 120,000 MWD/MTHM. Current materials constraints limit cycle burnups to an upper value of roughly 120,000 MWD/MTHM [T1].

For the twelve cases considered, the values calculated for k_∞ at the start of each depletion iteration are listed in Appendix B, Table [B.3]. As illustrated in Figs. [4.1-4.4], it can be seen that for all compositions, as expected, k_∞ decreases with fuel burnup, and for each composition, higher initial fissile enrichment results in higher values of k_∞ . A step decrease in k_∞ is noted during the first time increment due to the rapid saturation of xenon-135. All cases exhibited a nearly linear relation between k_∞ and burnup beyond 6000 MWD/MTHM.

At the beginning of life all compositions achieved criticality, with the exception of the case for which C/HM = 110 and ε_{BOL} = 2.0%. However, all cases for which ε_{BOL} = 2.0% were subcritical at a burnup of only 2000 MWD/MTHM and remained so for the duration of the cycle. In these cases, a rise in k_∞ was observed at mid-cycle, apparently due to an increase in fissile content. This will be addressed further in the next section.

The linear burnup model of Eq. (3.1) can be applied to each burn zone case, setting n = 1, since the calculations were done for batch loads. For each carbon-to-heavy metal atom ratio, the fissile enrichments necessary at the beginning-of-cycle necessary to achieve any given end-of-cycle burnup for either a batch-loaded or continuously-fueled system can then be determined.

A linear correlation of the form:

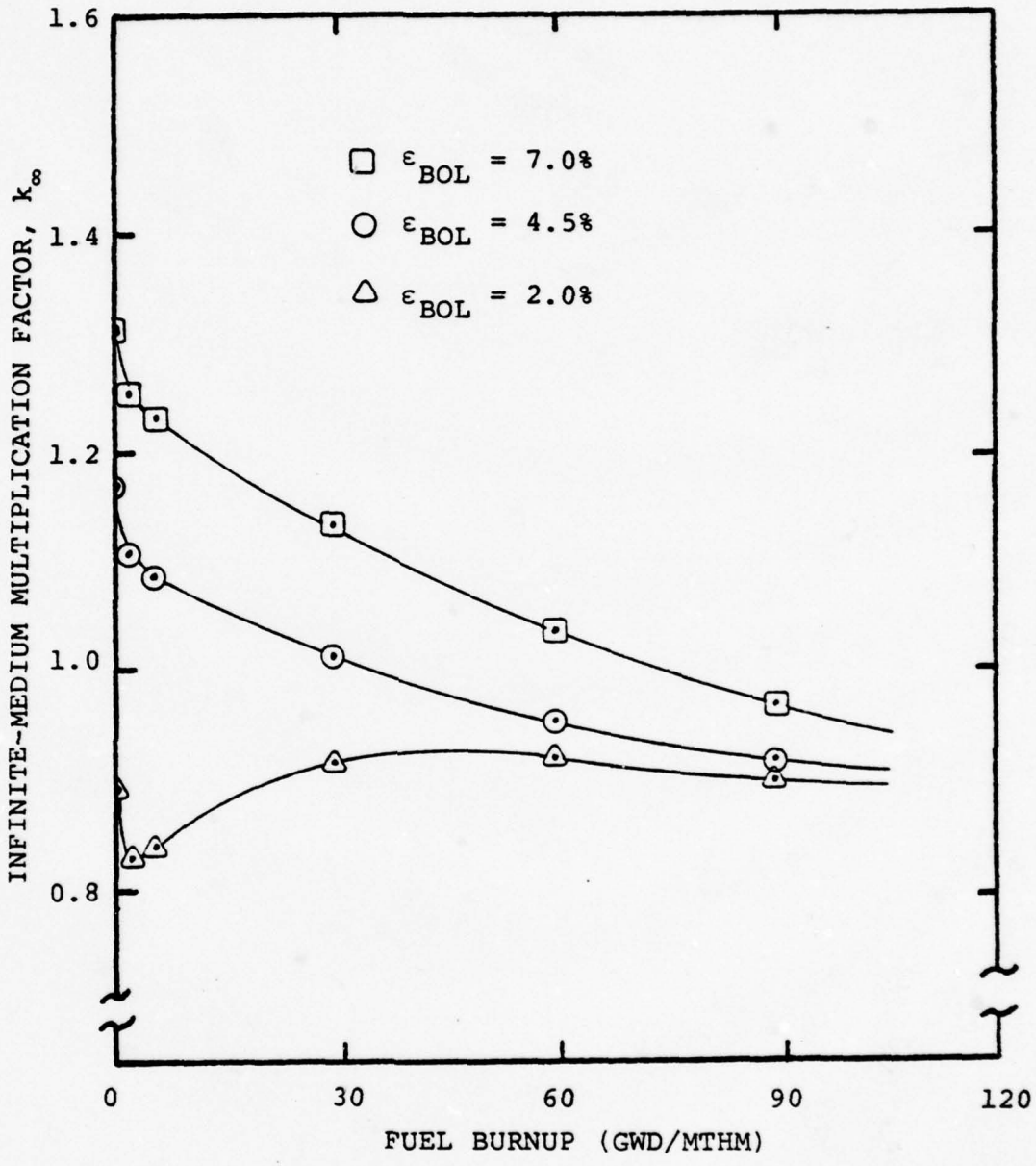

FIGURE 4.1: k_∞ VERSUS FUEL BURNUP FOR C/HM = 110

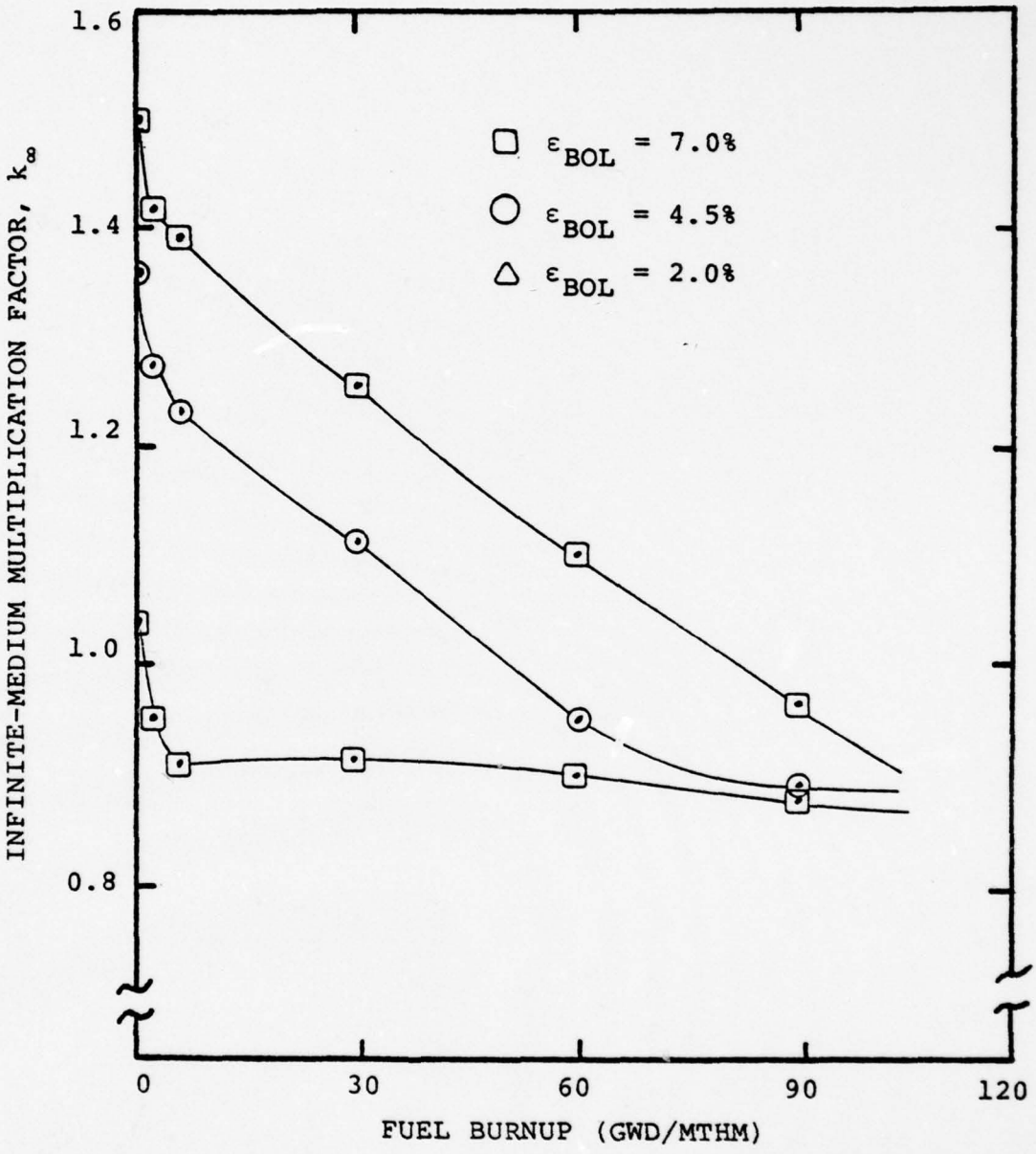

FIGURE 4.2: k_∞ VERSUS FUEL BURNUP FOR C/HM = 250

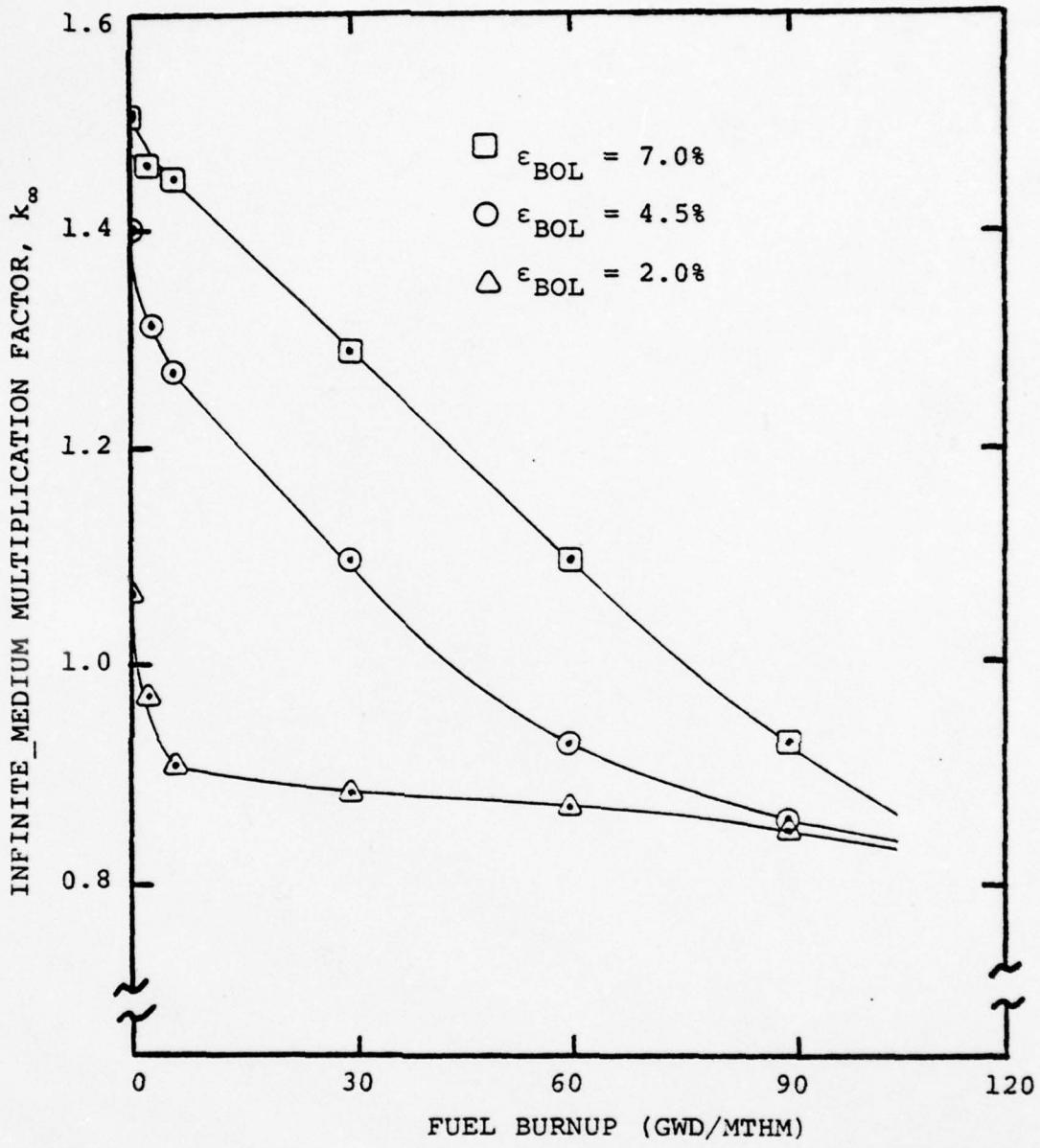

FIGURE 4.3: k_∞ VERSUS FUEL BURNUP FOR C/HM = 325

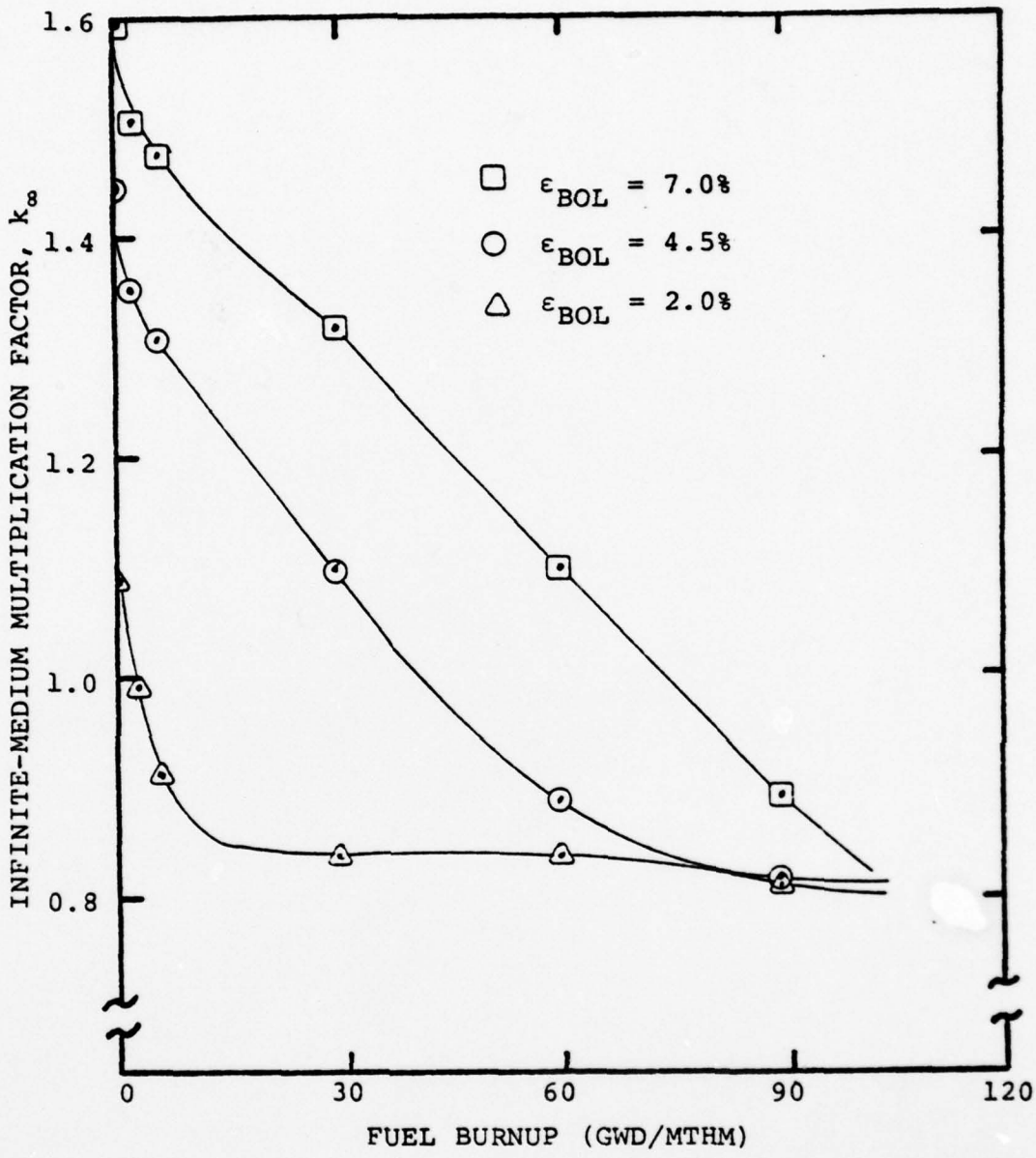

FIGURE 4.4: k_∞ VERSUS FUEL BURN FOR C/HM = 450

$$k_\infty = c_1 B + c_o \qquad (4.1)$$

was fit (linear least squares) to the linear region of each curve (i.e. for all burnups after initial Xe135 saturation) and the coefficients c_o and c_1 were determined. The resulting c_o and c_1 are listed in Appendix B, Table [B.5]. In this model, B is the average reactivity-limited fuel burnup.

Equation (4.1) can be solved for the burnup at which $k_\infty = 1.0$, $\hat{B}$, as :

$$1.0 = c_1 \hat{B} + c_o \quad , \qquad (4.2)$$

for each burn zone burnup history shown in Figs. [4.1 - 4.4]. Since initial enrichments of 2.0% resulted in subcritical systems (for all except the first time step) for all carbon-to-heavy metal atom ratios examined, these cases were excluded from further analysis. For the remaining two burnup histories for each burn zone composition (corresponding to initial enrichments of 4.5% and 7.0%) the linear burnup relation was applied. Simultaneous solution of the resulting two equations yields the coefficients a and b for each carbon-to-heavy metal atom ratio. These coefficients are listed in Appendix B, Table [B.6].

Thus, for any initial fissile enrichment, the end-of-cycle batch fuel burnups can be calculated; and setting $n \to \infty$ in Eq. (3.1) yields the burn zone burnup limit for continuous refueling. Table [4.1] lists the reactivity-limited burnups

TABLE 4.1

REACTIVITY-LIMITED BURNUP* FOR

CONTINUOUSLY-FUELED BURN ZONES

WITH $\varepsilon_{BOL_c} = \varepsilon_{ASY_{bz}}^{\dagger}$

		BURN ZONE C/HM ATOM RATIO			
		110	250	325	450
BREED ZONE C/HM ATOM RATIO	110	67400	97590	94480	86950
	250	28210	67390	65092	58500
	325	19920	61000	58880	52480
	450	13140	55780	53790	47560

* Values shown are MWD/MTHM

† Breed Zone ε_{ASY} values are given in Table [4.2] as ε_{EOC}.

for continuously-fueled burn zones as a function of the breed zone asymptotic limits given in Table [4.2]. These asymptotic enrichments, being the average end-of-cycle enrichments, ε_{EOC}, generated in the PDQ-7 calculations for each composition, approximate the asymptotic values predicted for each spectrum, as can be seen in Table [4.2].

The burnups obtained vary substantially with the breed and burn carbon-to-heavy metal atom ratio combinations, as shown in Fig. [4.5]. The highest values of fuel burnups are obtained for a breed zone for C/HM = 110 and a burn zone composition in the range of C/HM = 250 to 450.

4.3 Variation of ε^{23} with Fuel Burnup

Having met the objective of achieving system criticality, the next objective is to examine the fissile production potential. The analysis in Chapter 2 indicated that a maximum possible asymptotic fissile enrichment would be achieved, given adequate exposure time, dependent on the ambient spectrum. The fissile enrichments (U233 only, neglecting U235) for each zone composition are listed as a function of fuel burnup in Table [B.4]. As illustrated in Figs. [4.6 - 4.9], it is clear that an asymptotic limit is approached at very high fuel burnups, independent of the initial zone fissile enrichment. A comparison is made in Table [4.2] of the average U233 enrichment at end-of-cycle inferred from these results with the asymptotic enrichment limits predicted using the simplistic analysis of Chapter 2. As previously discussed, predicted values of ε_{ASY} should correspond nearly, but not

TABLE 4.2

COMPARISON OF ACTUAL END-OF-CYCLE U233

ENRICHMENTS AND PREDICTED ASYMPTOTIC LIMITS

	C/HM ATOM RATIO			
	110	250	325	450
ε_{ASY}*	0.03526	0.02686	0.02497	0.02302
ε_{EOC}	0.03697	0.02137	0.01807	0.01537
$\frac{\varepsilon_{ASY}}{\varepsilon_{EOC}}$	1.048	0.7956	0.7237	0.6677

* Predicted using $\frac{\sigma_c^{02}}{\sigma_a^{23}}$

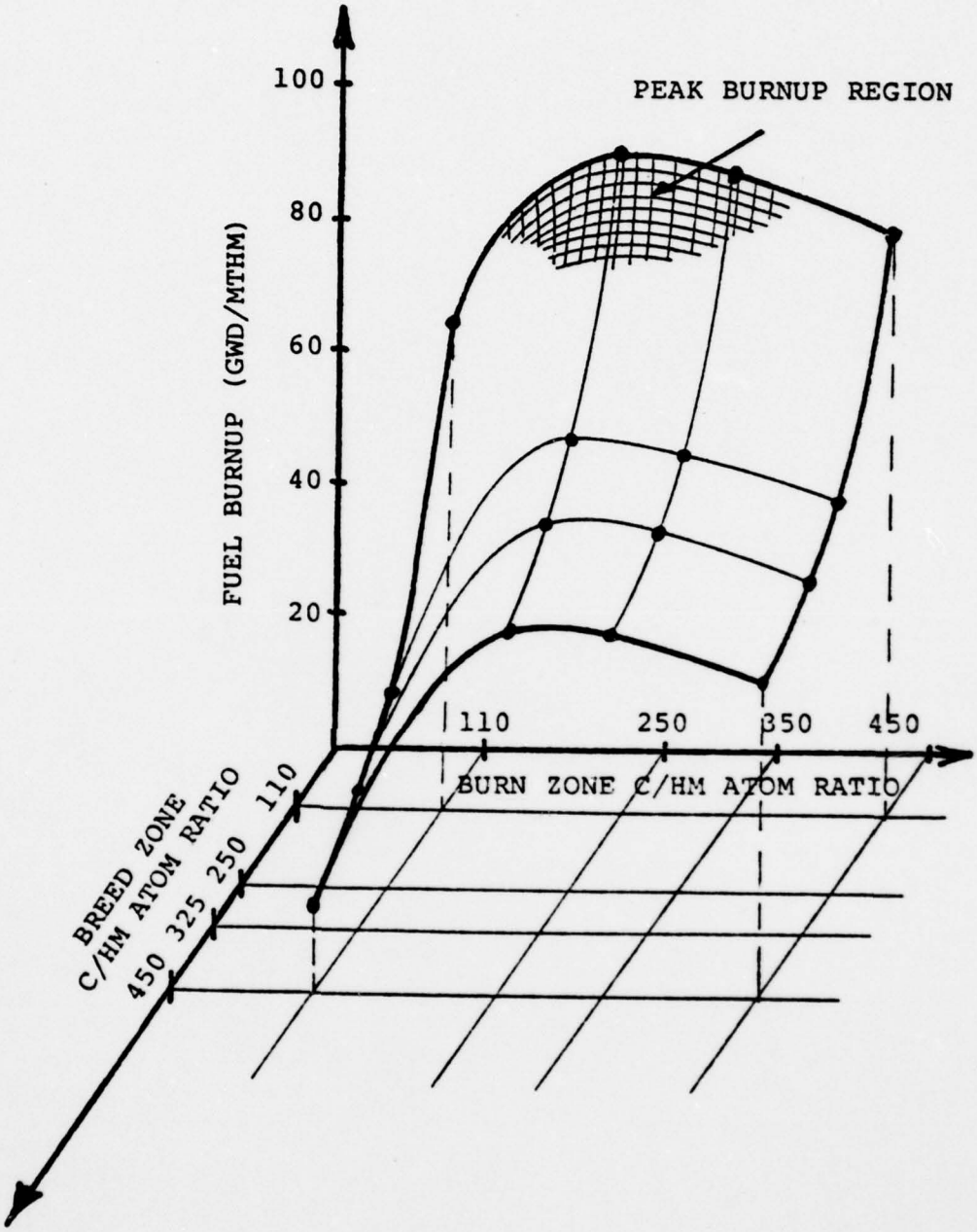

FIGURE 4.5: REACTIVITY LIMITED BURNUP FOR ASYMPTOTIC ENRICHMENT LOADINGS

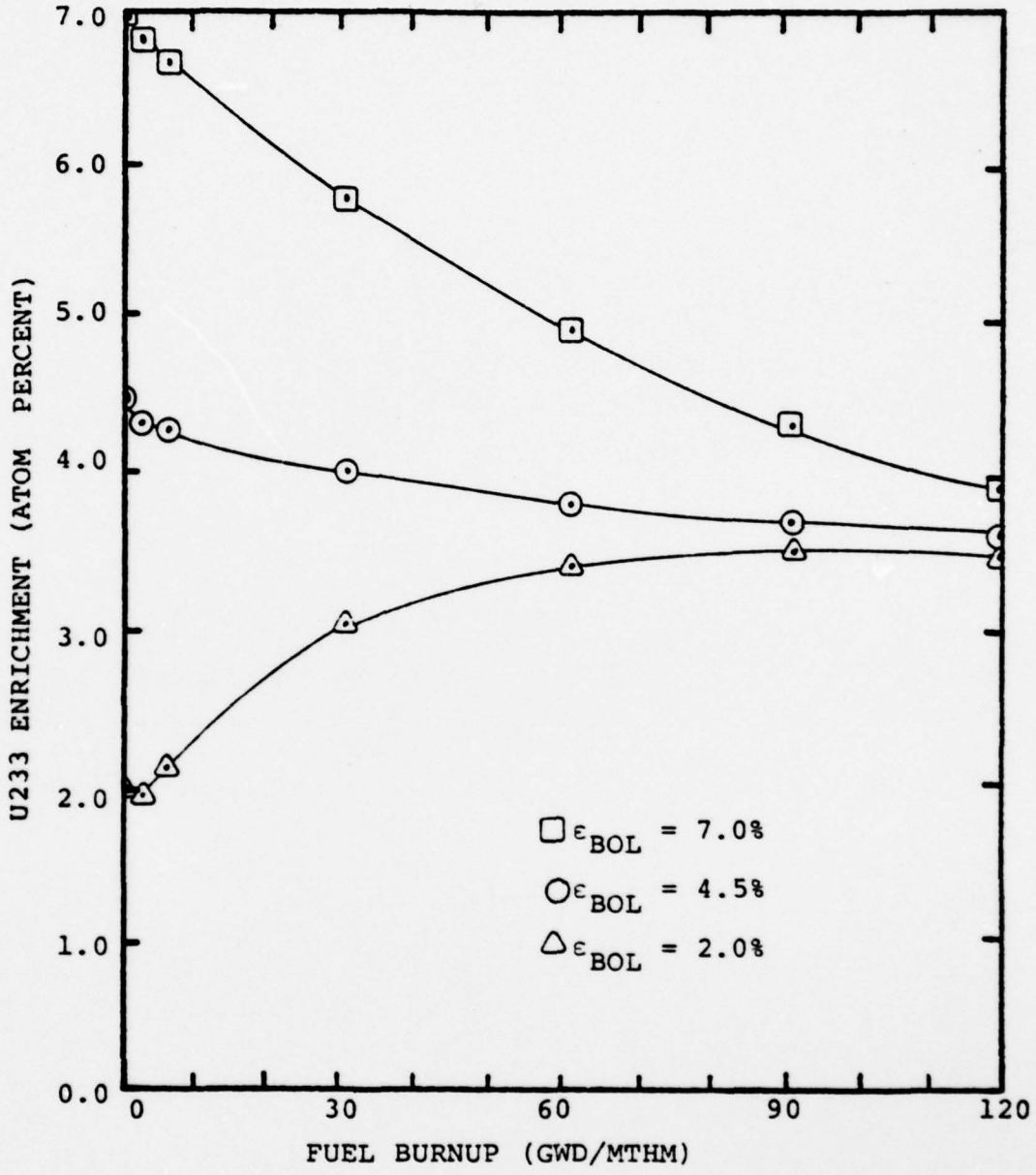

FIGURE 4.6: U233 ENRICHMENT VERSUS FUEL BURNUP FOR C/HM = 110

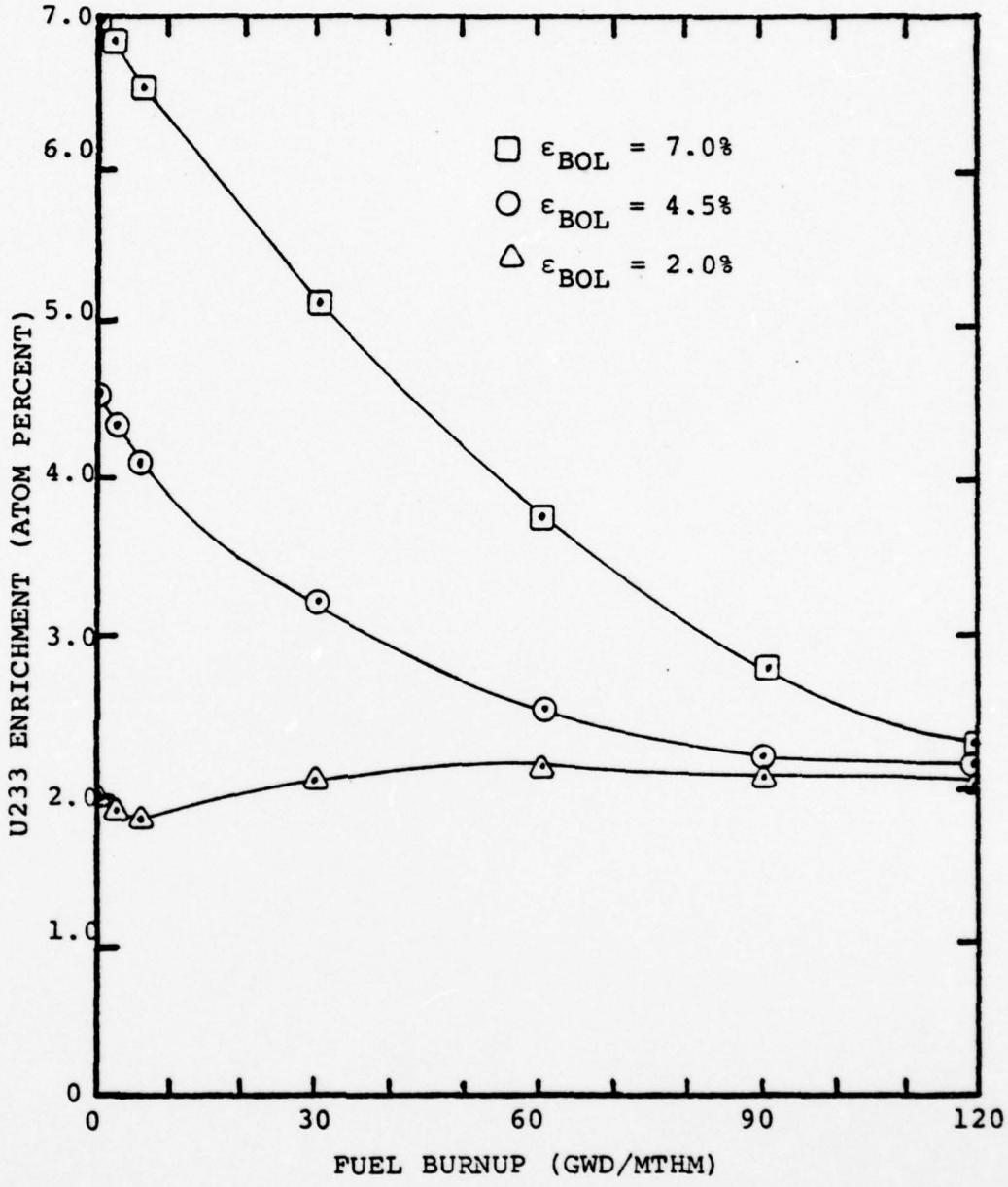

FIGURE 4.7: U233 ENRICHMENT VERSUS FUEL BURNUP FOR C/HM = 250

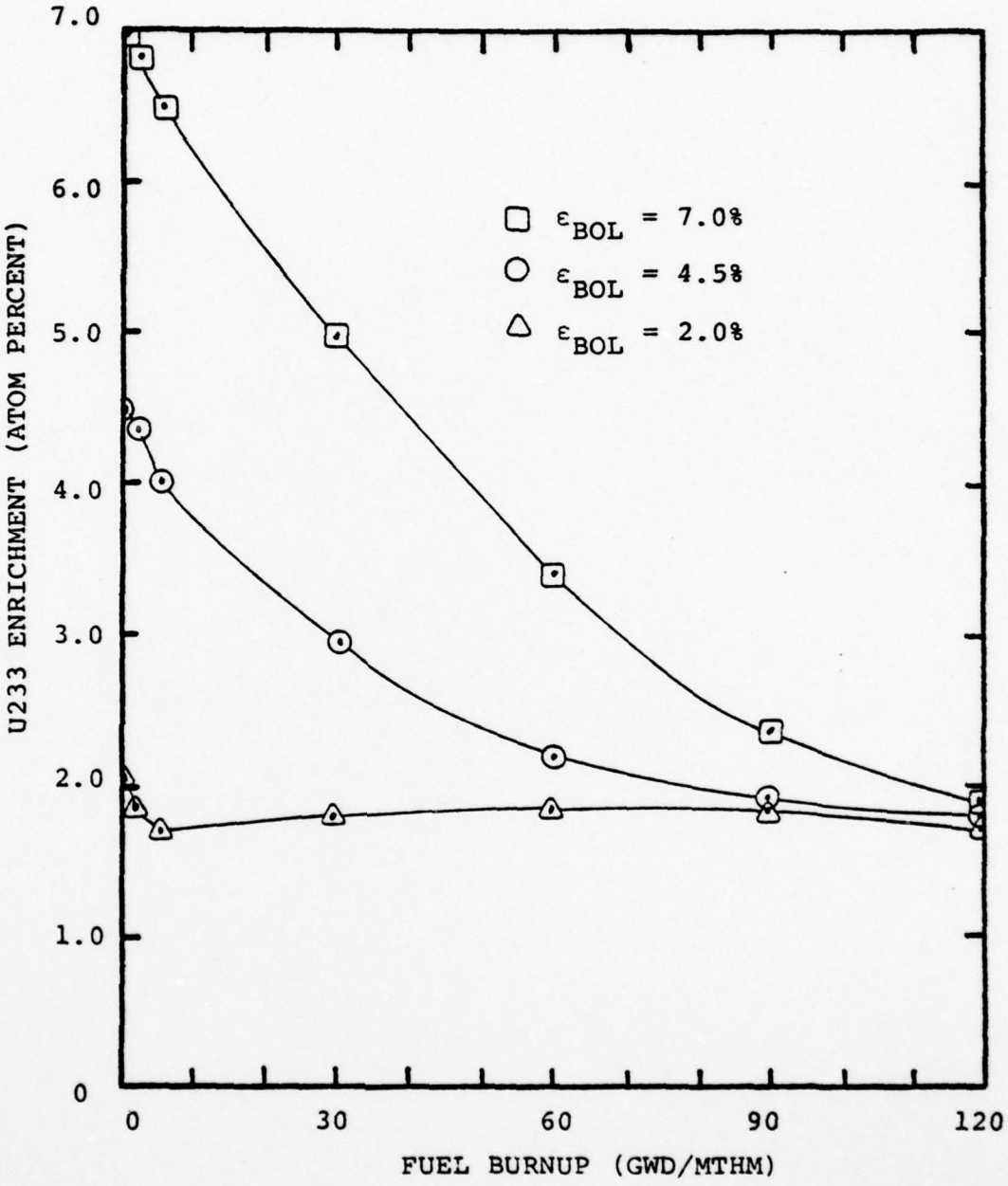

FIGURE 4.8: U233 ENRICHMENT VERSUS FUEL BURNUP FOR C/HM = 325

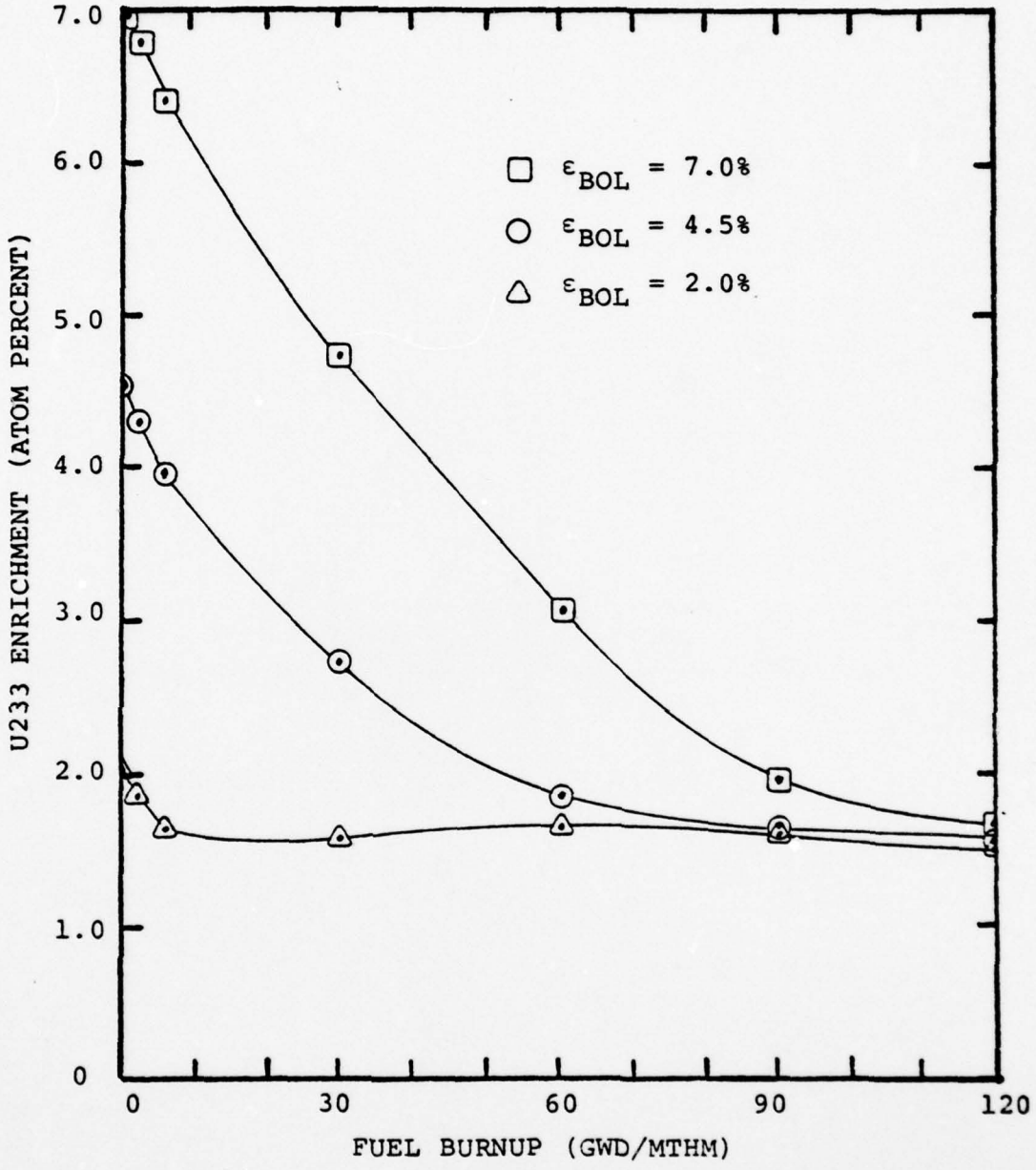

FIGURE 4.9: U233 ENRICHMENT VERSUS FUEL BURNUP for C/HM = 450

exactly, to ε_{EOL}, due to the more rigorous evaluation of other concurrent effects by PDQ-7.

A breed zone, initially having no fissile content, would eventually build up to a fissile concentration near the asymptotic limit, as indicated by the low-enriched (2.0% U233) depletion cases (which also exhibited an increase in k_∞ with burnup due to the high fissile production rate). It was noted in the previous section that an optimum combination of zone compositions to maximize obtainable burn zone burnup would use a breed zone where C/HM = 110 and a burn zone where C/HM = 250 to 450. Continuous refueling, which can be approached in pebble bed systems, would allow burn zone burnups in these cases approaching 100 GWD/MTHM. Recognizing that for continuous fueling very high burnups could be attained (Table [4.2]), the criteria for breed zone burnup, $\varepsilon_{BOL_c} \leq B_{EOL_{bz}}$, can be achieved. Additionally, it is clear from Appendix B, Table [B.3], that increasing the carbon-to-heavy metal atom ratio for a given initial fissile enrichment will increase $k_{\infty_{BOL}}$. This effect is illustrated in Fig. [4.10]. Because system criticality must be maintained, higher burn zone carbon-to-heavy metal atom ratios ($\sim$400 or greater) would therefore be preferred, even though the obtainable burn zone burnups are not quite the maximum possible.

Breed/burn system design in the pebble bed HTGR can, with careful selection of zone compositions, meet the rather conservative criterion established here for potential fissile production and hence breed/burn cycle operation <u>may</u> be

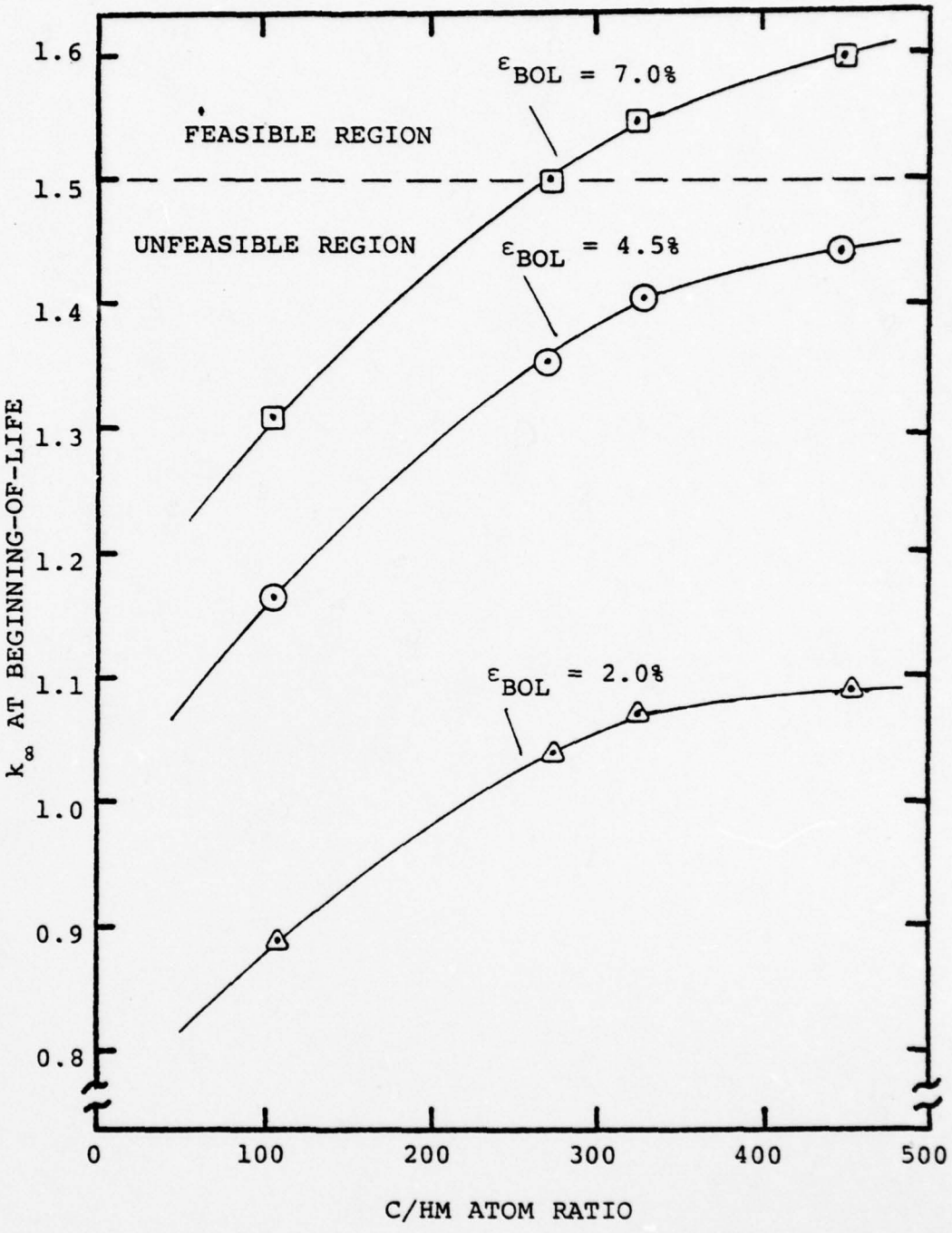

FIGURE 4.10: k_{∞} VERSUS C/HM ATOM RATIO AS A FUNCTION OF BOL ENRICHMENT

feasible. In this analysis, the effects of poisons, control materials and reactor vessel materials were neglected by analyzing an infinite homogeneous system. Therefore, these results are, in fact, extremely conservative estimates, indicating that true system performance might be substantially poorer. The operation of a two-zone system, however, as described in Chapter 3, requires an evaluation which accounts for zone-to-zone leakage.

4.4 Criticality with Zone Leakage

Equation (2.39) required, as a minimum, that at the beginning-of-life:

$$k_{\infty_c} \geq 1.5 \ . \qquad (2.39)$$

This was necessary to account for the significant neutron leakage out of the burn zone (into the breed zone). For the reference homogeneous systems evaluated, beginning-of-life values of k_∞ exceeded 1.5 only for initial enrichments of 7.0%. Since the asymptotic limit for fissile enrichment in a breed zone for which C/HM = 110 is 3.5%, as shown in Fig. [4.10], it can be seen that idealized core configurations yield no values of $k_{\infty_{BOL}} \geq 1.5$. This indicates that it is not possible to achieve a k_∞ high enough to accomodate zone leakage when using breed zone discharge fuel in the burn zone (depicted as the "feasible" range in Fig. [4.10]). Thus, no combination of the zone compositions evaluated in the present work are

AD-A072 680 NAVAL POSTGRADUATE SCHOOL MONTEREY CA F/G 18/12
FEASIBILITY OF BREED/BURN FUEL CYCLES IN PEBBLE BED HTGR REACTO--ETC(U)
SEP 78 T S JENKS

UNCLASSIFIED NL

2 OF 2
AD
A072680

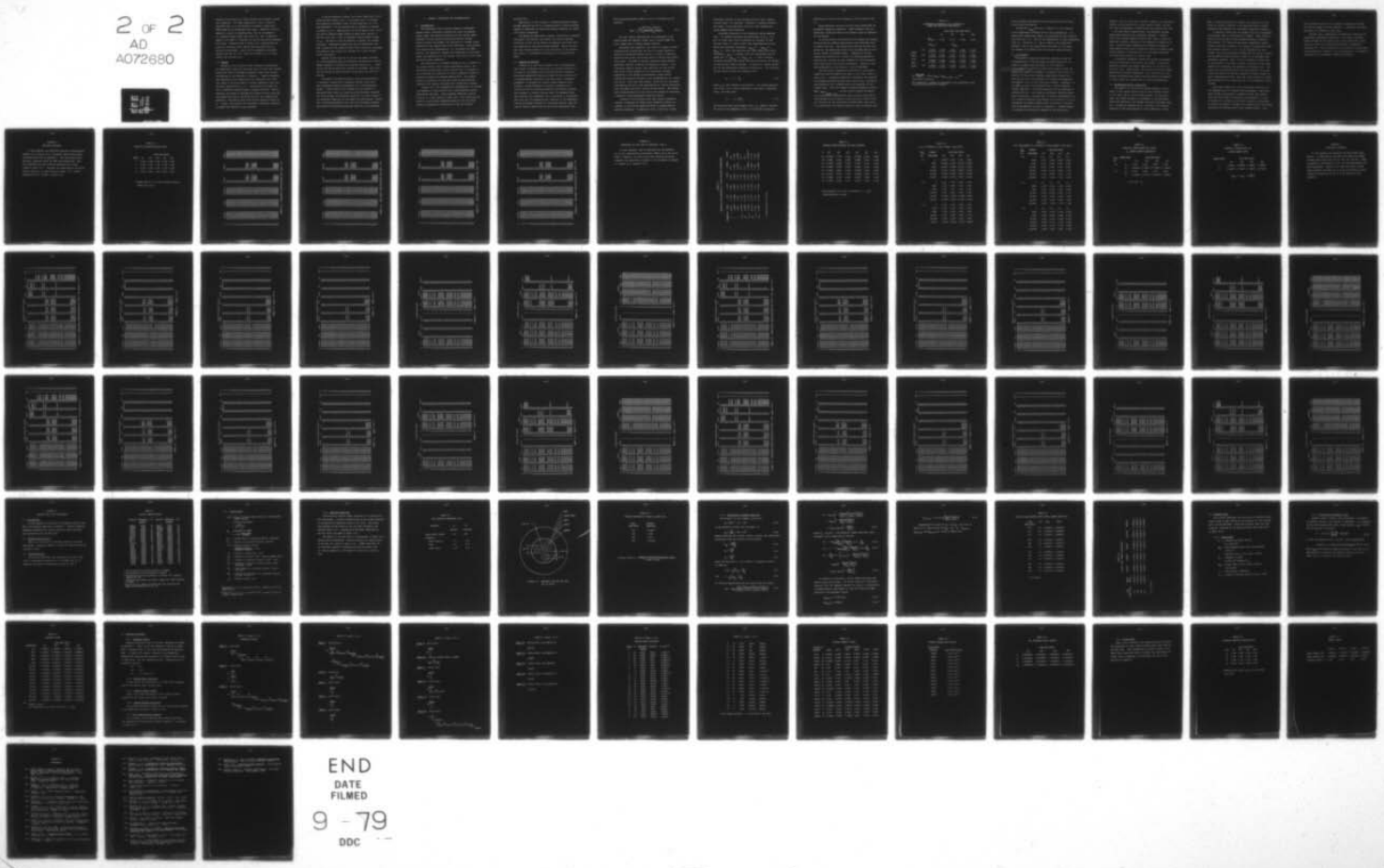

END
DATE
FILMED
9-79
DDC

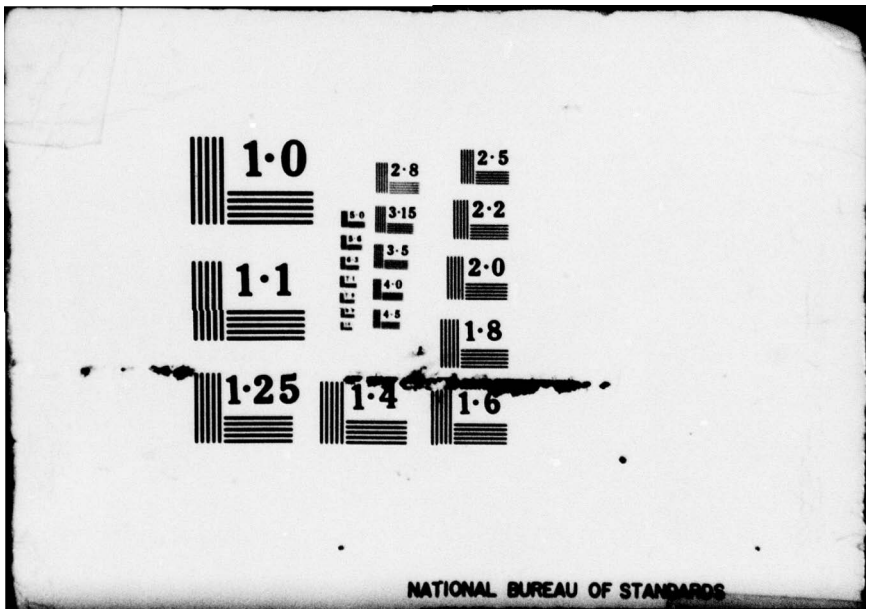
1·0
1·1
1·25
2·8
3·15
3·5
4·0
4·5
1·4
2·5
2·2
2·0
1·8
1·6
NATIONAL BUREAU OF STANDARDS

capable of satisfying all three criteria for successful breed/burn operation. For these compositions, then, it must be concluded that it is not feasible to operate a pebble bed HTGR system on the breed/burn fuel cycle. Moreover, since k_∞ appears to attain its maximum value (for all enrichments) at a carbon-to-heavy metal C/HM value of $\sim$ 450, it does not appear to be useful to consider the use of even softer spectrum burn zones. Referring back to Table [2.5], extrapolation to C/HM < 110 indicates that a harder spectrum breed zone, if physically practicable, might have an asymptotic enrichment greater than the 5% or so, which would permit $k_\infty \geq 1.5$ when cycled into the burn zone.

4.5 Summary

Analysis of the results of PDQ-7 depletion calculations for homogeneous zones has indicated that with high fuel burnups, breed zone fissile enrichments approach steady state values, as predicted in the analysis of Chapter 2. These enrichments, when appropriate zone compositions are employed, will allow burn zones of infinite extent to achieve adequately high burnups while maintaining $k_\infty \geq 1.0$. Considering only these criteria, breed/burn system operation appears feasible. However, requiring the system to overcome the effects of burn zone leakage showed that none of the breed and burn zone combinations examined in the present work could achieve adequate values of k_∞. Hence, the potential for successful breed/burn operation in pebble bed reactors in not confirmed.

It may be possible, however, by further reductions in the carbon-to-heavy metal ratio, in the breed zone, to increase the asymptotic enrichment limit of the breed zone (to $\gtrsim$ 5%, and preferably $\sim$ 7%) and thereby make it possible to achieve a system $k_\infty \geq 1.5$. Additionally, as can be seen in Fig. [4.4], the use of slightly higher carbon-to-heavy metal ratios in the burn zone (say $\sim$ 500) can produce slightly higher values of k_∞, and hence it may be possible to satisfy the leakage criterion. Reasonable compositions must be maintained, however, because as the carbon-to-heavy metal atom ratio increases, the required core volume will increase for a given thermal output requirement.

Another option would be to utilize the pebble bed HTGR in a near-breed/burn mode, by providing the additional fissile makeup necessary to achieve the required values of k_∞. Reactivity-limited burnups would thereby be increased, thus allowing the system to better utilize its potential for U233 production.

The goals of non-proliferation, while best-achieved by a successful "stand-alone" breed/burn system, might still have acceptable operating parameters for a near-breed/burn system. Fissile U235 or U233 loaded into the system in a denatured form, would not violate non-proliferation standards and could provide the necessary reactivity to effect successful breed/burn operation in the pebble bed HTGR system. Should such a modified breed/burn fuel cycle be considered, however, the effects of plutonium production would be to be evaluated.

V. SUMMARY, CONCLUSIONS AND RECOMMENDATIONS

5.1 Introduction

The realization that a growing number of nonnuclear weapons states, desiring to provide for their own growing energy needs, have opted to develop civilian nuclear power programs, and the implied relationship between nuclear electric plants and weapons, has resulted in a broader interpretation of the implications of proliferation. Both national and international reassessments, e.g. the NASAP and INFCE efforts, are underway to prepare new guidelines for the development and application of the nuclear fuel cycle for commercial electrical power production.

The transition to a breeder economy is not in prospect in the United States, under current governmental policy, and alternative options must utilize nuclear fuel in a manner so as to minimize the production of and/or commercial traffic in materials suitable for weapons applications. The present thesis is concerned with one such class of proliferation-resistant fuel cycles, designated the "breed/burn" concept.

Fischer et al [F1] proposed the implementation of a breed/burn system in a fast reactor core, using depleted uranium monocarbide feed fuel. After breeding sufficient fissile material in a hard spectrum "breed zone," fuel assemblies are moved to a more highly moderated region of the core where energy is generated by the burning of the now slightly

enriched fuel.

Application of this concept to thermal/epithermal reactor systems requires the use of a compositionally versatile system, capable of achieving the high fuel burnups necessary for effective fissile conversion.

The pebble bed HTGR offers inherent versatility in fueling strategies, core burnup, fuel design and neutron spectrum tailoring, as well as the ability to approach continuous fueling operation by using flow-through schemes. Hence, the present work focuses primarily on the utilization of the U233/Th fuel cycle in a breed/burn configuration of the pebble bed HTGR.

5.2 Summary of Analysis

Fischer et al [F1] have proposed that in implementing a fast reactor breed/burn fuel cycle, the primary objective is to maximize the breeding ratio through spectrum hardening. More highly-moderated regions are used for fuel burning, but a hardened ambient spectrum in the breed zone is required, presumably to increase the overall system breeding ratio. Primarily through decreases in parasitic absorption (in fissile as well as structural material and fissile products) and increases in fertile fission rates, the breeding ratio does increase with hardening, but it was found in the present work that this is accompanied by a decrease in the asymptotic fissile enrichment obtained for ultra-high burnups, when the rate of fertile capture equals the fissile absorption rate.

This spectrum-dependent apparent limit is expressed by the relation:

$$\varepsilon_{ASY} = \frac{(\sigma_c^{fertile}/\sigma_a^{fissile})}{1 + (\sigma_c^{fertile}/\sigma_a^{fissile})} \qquad (5.1)$$

For fast reactor applications, the preference is for softer breed zone spectra: softer than a typical LMFBR but still harder than in common thermal reactors.

Developing the breed/burn fuel cycle for thermal reactor configurations necessitates the use of a system capable of achieving regionwise spectral shifts (in order to segregate breed and burn zones) while being able to achieve high conversion ratios. The HTGR is the most versatile among thermal/epithermal reactors currently of commercial interest. This inherently superior system, when employed with the U233/Th fuel cycle (chosen because of its outstanding neutronic properties in the thermal and epithermal energy ranges) affords the required flexibility for implementation of a breed/burn cycle. Very high fuel burnups, relatively low enrichment requirements and the stated requirements for zoning flexibility made the pebble bed HTGR a logical system choice. The present work focused primarily on the use of this system for obtaining a feasible thermal/epithermal breed/burn design.

Contrary to the situation with fast reactor breed/burn systems, increasing the breed region asymptotic fissile enrichment in the U233/Th pebble bed HTGR is accomplished by spectrum hardening. In addition, the k_∞ values for a given

enrichment increase as the moderator-to-fuel ratio (carbon-to-heavy metal) is increased. Therefore, a system utilizing two zones; a very hard breed zone and a very thermal burn region appears most promising.

Successful operation of any breed/burn system requires that: (1) system criticality be maintained, or $k_\infty \geq 1.0$, and (2) breed zone fissile production be adequate to fuel the burn zone, or, using a very rough approximation for the breed zone discharge enrichment, $\varepsilon_{EOL_{bz}}$ (%) $\simeq \varepsilon_{ASY_{bx}}$ (%) $\simeq B_{EOL_c}$ (%). Burn zone operation must then require an initial enrichment, ε_{BOL_c}, no greater than that discharged from the breed zone, or $\varepsilon_{ASY_{bz}}$ (%) $\geq B_{EOL_c}$ (%). A final operating criterion requires that system criticality consider the effects of zone-to-zone neutron leakage. In applying a leakage correction to the macroscopic absorption cross-section, the criterion for criticality yields the necessity that:

$$k_\infty - 1 \geq 1 + \frac{\Sigma_L}{\Sigma_a} \quad , \tag{5.2}$$

where ε_L is the "leakage cross-section." By further manipulation of Eq. (5.2), using conservative (optimistic) approximations, one finds that:

$$k_\infty - 1 \geq \frac{1}{1 + b_c} \tag{5.3}$$

and since the burn zone breeding ratio, b_c, reaches a maximum of unity at the asymptotic limit, for successful operation,

accounting for zone-to-zone leakage, k_∞ must be greater than 1.5.

Three operating criteria have thus been established for successful breed/burn operation. These necessary (but not sufficient) conditions define the feasible range of operation for the system.

To fully evaluate the practicality of pebble bed systems, state-of-the-art computer calculations were performed using the PDQ-7 code [C1]. Four-group cross-section data was generated for the pebble bed system using the AMPX modular code system (NITAWL and XSDRNPM codes). Homogeneous one-zone regions were evaluated in a series of eigenvalue/depletion calculations, varying the zone composition (carbon-to-heavy metal atom ratios) and initial enrichments. Depletion runs were performed for fuel burnups to 120,000 MWD/MTHM.

For the various compositions evaluated in this thesis, asymptotic zone enrichments are shown in the first column of Table [5.1]. Increasing asymptotic enrichments are observed for decreasing carbon-to-heavy metal atom ratios, justifying the preference for a hardened breed zone spectrum in this reactor type. Using the highest available asymptotic enrichment, $\varepsilon_{ASY}\Big|_{C/HM = 110}$, as the initial fissile enrichment in a continuously-refueled burn zone, the burn zone end-of-life burnups are also shown in the first row of Table [5.1], as a function of the zone carbon-to-heavy metal atom ratio. It is clear that this reactor system is able to achieve high

TABLE 5.1

PERFORMANCE PARAMETERS AS A FUNCTION OF BREED AND BURN ZONE COMPOSITION

			BURN ZONE C/HM ATOM RATIO			
			110	250	325	450
		$B^{*}_{EOL_c}$, %	6.740	9.759	9.448	8.695
		$\varepsilon_{ASY_{bz}}$, %		$k^{\dagger}_{\infty_{BOL_c}}$		
BREED ZONE C/HM ATOM RATIO	110	0.0353	1.069 (1.110)	1.246 (1.256)	1.290 (1.286)	1.323 (1.313)
	250	0.0269	0.971 (0.952)	1.134 (1.095)	1.171 (1.125)	1.196 (1.152)
	325	0.0250	0.948 (0.910)	1.107 (1.052)	1.143 (1.082)	1.166 (1.109)
	450	0.0230	0.924 (0.865)	1.080 (1.005)	1.113 (1.035)	1.135 (1.062)

*In $\frac{\text{MWD/MTHM}}{10^4}$, using $\varepsilon_{BOL_c} = \varepsilon_{ASY_{bz\ C/HM\ =\ 110}}$ for continuous refueling.

†For comparison, numbers in parenthesis were predicted by the one-group calculation of Chapter 2.

infinite medium fuel burnups while requiring quite low beginning-of-life enrichments.

Values for k_{∞} are given in Table [5.1] as a function of the combination of breed and burn zone compositions. Although most combinations result in criticality for the infinite burn zone ($k_{\infty} > 1.0$), none of the combinations of zone composition reach k_{∞} values of 1.5. Hence, based on this simplistic analysis, none of the compositions evaluated in this thesis are capable of overcoming the zone-to-zone leakage effects.

5.3 Conclusions

Successful stand-alone breed/burn operation could not be accomplished in U233/Th pebble bed HTGR systems for the ranges of compositions considered in this analysis: $110 \leq C/HM \leq 450$. While the pebble bed system provides the flexibility needed to implement a successful fuel cycle, the effects of zone-to-zone leakage necessitates values of k_{∞} that are too high to be achieved with breed zone asymptotic enrichments (<3.5% in the C/HM range studied). Therefore, if the HTGR is still to be considered as a viable breed/burn system, additional breed zone hardening will be necessary to increase the attainable fisssile enrichment: carbon-to-heavy metal atom ratios much less than 110 must be contemplated, so as to achieve asymptotic enrichments on the order or 7% or so. Increasing the carbon-to-heavy metal atom ratio in the burn zone could possibly be used to increase k_{∞}, thereby helping to overcome the constraints imposed by the zone-to-zone

leakage. Such an action must consider, however, the additional reactor volume required for a given thermal output, and the fact that k_∞ approaches a broad maximum just beyond C/HM ≈ 450.

For fast reactor applications, the breed/burn concept offers good potential for successful operation. However, "soft" fast reactor spectra would be most likely to meet all operating criteria, contrary to the proposal by Fischer et al [F1]. The much higher asymptotic enrichments available in these spectra could allow a breed/burn system to produce large fissile masses in the breed zone in a time span consistent with lower fuel burnups in the burn zone.

A successful breed/burn system can satisfy the nonproliferation objectives of minimizing the traffic in sensitive materials suitable for weapons application at all points in the fuel cycle. Additionally, the use of fertile-only makeup makes fuel enrichment unnecessary, while the high burn zone burnups attainable help reduce discharge fissile enrichments to levels which are insufficient to justify reprocessing.

5.4 Recommendations for Future Work

The results of this analysis showed asymptotic enrichments in fast reactor spectra were at their highest levels in the "soft" end of the available spectra. On the other hand, the highest asymptotic enrichments in the epithermal range were obtained in the hardest available epithermal spectra. An apparent maximum exists, therefore, for a reactor operating in the range between a "soft" LMFBR and a "hard"

HTGR. Future analyses should examine the possibility of designing a system to operate in the described range, thereby maximizing the potential for successful breed/burn operation.

In addition, Karam [K1] has proposed the use of suspended-bed reactors (SBR) as alternatives to LMFBRs. These reactors would utilize pyrolytic carbon-coated dicarbide or metallic fuel kernels (i.e. HTGR fuel particles) suspended by upward flowing helium gas (coolant) in a cluster of pressurized tubes. High breeding ratios (1.2 to 1.38) are projected for this system, since the utilization of HTGR-type fuel kernels without the surrounding graphite matrix results in an extremely hard epithermal spectrum. Thus, it may be possible to adapt some of the features of the SBR to achieve a spectrum in the range required for maximizing the asymptotic enrichment limit. Combining the high breeding ratios and hard spectrum, and recognizing the ability to maintain composition zoning through the use of tube-contained fuel, this type system should be investigated carefully for its applicability to the breed/burn system concept.

Less exotic HTGRs still offer exceptional potential for the implementation of alternate fueling schemes. Even apart from the SBR, conventional or pebble bed type HTGR compositions for which C/HM < 110 should be investigated, as it may be possible to increase the available asymptotic enrichments to levels high enough to produce the necessary burn zone excess reactivity to overcome zone-to-zone leakage effects. Only

after thorough analysis of all possible compositions should the HTGR be judged as either feasible or unfeasible for implementation of a breed/burn fuel cycle.

Finally, once a combination of breed/burn zones pass the preliminary requirements proposed in this thesis, analyses should proceed to the logical step of multi-zone PDQ-7 calculations in which the zone-to-zone coupling is explicitly accounted for. This is essential if the extent to which zones can be spectrally isolated is to be established -- an essential prerequisite for successful breed/burn operation.

APPENDIX A

ONE-GROUP CONSTANTS

In this appendix are tabulated one-group cross-sections (Tables [A.2] through [A.5]) collapsed from the four-group cross-sections given in Appendix C. The four-group cross-sections, generated using the AMPX Code System [G2], were flux weighted using the relative groupwise flux values listed in table [A.1]. Nuclides are identified in the cross-section tables by an identification number, "I#", listed alphabetically by isotope in Table [D.1].

TABLE A.1

RELATIVE GROUPWISE NEUTRON FLUX*

		C/HM ATOM RATIO			
GROUP	Δu	110	250	325	450
1	4.400	1.000	1.000	1.000	1.000
2	5.750	1.534	1.533	1.533	1.534
3	5.750	1.025	1.194	1.236	1.282
4	5.916	0.920	2.305	2.939	3.874

* Normalized to ϕ_1 for each carbon-to-heavy metal atom ratio.

I#	TRANSPORT	TOTAL	ABSORPTION	FISSION	NUFISSION	CAPTURE
1	0.11539E+01	0.12760E+01	0.50337E-03	0.0	0.0	0.50337E-03
2	0.41195E+01	0.42774E+01	0.38296E-03	0.0	0.0	0.38296E-03
3	0.41195E+01	0.42774E+01	0.38296E-03	0.0	0.0	0.38296E-03
4	0.35196E+01	0.36665E+01	0.53058E-03	0.0	0.0	0.53058E-03
5	0.35196E+01	0.36724E+01	0.53058E-03	0.0	0.0	0.53058E-03
6	0.86931E-01	0.87373E-01	0.87373E-01	0.0	0.0	0.87373E-01
7	0.22220E+01	0.24490E+01	0.13582E-01	0.0	0.0	0.13582E-01
8	0.18021E+06	0.18372E+06	0.18372E+06	0.0	0.0	0.18372E+06
9	0.21892E+02	0.22243E+02	0.14759E+02	0.0	0.0	0.14759E+02
10	0.11610E+02	0.11681E+02	0.11681E+02	0.0	0.0	0.11681E+02
11	0.81374E+01	0.81375E+01	0.22017E+01	0.0	0.0	0.22017E+01
12	0.12123E+03	0.12189E+03	0.91808E+02	0.0	0.0	0.91808E+02
13	0.33677E+04	0.33746E+04	0.33746E+04	0.0	0.0	0.33746E+04
14	0.22483E+04	0.22371E+04	0.22371E+04	0.0	0.0	0.22371E+04
15	0.59164E+04	0.60128E+04	0.59471E+04	0.0	0.0	0.59471E+04
16	0.63150E+03	0.63822E+03	0.62789E+03	0.0	0.0	0.62789E+03
17	0.89566E+02	0.89972E+02	0.79091E+02	0.0	0.0	0.79091E+02
18	0.25240E+02	0.26091E+02	0.11310E+02	0.74426E-01	0.19877E+00	0.11256E+02
19	0.53153E+02	0.53524E+02	0.35814E+02	0.19344E+00	0.59177E+00	0.35621E+02
20	0.57751E+02	0.59166E+02	0.48422E+02	0.14359E+00	0.47416E+00	0.48279E+02
21	0.41293E+00	0.41802E+00	0.41802E+00	0.0	0.0	0.41802E+00
22	0.39200E+01	0.39282E+01	0.39282E+01	0.0	0.0	0.39282E+01
23	0.15641E+02	0.16146E+02	0.26814E+01	0.80965E-02	0.19318E-01	0.26733E+01
24	0.82180E+02	0.83088E+02	0.73194E+02	0.64537E+02	0.16158E+03	0.86064E+01
25	0.40066E+02	0.41412E+02	0.26569E+02	0.19894E+00	0.53432E+00	0.26370E+02
26	0.70241E+02	0.71215E+02	0.60816E+02	0.48192E+02	0.11726E+03	0.12624E+02
27	0.32214E+02	0.32346E+02	0.21866E+02	0.21860E+00	0.58712E+00	0.21647E+02
28	0.34257E+01	0.36516E+01	0.70052E-03	0.0	0.0	0.70052E-03
29	0.11495E+02	0.11336E+02	0.11336E+02	0.0	0.0	0.11336E+02
30	0.20299E+02	0.28713E+02	0.21879E+02	0.0	0.0	0.21879E+02
31	0.49673E+02	0.49682E+02	0.44230E+02	0.0	0.0	0.44230E+02
32	0.12997E+04	0.13068E+04	0.13068E+04	0.0	0.0	0.13068E+04
33	0.60509E+02	0.60752E+02	0.51910E+02	0.0	0.0	0.51910E+02
34	0.11672E+03	0.11550E+03	0.35976E+02	0.0	0.0	0.35976E+02
35	0.16458E+02	0.16547E+02	0.16547E+02	0.0	0.0	0.16547E+02
36	0.32987E+02	0.32914E+02	0.27025E+02	0.0	0.0	0.27025E+02
37	0.38554E+02	0.34283E+02	0.15800E+02	0.0	0.0	0.15800E+02
38	0.10804E+02	0.31933E+02	0.16827E+02	0.0	0.0	0.16827E+02
39	0.18732E+03	0.18596E+03	0.87445E+02	0.0	0.0	0.87445E+02
40	0.14749E+03	0.14825E+03	0.14347E+03	0.0	0.0	0.14347E+03
41	0.12143E+04	0.12206E+04	0.12151E+04	0.0	0.0	0.12151E+04
42	0.40615E+02	0.41231E+02	0.31581E+02	0.51716E-01	0.13425E+00	0.31529E+02
43	0.22259E+02	0.22995E+02	0.60959E+01	0.33322E-01	0.91067E-01	0.60626E+01
44	0.28341E+03	0.28295E+03	0.27270E+03	0.16843E+03	0.48403E+03	0.10427E+03
45	0.32223E+03	0.31875E+03	0.28499E+03	0.36387E+00	0.10983E+01	0.28462E+03
46	0.21313E+03	0.21427E+03	0.20361E+03	0.15125E+03	0.44358E+03	0.52356E+02

TABLE A.2: ONE-GROUP CROSS-SECTIONS FOR C/HM = 110

I#	TRANSPORT	TOTAL	ABSORPTION	FISSION	NUFISSION	CAPTURE
1	0.10720E+01	0.11512E+01	0.10946E-02	0.0	0.0	0.10946E-02
2	0.43909E+01	0.44026E+01	0.70947E-03	0.0	0.0	0.70947E-03
3	0.43909E+01	0.44026E+01	0.70947E-03	0.0	0.0	0.70947E-03
4	0.37037E+01	0.37116E+01	0.41458E-03	0.0	0.0	0.41458E-03
5	0.37171E+01	0.37250E+01	0.41458E-03	0.0	0.0	0.41458E-03
6	0.17069E+00	0.17117E+00	0.17117E+00	0.0	0.0	0.17117E+00
7	0.21756E+01	0.22939E+01	0.27087E-01	0.0	0.0	0.27087E-01
8	0.41570E+06	0.42128E+06	0.42128E+06	0.0	0.0	0.42128E+06
9	0.22111E+02	0.22284E+02	0.16404E+02	0.0	0.0	0.16404E+02
10	0.22852E+02	0.22917E+02	0.22917E+02	0.0	0.0	0.22917E+02
11	0.73795E+01	0.73001E+01	0.26647E+01	0.0	0.0	0.26647E+01
12	0.13403E+03	0.13451E+03	0.10716E+03	0.0	0.0	0.10716E+03
13	0.54263E+04	0.54375E+04	0.54375E+04	0.0	0.0	0.54375E+04
14	0.19510E+04	0.19479E+04	0.19479E+04	0.0	0.0	0.19479E+04
15	0.13280E+05	0.13419E+05	0.13343E+05	0.0	0.0	0.13343E+05
16	0.12974E+04	0.13020E+04	0.12921E+04	0.0	0.0	0.12921E+04
17	0.11638E+03	0.11663E+03	0.10708E+03	0.0	0.0	0.10708E+03
18	0.24020E+02	0.24575E+02	0.10866E+02	0.55620E-01	0.14853E+00	0.10810E+02
19	0.53660E+02	0.54096E+02	0.37757E+02	0.14431E+00	0.44148E+00	0.37613E+02
20	0.66753E+02	0.66564E+02	0.57296E+02	0.10728E+00	0.35429E+00	0.57180E+02
21	0.44622E+00	0.44945E+00	0.44945E+00	0.0	0.0	0.44945E+00
22	0.47728E+01	0.47814E+01	0.47814E+01	0.0	0.0	0.47814E+01
23	0.16422E+02	0.16688E+02	0.33377E+01	0.60505E-02	0.14434E-01	0.33316E+01
24	0.13375E+03	0.13131E+03	0.12071E+03	0.10800E+03	0.27036E+03	0.12711E+02
25	0.45115E+02	0.45693E+02	0.31096E+02	0.14836E+00	0.39848E+00	0.30948E+02
26	0.12114E+03	0.12201E+03	0.11096E+03	0.90690E+02	0.22048E+03	0.20177E+02
27	0.34905E+02	0.35360E+02	0.24435E+02	0.16312E+00	0.43814E+00	0.24272E+02
28	0.35902E+01	0.36566E+01	0.54038E-03	0.0	0.0	0.54038E-03
29	0.14069E+02	0.14016E+02	0.14016E+02	0.0	0.0	0.14016E+02
30	0.43316E+02	0.43493E+02	0.38005E+02	0.0	0.0	0.38005E+02
31	0.66567E+02	0.66062E+02	0.61854E+02	0.0	0.0	0.61854E+02
32	0.25568E+04	0.25641E+04	0.25641E+04	0.0	0.0	0.25641E+04
33	0.65225E+02	0.65336E+02	0.57759E+02	0.0	0.0	0.57759E+02
34	0.11769E+03	0.11742E+03	0.44035E+02	0.0	0.0	0.44035E+02
35	0.32387E+02	0.32479E+02	0.32479E+02	0.0	0.0	0.32479E+02
36	0.58207E+02	0.57781E+02	0.53064E+02	0.0	0.0	0.53064E+02
37	0.34799E+02	0.34564E+02	0.19660E+02	0.0	0.0	0.19660E+02
38	0.35006E+02	0.35630E+02	0.23132E+02	0.0	0.0	0.23132E+02
39	0.19430E+03	0.19401E+03	0.10192E+03	0.0	0.0	0.10192E+03
40	0.26986E+03	0.27057E+03	0.26688E+03	0.0	0.0	0.26688E+03
41	0.23881E+04	0.23947E+04	0.23903E+04	0.0	0.0	0.23903E+04
42	0.43975E+02	0.44174E+02	0.34799E+02	0.38648E-01	0.10031E+00	0.34760E+02
43	0.20750E+02	0.21187E+02	0.57043E+01	0.24900E-01	0.68040E-01	0.56794E+01
44	0.52367E+03	0.52168E+03	0.51178E+03	0.31846E+03	0.91508E+03	0.19332E+03
45	0.37768E+03	0.37360E+03	0.34004E+03	0.29989E+00	0.90100E+00	0.33974E+03
46	0.40298E+03	0.40334E+03	0.39260E+03	0.29042E+03	0.85166E+03	0.10218E+03

TABLE A.3: ONE-GROUP CROSS-SECTIONS FOR C/HM = 250

I#	TRANSPORT	TOTAL	ABSORPTION	FISSION	NUFISSION	CAPTURE
1	0.10491E+01	0.11177E+01	0.12946E-02	0.0	0.0	0.12946E-02
2	0.44737E+01	0.44397E+01	0.81909E-03	0.0	0.0	0.81909E-03
3	0.44737E+01	0.44397E+01	0.81909E-03	0.0	0.0	0.81909E-03
4	0.37581E+01	0.37262E+01	0.38113E-03	0.0	0.0	0.38113E-03
5	0.37740E+01	0.37421E+01	0.38113E-03	0.0	0.0	0.38113E-03
6	0.19878E+00	0.19920E+00	0.19920E+00	0.0	0.0	0.19920E+00
7	0.21614E+01	0.22173E+01	0.31602E-01	0.0	0.0	0.31602E-01
8	0.49041E+06	0.50448E+06	0.50448E+06	0.0	0.0	0.50448E+06
9	0.21723E+02	0.21964E+02	0.16608E+02	0.0	0.0	0.16608E+02
10	0.26619E+02	0.26675E+02	0.26675E+02	0.0	0.0	0.26675E+02
11	0.71345E+01	0.70304E+01	0.28119E+01	0.0	0.0	0.28119E+01
12	0.13542E+03	0.13592E+03	0.11018E+03	0.0	0.0	0.11018E+03
13	0.61143E+04	0.61246E+04	0.61246E+04	0.0	0.0	0.61246E+04
14	0.18464E+04	0.18448E+04	0.18448E+04	0.0	0.0	0.18448E+04
15	0.15943E+05	0.16015E+05	0.15910E+05	0.0	0.0	0.15910E+05
16	0.15277E+04	0.15304E+04	0.15206E+04	0.0	0.0	0.15206E+04
17	0.12409E+03	0.12424E+03	0.11514E+03	0.0	0.0	0.11514E+03
18	0.23447E+02	0.23929E+02	0.10596E+02	0.53062E-01	0.13368E+00	0.10536E+02
19	0.52538E+02	0.52972E+02	0.37178E+02	0.12984E+00	0.39724E+00	0.37048E+02
20	0.67451E+02	0.67498E+02	0.58192E+02	0.96561E-01	0.31887E+00	0.58295E+02
21	0.45626E+00	0.45900E+00	0.45900E+00	0.0	0.0	0.45900E+00
22	0.50115E+01	0.50223E+01	0.50223E+01	0.0	0.0	0.50223E+01
23	0.16581E+02	0.16779E+02	0.34056E+01	0.54457E-02	0.12990E-01	0.34002E+01
24	0.14623E+03	0.14667E+03	0.13588E+03	0.12193E+03	0.30521E+03	0.13948E+02
25	0.48559E+02	0.49306E+02	0.34840E+02	0.13349E+00	0.35853E+00	0.34706E+02
26	0.13451E+03	0.13906E+03	0.12798E+03	0.10532E+03	0.25605E+03	0.22657E+02
27	0.35466E+02	0.35952E+02	0.24983E+02	0.14679E+00	0.39425E+00	0.24836E+02
28	0.16282E+01	0.36586E+01	0.49405E-01	0.0	0.0	0.49405E-03
29	0.14853E+02	0.14818E+02	0.14818E+02	0.0	0.0	0.14818E+02
30	0.48292E+02	0.48385E+02	0.43357E+02	0.0	0.0	0.43357E+02
31	0.70461E+02	0.69913E+02	0.66094E+02	0.0	0.0	0.66094E+02
32	0.29785E+04	0.29849E+04	0.29849E+04	0.0	0.0	0.29849E+04
33	0.65155E+02	0.65272E+02	0.58229E+02	0.0	0.0	0.58229E+02
34	0.11562E+03	0.11551E+03	0.46105E+02	0.0	0.0	0.46105E+02
35	0.37730E+02	0.37809E+02	0.37809E+02	0.0	0.0	0.37809E+02
36	0.66721E+02	0.66191E+02	0.61855E+02	0.0	0.0	0.61855E+02
37	0.34646E+02	0.34395E+02	0.20738E+02	0.0	0.0	0.20738E+02
38	0.36086E+02	0.36596E+02	0.25032E+02	0.0	0.0	0.25032E+02
39	0.19210E+03	0.19201E+03	0.10470E+03	0.0	0.0	0.10470E+03
40	0.31086E+03	0.31146E+03	0.30810E+03	0.0	0.0	0.30810E+03
41	0.27817E+04	0.27874E+04	0.27834E+04	0.0	0.0	0.27834E+04
42	0.43943E+02	0.44038E+02	0.34760E+02	0.34785E-01	0.90282E-01	0.34725E+02
43	0.20062E+02	0.20420E+02	0.54595E+01	0.22411E-01	0.61236E-01	0.54371E+01
44	0.60074E+03	0.55820E+03	0.58843E+03	0.36677E+03	0.10539E+04	0.22166E+03
45	0.39000E+03	0.37594E+03	0.34364E+03	0.27797E+00	0.83406E+00	0.34337E+03
46	0.46593E+03	0.46593E+03	0.45517E+03	0.33654E+03	0.98688E+03	0.11863E+03

TABLE A.4: ONE-GROUP CROSS-SECTIONS FOR C/HM = 325

I#	TRANSPORT	TOTAL	ABSORPTION	FISSION	NUFISSION	CAPTURE
1	0.10191E+01	0.10750E+01	0.15354E-02	0.0	0.0	0.15354E-02
2	0.45716E+01	0.44841E+01	0.95073E-03	0.0	0.0	0.95073E-03
3	0.45716E+01	0.44841E+01	0.95073E-03	0.0	0.0	0.95073E-03
4	0.38223E+01	0.37436E+01	0.34094E-03	0.0	0.0	0.34094E-03
5	0.38414E+01	0.37626E+01	0.34094E-03	0.0	0.0	0.34094E-03
6	0.23255E+00	0.23286E+00	0.23286E+00	0.0	0.0	0.23286E+00
7	0.21439E+01	0.21914E+01	0.37024E-01	0.0	0.0	0.37024E-01
8	0.59909E+06	0.60567E+06	0.60567E+06	0.0	0.0	0.60567E+06
9	0.21408E+02	0.21480E+02	0.16743E+02	0.0	0.0	0.16743E+02
10	0.31146E+02	0.31188E+02	0.31188E+02	0.0	0.0	0.31188E+02
11	0.68469E+01	0.67138E+01	0.29880E+01	0.0	0.0	0.29880E+01
12	0.13629E+03	0.13573E+03	0.11314E+03	0.0	0.0	0.11314E+03
13	0.69419E+04	0.69500E+04	0.69500E+04	0.0	0.0	0.69500E+04
14	0.17224E+04	0.17221E+04	0.17221E+04	0.0	0.0	0.17221E+04
15	0.18945E+05	0.19140E+05	0.19023E+05	0.0	0.0	0.19023E+05
16	0.18072E+04	0.18071E+04	0.17976E+04	0.0	0.0	0.17976E+04
17	0.13294E+03	0.13297E+03	0.12440E+03	0.0	0.0	0.12440E+03
18	0.22545E+02	0.22936E+02	0.10027E+02	0.43370E-01	0.11581E+00	0.99841E+01
19	0.50302E+02	0.51214E+02	0.36099E+02	0.11250E+00	0.34417E+00	0.35977E+02
20	0.60567E+02	0.68022E+02	0.59106E+02	0.83654E-01	0.27625E+00	0.59023E+02
21	0.46830E+00	0.47050E+00	0.47050E+00	0.0	0.0	0.47050E+00
22	0.52857E+01	0.52953E+01	0.52953E+01	0.0	0.0	0.52953E+01
23	0.16735E+02	0.16856E+02	0.36299E+01	0.47177E-02	0.11253E-01	0.36252E+01
24	0.16458E+03	0.16485E+03	0.15393E+03	0.11844E+03	0.34655E+03	0.15384E+02
25	0.49117E+02	0.50251E+02	0.36461E+02	0.11561E+00	0.31053E+00	0.36345E+02
26	0.15922E+03	0.15956E+03	0.14830E+03	0.12268E+03	0.29821E+03	0.25620E+02
27	0.36034E+02	0.36335E+02	0.25516E+02	0.12714E+00	0.34148E+00	0.25409E+02
28	0.36847E+01	0.36611E+01	0.43842E-03	0.0	0.0	0.43842E-03
29	0.15774E+02	0.15754E+02	0.15754E+02	0.0	0.0	0.15754E+02
30	0.54247E+02	0.54241E+02	0.49768E+02	0.0	0.0	0.49768E+02
31	0.74602E+02	0.74036E+02	0.70644E+02	0.0	0.0	0.70644E+02
32	0.34953E+04	0.34900E+04	0.34900E+04	0.0	0.0	0.34900E+04
33	0.64609E+02	0.64693E+02	0.58326E+02	0.0	0.0	0.58326E+02
34	0.11221E+03	0.11222E+03	0.48347E+02	0.0	0.0	0.48347E+02
35	0.44150E+02	0.44210E+02	0.44210E+02	0.0	0.0	0.44210E+02
36	0.76972E+02	0.76310E+02	0.72438E+02	0.0	0.0	0.72438E+02
37	0.34409E+02	0.34131E+02	0.21970E+02	0.0	0.0	0.21970E+02
38	0.37255E+02	0.37616E+02	0.27231E+02	0.0	0.0	0.27231E+02
39	0.18772E+03	0.18779E+03	0.10724E+03	0.0	0.0	0.10724E+03
40	0.36013E+03	0.36054E+03	0.35758E+03	0.0	0.0	0.35758E+03
41	0.32547E+04	0.32588E+04	0.32554E+04	0.0	0.0	0.32554E+04
42	0.43551E+02	0.43520E+02	0.34350E+02	0.30134E-01	0.78210E-01	0.34328E+02
43	0.19182E+02	0.19451E+02	0.51249E+01	0.19415E-01	0.53048E-01	0.51055E+01
44	0.69195E+03	0.68977E+03	0.67916E+03	0.42404E+03	0.12104E+04	0.25512E+03
45	0.37748E+03	0.37350E+03	0.34309E+03	0.25087E+00	0.75143E+00	0.34284E+03
46	0.54123E+03	0.54076E+03	0.52999E+03	0.39170E+03	0.11486E+04	0.13829E+03

TABLE A.5: ONE-GROUP CROSS-SECTIONS FOR C/HM = 450

APPENDIX B

TABULATION OF DATA USED IN CHAPTERS 2 AND 4

In this appendix, data is tabulated for the Sheaffer et al [S1] cross-section correlation (Tables [B.1] and [B.2]) used in Chapter 2, as well as the data resulting from the computer runs specified in Chapter 3 and discussed in Chapter 4, (Tables [B.3] through [B.6]).

TABLE B.1

CONSTANTS FOR SHEAFFER[S1] CROSS-SECTION CORRELATION*

PARAMETER	Th232	U233	U238	Pu239	Oxygen	Carbon
ν	2.404	2.530	2.806	2.953	0.0	0.0
ξ	0.0086	0.0086	0.0084	0.0083	0.120	0.158
σ_r	2.685	2.987	2.736	3.040	0.1859	0.2396
$\sigma_{l,f}$	0.0389	2.111	0.1972	1.713	0.0	0.0
g_f	0.8059	-0.3491	0.7911	-0.1472	0.0	0.0
$\sigma_{l,a}$	0.1858	2.235	0.2147	1.813	2.468E-3	6.879E-6
g_a	-0.9775	-0.4273	-0.6249	-0.3067	0.6728	0.7102
$\sigma_{l,tr}$	6.284	6.194	6.331	6.661	3.307	2.753
g_{tr}	-0.2867	-0.3062	-0.2800	-0.2725	0.02695	-0.1601

* Cross-sections in barns.

TABLE B.2

NEUTRON CROSS-SECTIONS FOR FAST SPECTRA*

S	σ_a^{02}	σ_a^{23}	σ_f^{23}	σ_a^{28}	σ_a^{49}	σ_f^{49}
0.3	0.6028	3.739	3.214	0.4556	2.623	2.050
0.4	0.4550	3.306	2.907	0.3806	2.401	1.964
0.5	0.3658	3.005	2.689	0.3311	2.242	1.900
0.6	0.3061	2.780	2.523	0.2954	2.121	1.849
0.7	0.2633	2.603	2.391	0.2683	2.023	1.807
0.8	0.2311	2.459	2.282	0.2468	1.941	1.771
0.9	0.2060	2.338	2.190	0.2217	1.872	1.740
1.0	0.1858	2.235	2.111	0.2147	1.813	1.713

*From Sheaffer et al [S1] correlation, $\sigma = \sigma_1 S^g$.

Cross-sections in barns.

TABLE B.3

k_∞ AS A FUNCTION OF FUEL BURNUP (from PDQ-7)

ε^{235}_{BOL} (%)	BURNUP (MWD/MTHM)	C/HM ATOM RATIO 110	250	325	450
2.0	0	0.8863	1.036	1.067	1.086
	2000	0.8226	0.9450	0.9705	0.9853
	6000	0.8356	0.9038	0.9120	0.9072
	30,000	0.9114	0.9091	0.8837	0.8335
	60,000	0.9169	0.8949	0.8713	0.8343
	90,000	0.9046	0.8724	0.8477	0.8102
4.5	0	1.164	1.353	1.402	1.442
	2000	1.103	1.269	1.313	1.350
	6000	1.081	1.231	1.270	1.302
	30,000	1.010	1.086	1.095	1.090
	60,000	0.9529	0.9515	0.9288	0.8851
	90,000	0.9180	0.8827	0.8523	0.8062
7.0	0	1.307	1.495	1.548	1.597
	2000	1.253	1.416	1.463	1.506
	6000	1.230	1.386	1.431	1.473
	30,000	1.133	1.257	1.290	1.315
	60,000	1.036	1.098	1.103	1.094
	90,000	0.9651	0.9601	0.9352	0.8893

TABLE B.4

U233 ENRICHMENT AS A FUNCTION OF FUEL BURNUP (from PDQ-7)

ε^{233}_{BOL}	BURNUP	C/HM ATOM RATIO			
(%)	(MWD/MTHM)	110	250	325	450
2.0	0	2.0	2.0	2.0	2.0
	2000	1.937	1.845	1.828	1.814
	6000	2.114	1.758	1.681	1.603
	30,000	3.047	2.019	1.771	1.521
	60,000	3.422	2.116	1.846	1.615
	90,000	3.524	2.095	1.813	1.574
	120,000	3.513	2.038	1.753	1.512
4.5	0	4.5	4.5	4.5	4.5
	2000	4.367	4.310	4.300	4.292
	6000	4.291	4.061	4.013	3.964
	30,000	4.044	3.168	2.944	2.711
	60,000	3.844	2.487	2.158	1.845
	90,000	3.720	2.192	1.865	1.581
	120,000	3.616	2.072	1.772	1.524
7.0	0	7.0	7.0	7.0	7.0
	2000	6.840	6.799	6.792	6.785
	6000	6.667	6.494	6.458	6.419
	30,000	5.810	5.115	4.929	4.729
	60,000	4.956	3.719	3.388	3.059
	90,000	4.358	2.772	2.370	1.990
	120,000	3.962	2.272	1.897	1.575

TABLE B.5

CURVE-FIT COEFFICIENTS FOR LINEAR

k_∞ VERSUS BURNUP CORRELATION

ε_{BOL} (%)	COEFFICIENT	C/HM ATOM RATIO 110	250	325	450
4.5	c_0	1.092	1.251	1.292	1.326
	c_1	-2.092E-6	-4.445E-6	-5.336E-6	-6.359E-6
7.0	c_0	1.247	1.418	1.470	1.520
	c_1	-3.286E-6	-5.177E-6	-5.995E-6	-7.009E-6

$$k_\infty = c_1 B + c_0$$

TABLE B.6

CURVE-FIT COEFFICIENTS FOR

LINEAR BURNUP MODEL

COEFFICIENT	C/HM ATOM RATIO			
	110	250	325	450
a	1.256E+6	9.680E+5	9.420E+5	9.118E+5
b	1.014E-2	-1.344E-2	-1.318E-2	-1.071E-2

$$B_{BOL} = a(\varepsilon_{BOL} - b)\frac{2n}{n+1}$$

APPENDIX C

FOUR-GROUP CONSTANTS

In this appendix are tabulated the four-group cross-section data generated by the AMPX code system for carbon-to-heavy metal atom ratio of 110, 250, 325, and 450. Refer to Appendix D and Section [3.3.2] for code descriptions and input parameters. Table [D.13] shows the neutron energy group structure and Table [D.1] gives the identity of each nuclide corresponding to the I# in the tables of this appendix.

MICROSCOPIC CROSS-SECTIONS FOR GROUP 1

I#	TRANSPORT	TOTAL	N-GAMMA	FISSION	NU	CHI	N-ALPHA	N-2N	N-D	#SCT	I#
1	0.27442E+01	0.31442E+01	0.0	0.0	0.0	0.0	0.0	0.11945E-05	0.0	1	1
2	0.22560E+01	0.28100E+01	0.77269E-06	0.0	0.0	0.0	0.15001E-03	0.0	0.0	1	2
3	0.22560E+01	0.28100E+01	0.77269E-06	0.0	0.0	0.0	0.15001E-03	0.0	0.0	1	3
4	0.28217E+01	0.35639E+01	-0.12288E-09	0.0	0.0	0.0	0.23081E-02	0.38457E-05	0.0	1	4
5	0.28217E+01	0.35639E+01	-0.12288E-09	0.0	0.0	0.0	0.23081E-02	0.38457E-05	0.0	1	5
6	0.17118E-03	0.19318E-03	0.19318E-03	0.0	0.0	0.0	0.0	0.0	0.0	1	6
7	0.27634E+01	0.34127E+01	0.34366E-09	0.0	0.0	0.0	0.0	0.26321E-02	0.0	1	7
8	0.0	0.0	0.0	0.0	0.0	0.0	0.0	0.0	0.0	1	8
9	0.49742E+01	0.62440E+01	0.53245E-01	0.0	0.0	0.0	0.0	0.0	0.32874E-03	1	9
10	0.0	0.0	0.0	0.0	0.0	0.0	0.0	0.0	0.0	1	10
11	0.60621E+01	0.62249E+01	0.33689E-01	0.0	0.0	0.0	0.0	0.0	0.32874E-03	1	11
12	0.63820E+01	0.63721E+01	0.26491E+00	0.0	0.0	0.0	0.0	0.0	0.28946E-03	1	12
13	0.48181E+01	0.52134E+01	0.52134E+01	0.0	0.0	0.0	0.0	0.0	0.0	1	13
14	0.11572E+00	0.13516E+00	0.13516E+00	0.0	0.0	0.0	0.0	0.0	0.0	1	14
15	0.56735E+01	0.72581E+01	0.20495E+00	0.0	0.0	0.0	0.40064E-04	0.40064E-04	0.27360E-02	1	15
16	0.49377E+01	0.73971E+01	0.62561E+00	0.0	0.0	0.0	0.0	0.0	0.0	1	16
17	0.58545E+01	0.76708E+01	0.20415E+00	0.0	0.0	0.0	0.16424E-04	0.16424E-04	0.47045E-03	1	17
18	0.60176E+01	0.86004E+01	0.23365E+00	0.33360E+00	0.26707E+01	0.96749E+00	0.0	0.0	0.18250E-02	1	18
19	0.51515E+01	0.78568E+01	0.79904E-01	0.83234E+00	0.30694E+01	0.96903E+00	0.0	0.0	0.14038E-02	1	19
20	0.57510E+01	0.80469E+01	0.11265E+00	0.64197E+00	0.33031E+01	0.96903E+00	0.0	0.0	0.0	1	20
21	0.16892E-01	0.19740E-01	0.19740E-01	0.0	0.0	0.0	0.0	0.0	0.0	1	21
22	0.58675E-01	0.68788E-01	0.68788E-01	0.0	0.0	0.0	0.0	0.0	0.0	1	22
23	0.63399E+01	0.77860E+01	0.13324E+00	0.36291E-01	0.23860E+01	0.96673E+00	0.0	0.0	0.47208E-02	1	23
24	0.59665E+01	0.75901E+01	0.10622E+00	0.15937E+01	0.26033E+01	0.96673E+00	0.0	0.0	0.21294E-02	1	24
25	0.57910E+01	0.78029E+01	0.14841E+00	0.88203E+00	0.26877E+01	0.96749E+00	0.0	0.0	0.68266E-03	1	25
26	0.54243E+01	0.77555E+01	0.13438E+00	0.12361E+01	0.25709E+01	0.96749E+00	0.0	0.0	0.26123E-02	1	26
27	0.58681E+01	0.80492E+01	0.1775 E+00	0.97834E+00	0.26861E+01	0.96756E+00	0.0	0.0	0.28825E-02	1	27
28	0.26983E+01	0.37250E+01	0.47129E-04	0.0	0.0	0.0	0.30809E-02	0.41520E-05	0.0	1	28
29	0.83184E-02	0.99569E-02	0.99569E-02	0.0	0.0	0.0	0.0	0.0	0.0	1	29
30	0.54462E+01	0.57071E+01	0.69512E-01	0.0	0.0	0.0	0.0	0.0	0.17243E-04	1	30
31	0.61318E+01	0.65158E+01	0.16116E+00	0.0	0.0	0.0	0.0	0.0	0.14790E-03	1	31
32	0.24601E+01	0.28011E+01	0.20011E+01	0.0	0.0	0.0	0.0	0.0	0.0	1	32
33	0.60460E+01	0.64122E+01	0.35316E+00	0.0	0.0	0.0	0.0	0.0	0.20641E-03	1	33
34	0.61951E+01	0.63264E+01	0.74048E-01	0.0	0.0	0.0	0.0	0.0	0.35987E-03	1	34
35	0.0	0.0	0.0	0.0	0.0	0.0	0.0	0.0	0.0	1	35
36	0.64084E+01	0.64382E+01	0.45582E-01	0.0	0.0	0.0	0.0	0.0	0.97741E-03	1	36
37	0.64116E+01	0.64133E+01	0.41694E-01	0.0	0.0	0.0	0.0	0.0	0.97741E-03	1	37
38	0.50948E+01	0.71784E+01	0.45624E-01	0.0	0.0	0.0	0.0	0.0	0.26664E-02	1	38
39	0.50956E+01	0.71774E+01	0.46561E-01	0.0	0.0	0.0	0.0	0.0	0.26664E-02	1	39
40	0.71736E+01	0.73045E+01	0.47487E+00	0.0	0.0	0.0	0.0	0.0	0.41536E-03	1	40
41	0.70060E+01	0.71591E+01	0.16808E+00	0.0	0.0	0.0	0.0	0.0	0.40663E-03	1	41
42	0.55183E+01	0.76697E+01	0.23726E+00	0.23181E+00	0.25959E+01	0.96456E+00	0.0	0.0	0.94723E-03	1	42
43	0.55304E+01	0.82413E+01	0.95468E-01	0.14918E+00	0.27134E+01	0.96535E+00	0.0	0.0	0.38023E-02	1	43
44	0.56001E+01	0.80278E+01	0.74374E-01	0.16977E+01	0.30514E+01	0.96677E+00	0.0	0.0	0.79891E-03	1	44
45	0.55307E+01	0.79602E+01	0.11699E+00	0.97649E+00	0.31174E+01	0.96645E+00	0.0	0.0	0.31889E-03	1	45
46	0.56545E+01	0.89069E+01	0.13277E+00	0.16264E+01	0.31019E+01	0.96570E+00	0.0	0.0	0.56789E-02	1	46

TABLE C.1: FOUR-GROUP CROSS-SECTIONS FOR C/HM = 110 (page 1 of 7)

MICROSCOPIC CROSS-SECTIONS FOR GROUP 2

I#	TRANSPORT	TOTAL	N-GAMMA	FISSION	NU	CHI	N-ALPHA	N-2N	N-D	#SCT	I#
1	0.684512E+00	0.726C2E+C0	0.0	0.0	0.0	0.0	0.0	0.13188E-04	0.0	2	1
2	0.43526E+01	0.46317E+01	0.83131E-05	0.0	0.0	0.0	0.0	0.0	0.0	2	2
3	0.43526E+01	0.46317E+01	0.83131E-05	0.0	0.0	0.0	0.0	0.0	0.0	2	3
4	0.34990E+01	0.35913E+01	0.17946E-06	0.0	0.0	0.0	0.0	0.0	0.0	2	4
5	0.34990E+01	0.35913E+01	0.17946E-06	0.0	0.0	0.0	0.0	0.0	0.0	2	5
6	0.20280E-02	0.20784E-02	0.20784E-02	0.0	0.0	0.0	0.0	0.0	0.0	1	6
7	0.19814E+01	0.20121E+01	0.79831E-03	0.0	0.0	0.0	0.0	0.0	0.0	2	7
8	0.14988E-04	0.15216E-04	0.15216E-04	0.0	0.0	0.0	0.0	0.0	0.0	1	8
9	0.92221E+01	0.93304E+01	0.14040E+01	0.0	0.0	0.0	0.0	0.0	0.0	2	9
10	0.20927E+00	0.21660E+00	0.21660E+00	0.0	0.0	0.0	0.0	0.0	0.0	1	10
11	0.82711E+01	0.83459E+01	0.51293E+00	0.0	0.0	0.0	0.0	0.0	0.0	2	11
12	0.21742E+02	0.22293E+02	0.62396E+01	0.0	0.0	0.0	0.0	0.0	0.0	2	12
13	0.41660E+03	0.42607E+03	0.42607E+03	0.0	0.0	0.0	0.0	0.0	0.0	1	13
14	0.75559E+03	0.78585E+03	0.78585E+03	0.0	0.0	0.0	0.0	0.0	0.0	1	14
15	0.21179E+02	0.21537E+02	0.40655E+01	0.0	0.0	0.0	0.0	0.0	0.0	2	15
16	0.17756E+02	0.18405E+02	0.86401E+01	0.0	0.0	0.0	0.0	0.0	0.0	2	16
17	0.19635E+02	0.19927E+02	0.75709E+01	0.0	0.0	0.0	0.0	0.0	0.0	2	17
18	0.15935E+02	0.16404E+02	0.16040E+01	0.0	0.0	0.0	0.32508E-01	0.0	0.0	2	18
19	0.19151E+02	0.19956E+02	0.11647E+01	0.22634E-01	0.28153E+01	0.33966E-01	0.0	0.0	0.0	2	19
20	0.13175E+02	0.13551E+02	0.26870E+01	0.10325E-02	0.30480E+01	0.33966E-01	0.0	0.0	0.0	2	20
21	0.23516E+00	0.24095E+00	0.24095E+00	0.0	0.0	0.0	0.0	0.0	0.0	1	21
22	0.68531E+00	0.70139E+00	0.70139E+00	0.0	0.0	0.0	0.0	0.0	0.0	1	22
23	0.14600E+02	0.14651E+02	0.10725E+01	0.0	0.0	0.33273E-01	0.0	0.0	0.0	2	23
24	0.15909E+02	0.16572E+02	0.77017E+00	0.58342E+01	0.25629E+01	0.33273E-01	0.0	0.0	0.0	2	24
25	0.12206E+02	0.12736E+02	0.14756E+01	0.63238E-02	0.25120E+01	0.32508E-01	0.0	0.0	0.0	2	25
26	0.16065E+02	0.16766E+02	0.18293E+01	0.41060E+01	0.24436E+01	0.32508E-01	0.0	0.0	0.0	2	26
27	0.14837E+02	0.15522E+02	0.47879E+01	0.96829E-03	0.25140E+01	0.32436E-01	0.0	0.0	0.0	2	27
28	0.33964E+01	0.35741E+01	0.0	0.0	0.0	0.0	0.0	0.0	0.0	2	28
29	0.10495E+00	0.10756E+00	0.10756E+00	0.0	0.0	0.0	0.0	0.0	0.0	1	29
30	0.78121E+01	0.78926E+01	0.11099E+01	0.0	0.0	0.0	0.0	0.0	0.0	2	30
31	0.87905E+01	0.88516E+01	0.13369E+01	0.0	0.0	0.0	0.0	0.0	0.0	2	31
32	0.29466E+02	0.30198E+02	0.30198E+02	0.0	0.0	0.0	0.0	0.0	0.0	1	32
33	0.85521E+01	0.86162E+01	0.27254E+01	0.0	0.0	0.0	0.0	0.0	0.0	2	33
34	0.66657E+01	0.67132E+01	0.10297E+01	0.0	0.0	0.0	0.0	0.0	0.0	2	34
35	0.29372E+00	0.30400E+00	0.30400E+00	0.0	0.0	0.0	0.0	0.0	0.0	1	35
36	0.65848E+01	0.66296E+01	0.96031E+00	0.0	0.0	0.0	0.0	0.0	0.0	2	36
37	0.20948E+02	0.21474E+02	0.89488E+00	0.0	0.0	0.0	0.0	0.0	0.0	2	37
38	0.12703E+02	0.12815E+02	0.68938E+00	0.0	0.0	0.0	0.0	0.0	0.0	2	38
39	0.12240E+02	0.12601E+02	0.67519E+00	0.0	0.0	0.0	0.0	0.0	0.0	2	39
40	0.13228E+02	0.13459E+02	0.74859E+01	0.0	0.0	0.0	0.0	0.0	0.0	2	40
41	0.10676E+02	0.10823E+02	0.38227E+01	0.0	0.0	0.0	0.0	0.0	0.0	2	41
42	0.13971E+02	0.14393E+02	0.34394E+01	0.0	0.0	0.35436E-01	0.0	0.0	0.0	2	42
43	0.15475E+02	0.15970E+02	0.95625E+00	0.11812E-03	0.23217E+01	0.34654E-01	0.0	0.0	0.0	2	43
44	0.15412E+02	0.15926E+02	0.17667E+01	0.26648E+01	0.28763E+01	0.33231E-01	0.0	0.0	0.0	2	44
45	0.15869E+02	0.16612E+02	0.16181E+01	0.13416E+00	0.28727E+01	0.33502E-01	0.0	0.0	0.0	2	45
46	0.17090E+02	0.17930E+02	0.13129E+01	0.50791E+01	0.29346E+01	0.34297E-01	0.0	0.0	0.0	2	46

TABLE C.1: (page 2 of 7)

MICROSCOPIC CROSS-SECTIONS FOR GROUP 3

I#	TRANSPORT	TOTAL	N-GAMMA	FISSION	NU	CHI	N-ALPHA	N-2N	N-D	#SCT	I#
1	0.61028E+00	0.72621E+00	0.22034E-04	0.0	0.0	0.0	0.0	0.20119E-03	0.0	2	1
2	0.45137E+01	0.47539E+01	0.13029E-03	0.0	0.0	0.0	0.0	0.0	0.0	3	2
3	0.45137E+01	0.47539E+01	0.13029E-03	0.0	0.0	0.0	0.0	0.0	0.0	3	3
4	0.35682E+01	0.37078E+01	0.91331E-05	0.0	0.0	0.0	0.0	0.0	0.0	3	4
5	0.35682E+01	0.37078E+01	0.91331E-05	0.0	0.0	0.0	0.0	0.0	0.0	3	5
6	0.32708E-01	0.32577E-01	0.32577E-01	0.0	0.0	0.0	0.0	0.0	0.0	1	6
7	0.22264E+01	0.22735E+01	0.50376E-02	0.0	0.0	0.0	0.0	0.0	0.0	3	7
8	0.33363E+02	0.30167E+02	0.30167E+02	0.0	0.0	0.0	0.0	0.0	0.0	1	8
9	0.66533E+02	0.66956E+02	0.52131E+02	0.0	0.0	0.0	0.0	0.0	0.0	3	9
10	0.43623E+01	0.43649E+01	0.43649E+01	0.0	0.0	0.0	0.0	0.0	0.0	1	10
11	0.13941E+02	0.14016E+02	0.57873E+01	0.0	0.0	0.0	0.0	0.0	0.0	3	11
12	0.40904E+03	0.41096E+03	0.30933E+01	0.0	0.0	0.0	0.0	0.0	0.0	3	12
13	0.46166E+04	0.47660E+04	0.47660E+04	0.0	0.0	0.0	0.0	0.0	0.0	1	13
14	0.81836E+04	0.80861E+04	0.80861E+04	0.0	0.0	0.0	0.0	0.0	0.0	1	14
15	0.21515E+03	0.21613E+03	0.14078E+03	0.0	0.0	0.0	0.0	0.0	0.0	3	15
16	0.24914E+03	0.24787E+03	0.23046E+03	0.0	0.0	0.0	0.0	0.0	0.0	3	16
17	0.21596E+03	0.21492E+03	0.19704E+03	0.0	0.0	0.0	0.0	0.0	0.0	3	17
18	0.69807E+02	0.70521E+02	0.44405E+02	0.0	0.0	0.0	0.0	0.0	0.0	3	18
19	0.17854E+03	0.17633E+03	0.14136E+03	0.0	0.0	0.0	0.0	0.0	0.0	3	19
20	0.56250E+02	0.58192E+02	0.45591E+02	0.0	0.0	0.0	0.0	0.0	0.0	3	20
21	0.10549E+01	0.10634E+01	0.10634E+01	0.0	0.0	0.0	0.0	0.0	0.0	1	21
22	0.11926E+02	0.11062E+02	0.11062E+02	0.0	0.0	0.0	0.0	0.0	0.0	1	22
23	0.26892E+02	0.27116E+02	0.75589E+01	0.0	0.0	0.0	0.0	0.0	0.0	3	23
24	0.87426E+02	0.87418E+02	0.14054E+02	0.61511E+02	0.25029E+01	0.0	0.0	0.0	0.0	3	24
25	0.11763E+03	0.12021E+03	0.85637E+02	0.0	0.0	0.0	0.0	0.0	0.0	3	25
26	0.61992E+02	0.61964E+02	0.19788E+02	0.33409E+02	0.24420E+01	0.0	0.0	0.0	0.0	3	26
27	0.85100E+02	0.84999E+02	0.68618E+02	0.0	0.0	0.0	0.0	0.0	0.0	3	27
28	0.35623E+01	0.37065E+01	0.0	0.0	0.0	0.0	0.0	0.0	0.0	2	28
29	0.34612E+02	0.33814E+02	0.33814E+02	0.0	0.0	0.0	0.0	0.0	0.0	1	29
30	0.38086E+01	0.46298E+02	0.26065E+02	0.0	0.0	0.0	0.0	0.0	0.0	3	30
31	0.10005E+02	0.11304E+02	0.49873E+01	0.0	0.0	0.0	0.0	0.0	0.0	3	31
32	0.47557E+03	0.47363E+03	0.47363E+03	0.0	0.0	0.0	0.0	0.0	0.0	1	32
33	0.21265E+03	0.21344E+03	0.18952E+03	0.0	0.0	0.0	0.0	0.0	0.0	3	33
34	0.45284E+03	0.44760E+03	0.11453E+03	0.0	0.0	0.0	0.0	0.0	0.0	3	34
35	0.61487E+01	0.61242E+01	0.61242E+01	0.0	0.0	0.0	0.0	0.0	0.0	1	35
36	0.21570E+02	0.21522E+02	0.10917E+02	0.0	0.0	0.0	0.0	0.0	0.0	3	36
37	0.92251E+02	0.90826E+02	0.47016E+02	0.0	0.0	0.0	0.0	0.0	0.0	3	37
38	0.81791E+02	0.83869E+02	0.43070E+02	0.0	0.0	0.0	0.0	0.0	0.0	3	38
39	0.71979E+03	0.71134E+03	0.30541E+03	0.0	0.0	0.0	0.0	0.0	0.0	3	39
40	0.10181E+03	0.10170E+03	0.96395E+02	0.0	0.0	0.0	0.0	0.0	0.0	3	40
41	0.46964E+03	0.46781E+03	0.46071E+03	0.0	0.0	0.0	0.0	0.0	0.0	3	41
42	0.67596E+02	0.67424E+02	0.56184E+02	0.0	0.0	0.68975E-05	0.0	0.0	0.0	3	42
43	0.59963E+02	0.59610E+02	0.24065E+02	0.21907E-07	0.23195E+01	0.67444E-05	0.0	0.0	0.0	3	43
44	0.72277E+02	0.72279E+02	0.25020E+02	0.33494E+02	0.28733E+01	0.64523E-05	0.0	0.0	0.0	3	44
45	0.52924E+02	0.54989E+02	0.25915E+02	0.20458E+00	0.26698E+01	0.65194E-05	0.0	0.0	0.0	3	45
46	0.10501E+03	0.10461E+03	0.16436E+02	0.75802E+02	0.29325E+01	0.66708E-05	0.0	0.0	0.0	3	46

TABLE C.1: (page 3 of 7)

MICROSCOPIC CROSS-SECTIONS FOR GROUP 4

I#	TRANSPORT	TOTAL	N-GAMMA	FISSION	NU	CHI	N-ALPHA	N-2N	N-D	#SCT	I#
1	0.83844E+00	0.77910E+00	0.26643E-02	0.0	0.0	0.0	0.0	0.0	0.0	2	1
2	0.53127E+01	0.47490E+01	0.15370E-02	0.0	0.0	0.0	0.0	0.0	0.0	4	2
3	0.53128E+01	0.47490E+01	0.15370E-02	0.0	0.0	0.0	0.0	0.0	0.0	4	3
4	0.43091E+01	0.38349E+01	0.64587E-04	0.0	0.0	0.0	0.0	0.0	0.0	4	4
5	0.43376E+01	0.38637E+01	0.69507E-04	0.0	0.0	0.0	0.0	0.0	0.0	4	5
6	0.38192E+00	0.38424E+00	0.38424E+00	0.0	0.0	0.0	0.0	0.0	0.0	1	6
7	0.20276E+01	0.17795E+01	0.61479E-01	0.0	0.0	0.0	0.0	0.0	0.0	2	7
8	0.87460E+06	0.89186E+06	0.89186E+06	0.0	0.0	0.0	0.0	0.0	0.0	1	8
9	0.11694E+02	0.11374E+02	0.11374E+02	0.0	0.0	0.0	0.0	0.0	0.0	2	9
10	0.51177E+02	0.51468E+02	0.51468E+02	0.0	0.0	0.0	0.0	0.0	0.0	1	10
11	0.36966E+01	0.33429E+01	0.33429E+01	0.0	0.0	0.0	0.0	0.0	0.0	2	11
12	0.91283E+02	0.91553E+02	0.91553E+02	0.0	0.0	0.0	0.0	0.0	0.0	2	12
13	0.10312E+05	0.10375E+05	0.10375E+05	0.0	0.0	0.0	0.0	0.0	0.0	1	13
14	0.57287E+03	0.57636E+03	0.57636E+03	0.0	0.0	0.0	0.0	0.0	0.0	1	14
15	0.28435E+05	0.28700E+05	0.28700E+05	0.0	0.0	0.0	0.0	0.0	0.0	3	15
16	0.27516E+04	0.27839E+04	0.27766E+04	0.0	0.0	0.0	0.0	0.0	0.0	2	16
17	0.15614E+03	0.15674E+03	0.15229E+03	0.0	0.0	0.0	0.0	0.0	0.0	3	17
18	0.12032E+02	0.11793E+02	0.24197E+01	0.0	0.0	0.0	0.0	0.0	0.0	2	18
19	0.22402E+02	0.22381E+02	0.13365E+02	0.0	0.0	0.0	0.0	0.0	0.0	3	19
20	0.18749E+03	0.18649E+03	0.17913E+03	0.0	0.0	0.0	0.0	0.0	0.0	3	20
21	0.42611E+00	0.42689E+00	0.42689E+00	0.0	0.0	0.0	0.0	0.0	0.0	1	21
22	0.55021E+01	0.56129E+01	0.56129E+01	0.0	0.0	0.0	0.0	0.0	0.0	1	22
23	0.15505E+02	0.15172E+02	0.20544E+01	0.0	0.0	0.0	0.0	0.0	0.0	2	23
24	0.28147E+03	0.27084E+03	0.24866E+02	0.23310E+03	0.25039E+01	0.0	0.0	0.0	0.0	2	24
25	0.40041E+02	0.39995E+02	0.39982E+02	0.0	0.0	0.0	0.0	0.0	0.0	2	25
26	0.23755E+03	0.24062E+03	0.36117E+02	0.19199E+03	0.24302E+01	0.0	0.0	0.0	0.0	4	26
27	0.33938E+02	0.30765E+02	0.20745E+02	0.0	0.0	0.0	0.0	0.0	0.0	2	27
28	0.41105E+01	0.36465E+01	0.68545E-04	0.0	0.0	0.0	0.0	0.0	0.0	2	28
29	0.17166E+02	0.17291E+02	0.17291E+02	0.0	0.0	0.0	0.0	0.0	0.0	1	29
30	0.75340E+02	0.75337E+02	0.75337E+02	0.0	0.0	0.0	0.0	0.0	0.0	2	30
31	0.20875E+03	0.20674E+03	0.20674E+03	0.0	0.0	0.0	0.0	0.0	0.0	2	31
32	0.57287E+04	0.57636E+04	0.57636E+04	0.0	0.0	0.0	0.0	0.0	0.0	1	32
33	0.36864E+02	0.36674E+02	0.36674E+02	0.0	0.0	0.0	0.0	0.0	0.0	2	33
34	0.45922E+02	0.45714E+02	0.45714E+02	0.0	0.0	0.0	0.0	0.0	0.0	2	34
35	0.72564E+02	0.73006E+02	0.73006E+02	0.0	0.0	0.0	0.0	0.0	0.0	1	35
36	0.11926E+03	0.11739E+03	0.11739E+03	0.0	0.0	0.0	0.0	0.0	0.0	2	36
37	0.23570E+02	0.22963E+02	0.22963E+02	0.0	0.0	0.0	0.0	0.0	0.0	2	37
38	0.32779E+02	0.32661E+02	0.32661E+02	0.0	0.0	0.0	0.0	0.0	0.0	2	38
39	0.84220E+02	0.84203E+02	0.84203E+02	0.0	0.0	0.0	0.0	0.0	0.0	2	39
40	0.57309E+03	0.57636E+03	0.57636E+03	0.0	0.0	0.0	0.0	0.0	0.0	2	40
41	0.53472E+04	0.53794E+04	0.53794E+04	0.0	0.0	0.0	0.0	0.0	0.0	2	41
42	0.92915E+02	0.93212E+02	0.84688E+02	0.0	0.0	0.73006E-10	0.0	0.0	0.0	4	42
43	0.10227E+02	0.99884E+01	0.16815E+01	0.64225E-08	0.23155E+01	0.12159E-08	0.0	0.0	0.0	3	43
44	0.12636E+04	0.12579E+04	0.47462E+03	0.77405E+03	0.28733E+01	0.11632E-06	0.0	0.0	0.0	3	44
45	0.14729E+04	0.14498E+04	0.13498E+04	0.25880E+03	0.28696E+01	0.11754E-08	0.0	0.0	0.0	3	45
46	0.88334E+03	0.88442E+03	0.23354E+03	0.63976E+03	0.29323E+01	0.12026E-08	0.0	0.0	0.0	2	46

TABLE C.1: (page 4 of 7)

SCATTERING CROSS-SECTIONS

	GROUP 1					GROUP 2			
I#	G--G	(G-1)--G	(G-2)--G	(G-3)--G	I#	G--G	(G-1)--G	(G-2)--G	(G-3)--G
1	0.297375E+01	0.0	0.0	0.0	1	0.67633E+00	0.17036E+00	0.0	0.0
2	0.261402E+01	0.0	0.0	0.0	2	0.45120E+01	0.19574E+00	0.0	0.0
3	0.261405E+01	0.0	0.0	0.0	3	0.45119E+01	0.19574E+00	0.0	0.0
4	0.344442E+01	0.0	0.0	0.0	4	0.35209E+01	0.13720E+00	0.0	0.0
5	0.344443E+01	0.0	0.0	0.0	5	0.35209E+01	0.13720E+00	0.0	0.0
6	0.0	0.0	0.0	0.0	6	0.0	0.0	0.0	0.0
7	0.368496E+01	0.0	0.0	0.0	7	0.19848E+01	0.22462E+00	0.0	0.0
8	0.0	0.0	0.0	0.0	8	0.0	0.0	0.0	0.0
9	0.594062E+01	0.0	0.0	0.0	9	0.79017E+01	0.24998E+00	0.0	0.0
10	0.0	0.0	0.0	0.0	10	0.0	0.0	0.0	0.0
11	0.594401E+01	0.0	0.0	0.0	11	0.77921E+01	0.25012E+00	0.0	0.0
12	0.600795E+01	0.0	0.0	0.0	12	0.16027E+02	0.99440E-01	0.0	0.0
13	0.0	0.0	0.0	0.0	13	0.0	0.0	0.0	0.0
14	0.0	0.0	0.0	0.0	14	0.0	0.0	0.0	0.0
15	0.675428E+01	0.0	0.0	0.0	15	0.16802E+02	0.34126E+00	0.0	0.0
16	0.840344E+01	0.0	0.0	0.0	16	0.97570E+01	0.38262E+00	0.0	0.0
17	0.671402E+01	0.0	0.0	0.0	17	0.12319E+02	0.75238E+00	0.0	0.0
18	0.780844E+01	0.0	0.0	0.0	18	0.14756E+02	0.22606E+00	0.0	0.0
19	0.682702E+01	0.0	0.0	0.0	19	0.18722E+02	0.12033E+00	0.0	0.0
20	0.669768E+01	0.0	0.0	0.0	20	0.10849E+02	0.59385E+00	0.0	0.0
21	0.0	0.0	0.0	0.0	21	0.0	0.0	0.0	0.0
22	0.0	0.0	0.0	0.0	22	0.0	0.0	0.0	0.0
23	0.740152E+01	0.0	0.0	0.0	23	0.13741E+02	0.21960E+00	0.0	0.0
24	0.534594E+01	0.0	0.0	0.0	24	0.10004E+02	0.15216E+00	0.0	0.0
25	0.660494E+01	0.0	0.0	0.0	25	0.11235E+02	0.17014E+00	0.0	0.0
26	0.622522E+01	0.0	0.0	0.0	26	0.10814E+02	0.16193E+00	0.0	0.0
27	0.646031E+01	0.0	0.0	0.0	27	0.10715E+02	0.43529E+00	0.0	0.0
28	0.360331E+01	0.0	0.0	0.0	28	0.35037E+01	0.11891E+00	0.0	0.0
29	0.0	0.0	0.0	0.0	29	0.0	0.0	0.0	0.0
30	0.555413E+01	0.0	0.0	0.0	30	0.67566E+01	0.83152E-01	0.0	0.0
31	0.622086E+01	0.0	0.0	0.0	31	0.74958E+01	0.13332E+00	0.0	0.0
32	0.0	0.0	0.0	0.0	32	0.0	0.0	0.0	0.0
33	0.589972E+01	0.0	0.0	0.0	33	0.58644E+01	0.15893E+00	0.0	0.0
34	0.612695E+01	0.0	0.0	0.0	34	0.56718E+01	0.12510E+00	0.0	0.0
35	0.0	0.0	0.0	0.0	35	0.0	0.0	0.0	0.0
36	0.610478E+01	0.0	0.0	0.0	36	0.56513E+01	0.86366E-01	0.0	0.0
37	0.628302E+01	0.0	0.0	0.0	37	0.20544E+02	0.88970E-01	0.0	0.0
38	0.693711E+01	0.0	0.0	0.0	38	0.11026E+02	0.19625E+00	0.0	0.0
39	0.693684E+01	0.0	0.0	0.0	39	0.11026E+02	0.19624E+00	0.0	0.0
40	0.661444E+01	0.0	0.0	0.0	40	0.59616E+01	0.21941E+00	0.0	0.0
41	0.678292E+01	0.0	0.0	0.0	41	0.69851E+01	0.20819E+00	0.0	0.0
42	0.626338E+01	0.0	0.0	0.0	42	0.10847E+02	0.93713E+00	0.0	0.0
43	0.779422E+01	0.0	0.0	0.0	43	0.14999E+02	0.20554E+00	0.0	0.0
44	0.610866E+01	0.0	0.0	0.0	44	0.11464E+02	0.14741E+00	0.0	0.0
45	0.672402E+01	0.0	0.0	0.0	45	0.14846E+02	0.14233E+00	0.0	0.0
46	0.686702E+01	0.0	0.0	0.0	46	0.11521E+02	0.27986E+00	0.0	0.0

TABLE C.1: (page 5 of 7)

SCATTERING CROSS-SECTIONS

I#	GROUP 3 G--G	(G-1)--G	(G-2)--G	(G-3)--G	I#	GROUP 4 G--G	(G-1)--G	(G-2)--G	(G-3)--G
1	0.68520E+00	0.49671E-01	0.0	0.0	1	0.77640E+00	0.38775E-01	0.0	0.0
2	0.46616E+01	0.11976E+00	0.25055E-06	0.0	2	0.47472E+01	0.92138E-01	0.0	0.62149E-09
3	0.46616E+01	0.11976E+00	0.25055E-06	0.0	3	0.47474E+01	0.92138E-01	0.0	0.62149E-09
4	0.36526E+01	0.70342E-01	0.77442E-07	0.0	4	0.38346E+01	0.55214E-01	0.0	0.68994E-10
5	0.36525E+01	0.70342E-01	0.77442E-07	0.0	5	0.38633E+01	0.55214E-01	0.0	0.68994E-10
6	0.0	0.0	0.0	0.0	6	0.0	0.0	0.0	0.0
7	0.22493E+01	0.26482E-01	0.93927E-08	0.0	7	0.17180E+01	0.19180E-01	0.0	0.0
8	0.0	0.0	0.0	0.0	8	0.0	0.0	0.0	0.0
9	0.14811E+02	0.24658E-01	0.37687E-05	0.0	9	0.0	0.13907E-01	0.0	0.0
10	0.0	0.0	0.0	0.0	10	0.0	0.0	0.0	0.0
11	0.82095E+01	0.20795E-01	0.37687E-05	0.0	11	0.0	0.13539E-01	0.0	0.0
12	0.10155E+03	0.26430E-01	0.10527E-05	0.0	12	0.0	0.89495E-02	0.0	0.0
13	0.0	0.0	0.0	0.0	13	0.0	0.0	0.0	0.0
14	0.0	0.0	0.0	0.0	14	0.0	0.0	0.0	0.0
15	0.75337E+02	0.79734E-01	0.36820E-04	0.0	15	0.19925E+03	0.18544E-01	0.96830E-08	0.0
16	0.17311E+02	0.18125E-01	0.71175E-05	0.0	16	0.72456E+01	0.69081E-02	0.0	0.0
17	0.17834E+02	0.37240E-01	0.54102E-04	0.0	17	0.44085E+01	0.30088E-02	0.11021E-06	0.0
18	0.26137E+02	0.44447E-01	0.66037E-07	0.0	18	0.93738E+01	0.91503E-02	0.0	0.0
19	0.34451E+02	0.47148E-01	0.63495E-08	0.0	19	0.90155E+01	0.28833E-02	0.84178E-09	0.0
20	0.12563E+02	0.16493E-01	0.11082E-04	0.0	20	0.73629E+01	0.17713E-01	0.0	0.0
21	0.0	0.0	0.0	0.0	21	0.0	0.0	0.0	0.0
22	0.0	0.0	0.0	0.0	22	0.0	0.0	0.0	0.0
23	0.19545E+02	0.36523E-01	0.34639E-05	0.0	23	0.12517E+02	0.12775E-01	0.0	0.0
24	0.11836E+02	0.16279E-01	0.34921E-05	0.0	24	0.12521E+02	0.12909E-01	0.0	0.0
25	0.35159E+02	0.16486E-01	0.26796E-05	0.0	25	0.90124E+01	0.10683E-01	0.0	0.0
26	0.11753E+02	0.16479E-01	0.30367E-04	0.0	26	0.12517E+02	0.13931E-01	0.12086E-07	0.19825E-06
27	0.16370E+02	0.19301E-01	0.88455E-05	0.0	27	0.10016E+02	0.10728E-01	0.0	0.0
28	0.36465E+01	0.70372E-01	0.0	0.0	28	0.36461E+01	0.53914E-01	0.0	0.0
29	0.0	0.0	0.0	0.0	29	0.0	0.0	0.0	0.0
30	0.14215E+02	0.26085E-01	0.43350E-06	0.0	30	0.0	0.18218E-01	0.0	0.0
31	0.63795E+01	0.19108E-01	0.12186E-05	0.0	31	0.0	0.16761E-01	0.0	0.0
32	0.0	0.0	0.0	0.0	32	0.0	0.0	0.0	0.0
33	0.23924E+02	0.26264E-01	0.17932E-05	0.0	33	0.0	0.13410E-01	0.0	0.0
34	0.33308E+03	0.11670E-01	0.14298E-05	0.0	34	0.0	0.21225E-01	0.0	0.0
35	0.0	0.0	0.0	0.0	35	0.0	0.0	0.0	0.0
36	0.10543E+02	0.12203E-01	0.87145E-06	0.0	36	0.0	0.61057E-01	0.0	0.0
37	0.43782E+02	0.35330E-01	0.87144E-06	0.0	37	0.0	0.26900E-01	0.0	0.0
38	0.43808E+02	0.99252E-01	0.26879E-05	0.0	38	0.0	0.11386E-01	0.0	0.0
39	0.43591E+03	0.99252E-01	0.26878E-05	0.0	39	0.0	0.16856E-01	0.0	0.0
40	0.53014E+01	0.11773E-01	0.32178E-05	0.0	40	0.0	0.79175E-02	0.0	0.0
41	0.70813E+01	0.15037E-01	0.29146E-05	0.0	41	0.0	0.12586E-01	0.0	0.0
42	0.11226E+02	0.15395E-01	0.24022E-04	0.0	42	0.85244E+01	0.13720E-01	0.17979E-08	0.40799E-10
43	0.35595E+02	0.14422E-01	0.15975E-05	0.0	43	0.89068E+01	0.88946E-02	0.31552E-08	0.0
44	0.13156E+02	0.28075E-01	0.22614E-05	0.0	44	0.92687E+01	0.99476E-02	0.15797E-08	0.0
45	0.28840E+02	0.13028E-01	0.71449E-06	0.0	45	0.99707E+02	0.29057E-01	0.23178E-09	0.0
46	0.12363E+02	0.17353E-01	0.15484E-05	0.0	46	0.11120E+02	0.87371E-02	0.0	0.0

TABLE C.1: (page 6 of 7)

CALCULATED CROSS-SECTIONS

REMOVAL

I#	GROUP 1	GROUP 2	GROUP 3	GROUP 4
1	0.17086E+00	0.49671E-01	0.38775E-01	0.0
2	0.19574E+00	0.11976E+00	0.92136E-01	0.0
3	0.19574E+00	0.11976E+00	0.92136E-01	0.0
4	0.13720E+00	0.70342E-01	0.55214E-01	0.0
5	0.13720E+00	0.70342E-01	0.55214E-01	0.0
6	0.0	0.0	0.0	0.0
7	0.22462E+00	0.26492E-01	0.19180E-01	0.0
8	0.0	0.0	0.0	0.0
9	0.24999E+00	0.24658E-01	0.13907E-01	0.0
10	0.0	0.0	0.0	0.0
11	0.25012E+00	0.20796E-01	0.13539E-01	0.0
12	0.19440E-01	0.26430E-01	0.89495E-02	0.0
13	0.0	0.0	0.0	0.0
14	0.0	0.0	0.0	0.0
15	0.34126E+00	0.79734E-01	0.18544E-01	0.0
16	0.38262E+00	0.18125E-01	0.69081E-02	0.0
17	0.75284E+00	0.37240E-01	0.30066E-02	0.0
18	0.22606E+00	0.44497E-01	0.91503E-02	0.0
19	0.12033E+00	0.47148E-01	0.28833E-02	0.0
20	0.59365E+00	0.16493E-01	0.17713E-01	0.0
21	0.0	0.0	0.0	0.0
22	0.0	0.0	0.0	0.0
23	0.21960E+00	0.36523E-01	0.12775E-01	0.0
24	0.15216E+00	0.16279E-01	0.12909E-01	0.0
25	0.17014E+00	0.18486E-01	0.10083E-01	0.0
26	0.16193E+00	0.16479E-01	0.13931E-01	0.0
27	0.43529E+00	0.19301E-01	0.10720E-01	0.0
28	0.11691E+00	0.70372E-01	0.53914E-01	0.0
29	0.0	0.0	0.0	0.0
30	0.83152E-01	0.26045E-01	0.18218E-01	0.0
31	0.13332E+00	0.19108E-01	0.16761E-01	0.0
32	0.0	0.0	0.0	0.0
33	0.15893E+00	0.26264E-01	0.13410E-01	0.0
34	0.12510E+00	0.11670E-01	0.21225E-01	0.0
35	0.0	0.0	0.0	0.0
36	0.88366E-01	0.12203E-01	0.61657E-01	0.0
37	0.88972E-01	0.35330E-01	0.26900E-01	0.0
38	0.19625E+00	0.99252E-01	0.11386E-01	0.0
39	0.19624E+00	0.99252E-01	0.10656E-01	0.0
40	0.21941E+00	0.11773E-01	0.79175E-02	0.0
41	0.20819E+00	0.15037E-01	0.12586E-01	0.0
42	0.93713E+00	0.15395E-01	0.13720E-01	0.0
43	0.20554E+00	0.14422E-01	0.88446E-02	0.0
44	0.14741E+00	0.26075E-01	0.99476E-02	0.0
45	0.14233E+00	0.13020E-01	0.29057E-01	0.0
46	0.27986E+00	0.17353E-01	0.87371E-02	0.0

ABSORPTION

I#	GROUP 1	GROUP 2	GROUP 3	GROUP 4
1	-0.11945E-05	-0.13188E-04	-0.17836E-03	0.26643E-02
2	0.15079E-03	0.83131E-05	0.13029E-03	0.15370E-02
3	0.15079E-03	0.83131E-05	0.13029E-03	0.15370E-02
4	0.23043E-02	0.17946E-06	0.91330E-05	0.69587E-04
5	0.23043E-02	0.17946E-06	0.91330E-05	0.69587E-04
6	0.19311E-03	0.20784E-02	0.32577E-01	0.38424E+00
7	-0.22884E-02	0.79831E-03	0.50376E-02	0.61479E-01
8	0.0	0.15216E-04	0.30167E+02	0.89166E+06
9	0.53573E-01	0.14040E+01	0.52131E+02	0.11374E+02
10	0.0	0.21660E+00	0.43649E+01	0.51488E+02
11	0.31018E-01	0.53293E+00	0.57873E+01	0.33429E+01
12	0.26520E+00	0.62396E+01	0.30933E+03	0.91553E+02
13	0.52134E+01	0.42607E+03	0.47660E+04	0.10375E+05
14	0.13516E+00	0.78585E+03	0.80861E+04	0.57636E+03
15	0.20769E+00	0.46552E+01	0.14076E+03	0.28700E+05
16	0.62961E+00	0.86401E+01	0.23046E+03	0.27766E+04
17	0.20462E+00	0.75709E+01	0.19708E+03	0.15229E+03
18	0.56907E+00	0.16030E+01	0.44405E+02	0.24197E+01
19	0.91371E+00	0.11874E+01	0.14188E+03	0.13365E+02
20	0.75462E+00	0.26880E+01	0.45591E+02	0.17913E+03
21	0.19746E-01	0.24095E+00	0.10634E+01	0.42689E+00
22	0.68788E-01	0.70139E+00	0.11002E+02	0.56129E+01
23	0.17425E+00	0.10725E+01	0.75580E+01	0.26544E+01
24	0.20961E+01	0.65524E+01	0.75566E+02	0.25797E+03
25	0.10281E+01	0.14819E+01	0.85037E+02	0.30982E+02
26	0.13731E+01	0.59353E+01	0.50197E+02	0.22810E+03
27	0.11508E+01	0.47882E+01	0.60618E+02	0.20749E+02
28	0.30764E-02	0.0	0.0	0.68395E-04
29	0.99569E-02	0.10756E+00	0.33814E+02	0.17291E+02
30	0.69530E-01	0.11099E+01	0.26065E+02	0.75337E+02
31	0.16131E+00	0.13368E+01	0.49873E+01	0.20674E+03
32	0.28011E+01	0.30198E+02	0.47363E+03	0.57636E+04
33	0.35337E+00	0.27254E+01	0.18950E+03	0.36674E+02
34	0.74408E-01	0.10297E+01	0.11450E+03	0.45714E+02
35	0.0	0.30400E+00	0.61242E+01	0.73006E+02
36	0.46560E-01	0.96633E+00	0.10017E+02	0.11739E+03
37	0.42671E-01	0.89488E+00	0.47016E+02	0.22963E+02
38	0.48290E-01	0.68939E+00	0.43070E+02	0.32661E+02
39	0.49228E-01	0.67518E+00	0.30541E+03	0.84203E+02
40	0.47528E+00	0.74859E+01	0.96395E+02	0.57636E+03
41	0.10849E+00	0.38227E+01	0.46071E+03	0.53794E+04
42	0.47002E+00	0.34394E+01	0.56184E+02	0.84688E+02
43	0.24846E+00	0.95636E+00	0.24005E+02	0.10815E+01
44	0.17729E+01	0.44336E+01	0.59114E+02	0.12487E+04
45	0.10938E+01	0.17522E+01	0.26120E+02	0.13501E+04
46	0.17649E+01	0.63920E+01	0.92238E+02	0.87330E+03

TABLE C.1: (page 7 of 7)

MICROSCOPIC CROSS-SECTIONS FOR GROUP 1

I#	TRANSPORT	TOTAL	N-GAMMA	FISSION	NU	CHI	N-ALPHA	N-2N	N-D	ISCT	I#
1	0.27499E+01	0.31559E+01	0.0	0.0	0.0	0.0	0.0	0.11935E-05	0.0	1	1
2	0.22520E+01	0.28052E+01	0.770928E-06	0.0	0.0	0.0	0.14959E-03	0.0	0.0	1	2
3	0.22520E+01	0.28052E+01	0.770918E-06	0.0	0.0	0.0	0.14959E-03	0.0	0.0	1	3
4	0.29161E+01	0.35787E+01	-0.12241E-09	0.0	0.0	0.0	0.23141E-02	0.38260E-05	0.0	1	4
5	0.29161E+01	0.35787E+01	-0.12241E-09	0.0	0.0	0.0	0.23141E-02	0.38260E-05	0.0	1	5
6	0.17378E-03	0.19274E-03	0.19274E-03	0.0	0.0	0.0	0.0	0.0	0.0	1	6
7	0.27591E+01	0.34055E+01	0.34457E-03	0.0	0.0	0.0	0.0	0.26357E-02	0.0	1	7
8	0.0	0.0	0.0	0.0	0.0	0.0	0.0	0.0	0.0	1	8
9	0.43698E+01	0.62431E+01	0.530448E-01	0.0	0.0	0.0	0.0	0.0	0.32735E-03	1	9
10	0.0	0.0	0.0	0.0	0.0	0.0	0.0	0.0	0.0	1	10
11	0.60812E+01	0.62242E+01	0.305B2E-01	0.0	0.0	0.0	0.0	0.0	0.32735E-03	1	11
12	0.60839E+01	0.63742E+01	0.284448E+00	0.0	0.0	0.0	0.0	0.0	0.28824E-03	1	12
13	0.46073E+01	0.52015E+01	0.52015E+01	0.0	0.0	0.0	0.0	0.0	0.0	1	13
14	0.11945E+00	0.13485E+00	0.13485E+00	0.0	0.0	0.0	0.0	0.0	0.0	1	14
15	0.56637E+01	0.72965E+01	0.20397E+00	0.0	0.0	0.0	0.40127E-04	0.40127E-04	0.27329E-02	1	15
16	0.49336E+01	0.73945E+01	0.62769E+00	0.0	0.0	0.0	0.0	0.0	0.0	1	16
17	0.59636E+01	0.76674E+01	0.20330E+00	0.0	0.0	0.0	0.16450E-04	0.16450E-04	0.46853E-03	1	17
18	0.60094E+01	0.85931E+01	0.23336E+00	0.33547E+00	0.2e704E+01	0.96749E+00	0.0	0.0	0.18228E-02	1	18
19	0.51458E+01	0.78535E+01	0.79751E-01	0.83593E+00	0.30694E+01	0.96903E+00	0.0	0.0	0.14029E-02	1	19
20	0.57488E+01	0.80445E+01	0.11202E+00	0.64550E+00	0.33050E+01	0.96903E+00	0.0	0.0	0.0	1	20
21	0.10627E-01	0.19688E-01	0.19688E-01	0.0	0.0	0.0	0.0	0.0	0.0	1	21
22	0.58490E-01	0.68585E-01	0.68585E-01	0.0	0.0	0.0	0.0	0.0	0.0	1	22
23	0.61323E+01	0.77760E+01	0.13291E+00	0.36493E-01	0.23655E+01	0.96673E+00	0.0	0.0	0.47203E-02	1	23
24	0.54629E+01	0.75840E+01	0.99776E-01	0.19928E+01	0.26037E+01	0.96673E+00	0.0	0.0	0.21304E-02	1	24
25	0.51455E+01	0.77964E+01	0.14498E+00	0.88522E+00	0.26876E+01	0.96749E+00	0.0	0.0	0.68105E-03	1	25
26	0.54106E+01	0.77491E+01	0.13394E+00	0.12359E+01	0.25713E+01	0.96749E+00	0.0	0.0	0.26140E-02	1	26
27	0.58665E+01	0.80460E+01	0.17e[illegible]E+00	0.98239E+00	0.26862E+01	0.96756E+00	0.0	0.0	0.20811E-02	1	27
28	0.26944E+01	0.37195E+01	0.46942E-08	0.0	0.0	0.0	0.30877E-02	0.41312E-05	0.0	1	28
29	0.87978E-02	0.99340E-02	0.99340E-02	0.0	0.0	0.0	0.0	0.0	0.0	1	29
30	0.54410E+01	0.57037E+01	0.69295E-01	0.0	0.0	0.0	0.0	0.0	0.17130E-04	1	30
31	0.61261E+01	0.65099E+01	0.16075E+00	0.0	0.0	0.0	0.0	0.0	0.14718E-03	1	31
32	0.24745E+01	0.27947E+01	0.27947E+01	0.0	0.0	0.0	0.0	0.0	0.0	1	32
33	0.60405E+01	0.64066E+01	0.35232E+00	0.0	0.0	0.0	0.0	0.0	0.20545E-03	1	33
34	0.61945E+01	0.65263E+01	0.73854E-01	0.0	0.0	0.0	0.0	0.0	0.35856E-03	1	34
35	0.0	0.0	0.0	0.0	0.0	0.0	0.0	0.0	0.0	1	35
36	0.64099E+01	0.64400E+01	0.45438E-01	0.0	0.0	0.0	0.0	0.0	0.97526E-03	1	36
37	0.64134E+01	0.64153E+01	0.41558E-01	0.0	0.0	0.0	0.0	0.0	0.97527E-03	1	37
38	0.50923E+01	0.71740E+01	0.45503E-01	0.0	0.0	0.0	0.0	0.0	0.26640E-02	1	38
39	0.50931E+01	0.71755E+01	0.46439E-01	0.0	0.0	0.0	0.0	0.0	0.26640E-02	1	39
40	0.71703E+01	0.73083E+01	0.47427E+00	0.0	0.0	0.0	0.0	0.0	0.41367E-03	1	40
41	0.70350E+01	0.71565E+01	0.16777E+00	0.0	0.0	0.0	0.0	0.0	0.40498E-03	1	41
42	0.55105E+01	0.76637E+01	0.23702E+00	0.23310E+00	0.25955E+01	0.96456E+00	0.0	0.0	0.94526E-03	1	42
43	0.55234E+01	0.82342E+01	0.95360E-01	0.15000E+00	0.27330E+01	0.96535E+00	0.0	0.0	0.38010E-02	1	43
44	0.55945E+01	0.80220E+01	0.73969E-01	0.16986E+01	0.30520E+01	0.96677E+00	0.0	0.0	0.79930E-03	1	44
45	0.55253E+01	0.79541E+01	0.11671E+00	0.98040E+00	0.31175E+01	0.96645E+00	0.0	0.0	0.31836E-03	1	45
46	0.56471E+01	0.86924E+01	0.13254E+00	0.16265E+01	0.31025E+01	0.96570E+00	0.0	0.0	0.56874E-02	1	46

TABLE C.2: FOUR-GROUP CROSS-SECTIONS FOR C/HM = 250 (page 1 of 7)

MICROSCOPIC CROSS-SECTIONS FOR GROUP 2

I#	TRANSPORT	TOTAL	N-GAMMA	FISSION	NU	CHI	N-ALPHA	N-2N	N-D	#SCT	I#
1	0.6d331E+00	0.726008E+00	0.0	0.0	0.0	0.0	0.0	0.13306E-04	0.0	2	1
2	0.435222E+01	0.463278E+01	0.83d26E-05	0.0	0.0	0.0	0.0	0.0	0.0	2	2
3	0.435222E+01	0.463278E+01	0.83b2[illegible]E-05	0.0	0.0	0.0	0.0	0.0	0.0	2	3
4	0.345806E+01	0.359188E+01	0.184128E-06	0.0	0.0	0.0	0.0	0.0	0.0	2	4
5	0.344796E+01	0.359188E+01	0.184128E-06	0.0	0.0	0.0	0.0	0.0	0.0	2	5
6	0.204497E-02	0.209578E-02	0.209578E-02	0.0	0.0	0.0	0.0	0.0	0.0	1	6
7	0.194559E+01	0.201648E+01	0.799468E-03	0.0	0.0	0.0	0.0	0.0	0.0	2	7
8	0.150193E-04	0.156038E-04	0.156038E-04	0.0	0.0	0.0	0.0	0.0	0.0	1	8
9	0.925191E+01	0.935448E+01	0.142008E+01	0.0	0.0	0.0	0.0	0.0	0.0	2	9
10	0.212658E+00	0.219348E+00	0.219348E+00	0.0	0.0	0.0	0.0	0.0	0.0	1	10
11	0.820468E+01	0.835738E+01	0.539228E+00	0.0	0.0	0.0	0.0	0.0	0.0	2	11
12	0.219278E+02	0.224488E+02	0.631708E+01	0.0	0.0	0.0	0.0	0.0	0.0	2	12
13	0.419318E+03	0.433068E+03	0.433068E+03	0.0	0.0	0.0	0.0	0.0	0.0	1	13
14	0.774308E+03	0.799568E+03	0.799568E+03	0.0	0.0	0.0	0.0	0.0	0.0	1	14
15	0.213478E+02	0.216748E+02	0.476648E+01	0.0	0.0	0.0	0.0	0.0	0.0	2	15
16	0.176378E+02	0.186678E+02	0.676748E+01	0.0	0.0	0.0	0.0	0.0	0.0	2	16
17	0.197628E+02	0.200308E+02	0.764598E+01	0.0	0.0	0.0	0.0	0.0	0.0	2	17
18	0.160108E+02	0.164638E+02	0.161768E+01	0.0	0.0	0.0	0.32508E-01	0.0	0.0	2	18
19	0.172598E+02	0.206408E+02	0.117718E+01	0.22472E-01	0.28152E+01	0.30966E-01	0.0	0.0	0.0	2	19
20	0.132228E+02	0.135908E+02	0.271418E+01	0.10233E-02	0.30480E+01	0.30966E-01	0.0	0.0	0.0	2	20
21	0.237658E+00	0.242928E+00	0.242928E+00	0.0	0.0	0.0	0.0	0.0	0.0	1	21
22	0.692268E+00	0.706898E+00	0.706898E+00	0.0	0.0	0.0	0.0	0.0	0.0	1	22
23	0.146798E+02	0.149198E+02	0.111388E+01	0.0	0.0	0.33273E-01	0.0	0.0	0.0	2	23
24	0.153748E+02	0.166218E+02	0.724278E+00	0.58685E+01	0.25029E+01	0.33273E-01	0.0	0.0	0.0	2	24
25	0.122738E+02	0.127368E+02	0.148268E+01	0.62662E-02	0.25120E+01	0.32508E-01	0.0	0.0	0.0	2	25
26	0.161348E+02	0.166168E+02	0.184628E+01	0.41342E+01	0.24436E+01	0.32508E-01	0.0	0.0	0.0	2	26
27	0.148928E+02	0.155878E+02	0.483138E+01	0.95937E-03	0.25140E+01	0.32436E-01	0.0	0.0	0.0	2	27
28	0.336658E+01	0.357498E+01	0.0	0.0	0.0	0.0	0.0	0.0	0.0	2	28
29	0.106078E+00	0.110468E+00	0.100468E+00	0.0	0.0	0.0	0.0	0.0	0.0	1	29
30	0.762608E+01	0.796408E+01	0.112128E+01	0.0	0.0	0.0	0.0	0.0	0.0	2	30
31	0.879598E+01	0.886568E+01	0.134688E+01	0.0	0.0	0.0	0.0	0.0	0.0	2	31
32	0.297d0E+02	0.304518E+02	0.304518E+02	0.0	0.0	0.0	0.0	0.0	0.0	1	32
33	0.857258E+01	0.863268E+01	0.273748E+01	0.0	0.0	0.0	0.0	0.0	0.0	2	33
34	0.667528E+01	0.672848E+01	0.104228E+01	0.0	0.0	0.0	0.0	0.0	0.0	2	34
35	0.298458E+00	0.307658E+00	0.307858E+00	0.0	0.0	0.0	0.0	0.0	0.0	1	35
36	0.659858E+01	0.664088E+01	0.979638E+00	0.0	0.0	0.0	0.0	0.0	0.0	2	36
37	0.219938E+02	0.216308E+02	0.906678E+00	0.0	0.0	0.0	0.0	0.0	0.0	2	37
38	0.123578E+02	0.126038E+02	0.698718E+00	0.0	0.0	0.0	0.0	0.0	0.0	2	38
39	0.123438E+02	0.126498E+02	0.648258E+00	0.0	0.0	0.0	0.0	0.0	0.0	2	39
40	0.133268E+02	0.135388E+02	0.756678E+01	0.0	0.0	0.0	0.0	0.0	0.0	2	40
41	0.107348E+02	0.108708E+02	0.386958E+01	0.0	0.0	0.0	0.0	0.0	0.0	2	41
42	0.143128E+02	0.147358E+02	0.347148E+01	0.0	0.0	0.35436E-01	0.0	0.0	0.0	2	42
43	0.155248E+02	0.160088E+02	0.965238E+00	0.12014E-03	0.23217E+01	0.34654E-01	0.0	0.0	0.0	2	43
44	0.154718E+02	0.159718E+02	0.178678E+01	0.26801E+01	0.28763E+01	0.33231E-01	0.0	0.0	0.0	2	44
45	0.159328E+02	0.166598E+02	0.163358E+01	0.13500E+00	0.28727E+01	0.33558E-01	0.0	0.0	0.0	2	45
46	0.171678E+02	0.179868E+02	0.132458E+01	0.51154E+01	0.29346E+01	0.34297E-01	0.0	0.0	0.0	2	46

TABLE C.2: (page 2 of 7)

MICROSCOPIC CROSS-SECTIONS FOR GROUP 3

I#	TRANSPORT	TOTAL	N-GAMMA	FISSION	NU	CHI	N-ALPHA	N-2N	N-D	#SCT	I#
1	0.607095E+00	0.724252E+00	0.268452E-04	0.0	0.0	0.0	0.0	0.213278-03	0.0	2	1
2	0.450306E+01	0.475412E+01	0.139579E-03	0.0	0.0	0.0	0.0	0.0	0.0	3	2
3	0.450311E+01	0.475411E+01	0.139598-03	0.0	0.0	0.0	0.0	0.0	0.0	3	3
4	0.350837E+01	0.371C0E+01	0.939668-05	0.0	0.0	0.0	0.0	0.0	0.0	3	4
5	0.350836E+01	0.371008+01	0.939C6E-05	0.0	0.0	0.0	0.0	0.0	0.0	3	5
6	0.349684E-01	0.349011E-01	0.349012E-01	0.0	0.0	0.0	0.0	0.0	0.0	1	6
7	0.222303E+01	0.227278+01	0.541838-02	0.0	0.0	0.0	0.0	0.0	0.0	3	7
8	0.349068+02	0.347988+02	0.347988+02	0.0	0.0	0.0	0.0	0.0	0.0	1	8
9	0.707018+02	0.710198+02	0.506838+02	0.0	0.0	0.0	0.0	0.0	0.0	3	9
10	0.466456+01	0.467628+01	0.467628+01	0.0	0.0	0.0	0.0	0.0	0.0	1	10
11	0.136918+02	0.137448+02	0.554968+01	0.0	0.0	0.0	0.0	0.0	0.0	3	11
12	0.450888+03	0.450158+03	0.337408+03	0.0	0.0	0.0	0.0	0.0	0.0	3	12
13	0.460938+04	0.458198+04	0.458198+04	0.0	0.0	0.0	0.0	0.0	0.0	1	13
14	0.762788+04	0.757478+04	0.757478+04	0.0	0.0	0.0	0.0	0.0	0.0	1	14
15	0.219048+03	0.219708+03	0.146718+03	0.0	0.0	0.0	0.0	0.0	0.0	3	15
16	0.270088+03	0.269468+03	0.251218+03	0.0	0.0	0.0	0.0	0.0	0.0	3	16
17	0.231338+03	0.230888+03	0.213318+03	0.0	0.0	0.0	0.0	0.0	0.0	3	17
18	0.720628+02	0.725748+02	0.471838+02	0.0	0.0	0.0	0.0	0.0	0.0	3	18
19	0.197348+03	0.196078+03	0.160938+03	0.0	0.0	0.0	0.0	0.0	0.0	3	19
20	0.602478+02	0.602928+02	0.477478+02	0.0	0.0	0.0	0.0	0.0	0.0	3	20
21	0.101918+01	0.102368+01	0.102368+01	0.0	0.0	0.0	0.0	0.0	0.0	1	21
22	0.113238+02	0.113198+02	0.113198+02	0.0	0.0	0.0	0.0	0.0	0.0	1	22
23	0.241898+02	0.238438+02	0.940378+01	0.0	0.0	0.0	0.0	0.0	0.0	3	23
24	0.932178+02	0.932498+02	0.151678+02	0.66187E+02	0.250298+01	0.0	0.0	0.0	0.0	3	24
25	0.121408+03	0.121818+03	0.855768+02	0.0	0.0	0.0	0.0	0.0	0.0	3	25
26	0.629928+02	0.630078+02	0.203698+02	0.30971E+02	0.244208+01	0.0	0.0	0.0	0.0	3	26
27	0.879308+02	0.878968+02	0.716228+02	0.0	0.0	0.0	0.0	0.0	0.0	3	27
28	0.355588+01	0.370058+01	0.0	0.0	0.0	0.0	0.0	0.0	0.0	2	28
29	0.333308+02	0.334528+02	0.334528+02	0.0	0.0	0.0	0.0	0.0	0.0	1	29
30	0.400458+02	0.410018+02	0.267038+02	0.0	0.0	0.0	0.0	0.0	0.0	3	30
31	0.113028+02	0.113138+02	0.501048+01	0.0	0.0	0.0	0.0	0.0	0.0	3	31
32	0.560578+03	0.597628+03	0.507628+03	0.0	0.0	0.0	0.0	0.0	0.0	1	32
33	0.235958+03	0.236638+03	0.210988+03	0.0	0.0	0.0	0.0	0.0	0.0	3	33
34	0.481548+03	0.480808+03	0.122578+03	0.0	0.0	0.0	0.0	0.0	0.0	3	34
35	0.657288+01	0.656108+01	0.656108+01	0.0	0.0	0.0	0.0	0.0	0.0	1	35
36	0.219008+02	0.219688+02	0.107648+02	0.0	0.0	0.0	0.0	0.0	0.0	3	36
37	0.920898+02	0.920698+02	0.480778+02	0.0	0.0	0.0	0.0	0.0	0.0	3	37
38	0.860578+02	0.874538+02	0.450348+02	0.0	0.0	0.0	0.0	0.0	0.0	3	38
39	0.760468+03	0.779258+03	0.335298+03	0.0	0.0	0.0	0.0	0.0	0.0	3	39
40	0.101018+03	0.102968+03	0.976658+02	0.0	0.0	0.0	0.0	0.0	0.0	3	40
41	0.500838+03	0.499968+03	0.492858+03	0.0	0.0	0.0	0.0	0.0	0.0	3	41
42	0.712998+02	0.712508+02	0.600128+02	0.0	0.0	0.68975E-05	0.0	0.0	0.0	3	42
43	0.603158+02	0.600748+02	0.256698+02	0.226448-07	0.231958+01	0.674448-05	0.0	0.0	0.0	3	43
44	0.732758+02	0.732878+02	0.259798+02	0.343878+02	0.287338+01	0.645238-05	0.0	0.0	0.0	3	44
45	0.525138+02	0.541138+02	0.256438+02	0.195978+00	0.268988+01	0.651948-05	0.0	0.0	0.0	3	45
46	0.109798+03	0.109638+03	0.172458+02	0.601418+02	0.293258+01	0.667008-05	0.0	0.0	0.0	3	46

TABLE C.2: (page 3 of 7)

MICROSCOPIC CROSS-SECTIONS FOR GROUP 4

I#	TRANSPORT	TOTAL	N-GAMMA	FISSION	NU	CHI	N-ALPHA	N-2N	N-D	#SCT	I#
1	0.84326E+00	0.79043E+00	0.29701E-02	0.0	0.0	0.0	0.0	0.0	0.0	2	1
2	0.52865E+01	0.47605E+01	0.17134E-02	0.0	0.0	0.0	0.0	0.0	0.0	4	2
3	0.52865E+01	0.47605E+01	0.17134E-02	0.0	0.0	0.0	0.0	0.0	0.0	4	3
4	0.42582E+01	0.38498E+01	0.77555E-04	0.0	0.0	0.0	0.0	0.0	0.0	4	4
5	0.43331E+01	0.38847E+01	0.77556E-04	0.0	0.0	0.0	0.0	0.0	0.0	4	5
6	0.42736E+00	0.42835E+00	0.42835E+00	0.0	0.0	0.0	0.0	0.0	0.0	1	6
7	0.20241E+01	0.17904E+01	0.68536E-01	0.0	0.0	0.0	0.0	0.0	0.0	2	7
8	0.10878E+07	0.11024E+07	0.11024E+07	0.0	0.0	0.0	0.0	0.0	0.0	1	8
9	0.12933E+02	0.12602E+02	0.12602E+02	0.0	0.0	0.0	0.0	0.0	0.0	2	9
10	0.57229E+02	0.57399E+02	0.57399E+02	0.0	0.0	0.0	0.0	0.0	0.0	1	10
11	0.40722E+01	0.37267E+01	0.37267E+01	0.0	0.0	0.0	0.0	0.0	0.0	2	11
12	0.10110E+03	0.10115E+03	0.10115E+03	0.0	0.0	0.0	0.0	0.0	0.0	2	12
13	0.11531E+05	0.11565E+05	0.11565E+05	0.0	0.0	0.0	0.0	0.0	0.0	1	13
14	0.64036E+03	0.64252E+03	0.64252E+03	0.0	0.0	0.0	0.0	0.0	0.0	1	14
15	0.34819E+05	0.35034E+05	0.34835E+05	0.0	0.0	0.0	0.0	0.0	0.0	3	15
16	0.32410E+04	0.32520E+04	0.32443E+04	0.0	0.0	0.0	0.0	0.0	0.0	2	16
17	0.16904E+03	0.16896E+03	0.16855E+03	0.0	0.0	0.0	0.0	0.0	0.0	3	17
18	0.12280E+02	0.12048E+02	0.26729E+01	0.0	0.0	0.0	0.0	0.0	0.0	2	18
19	0.23329E+02	0.23278E+02	0.14259E+02	0.0	0.0	0.0	0.0	0.0	0.0	3	19
20	0.13215E+03	0.13043E+03	0.12307E+03	0.0	0.0	0.0	0.0	0.0	0.0	3	20
21	0.47449E+00	0.47590E+00	0.47590E+00	0.0	0.0	0.0	0.0	0.0	0.0	1	21
22	0.61390E+01	0.61550E+01	0.61550E+01	0.0	0.0	0.0	0.0	0.0	0.0	1	22
23	0.15865E+02	0.15538E+02	0.30164E+01	0.0	0.0	0.0	0.0	0.0	0.0	2	23
24	0.28086E+03	0.28098E+03	0.24889E+02	0.24357E+03	0.25030E+01	0.0	0.0	0.0	0.0	2	24
25	0.44769E+02	0.44629E+02	0.35613E+02	0.0	0.0	0.0	0.0	0.0	0.0	2	25
26	0.27100E+03	0.27210E+03	0.40962E+02	0.21801E+03	0.24301E+01	0.0	0.0	0.0	0.0	4	26
27	0.33365E+02	0.33150E+02	0.23131E+02	0.0	0.0	0.0	0.0	0.0	0.0	2	27
28	0.40994E+01	0.38667E+01	0.76246E-04	0.0	0.0	0.0	0.0	0.0	0.0	2	28
29	0.19219E+02	0.19276E+02	0.19276E+02	0.0	0.0	0.0	0.0	0.0	0.0	1	29
30	0.86043E+02	0.86844E+02	0.86844E+02	0.0	0.0	0.0	0.0	0.0	0.0	2	30
31	0.15953E+03	0.15829E+03	0.15829E+03	0.0	0.0	0.0	0.0	0.0	0.0	2	31
32	0.64062E+04	0.64253E+04	0.64253E+04	0.0	0.0	0.0	0.0	0.0	0.0	1	32
33	0.40158E+02	0.39897E+02	0.39897E+02	0.0	0.0	0.0	0.0	0.0	0.0	2	33
34	0.51432E+02	0.51026E+02	0.51026E+02	0.0	0.0	0.0	0.0	0.0	0.0	2	34
35	0.81145E+02	0.81386E+02	0.81386E+02	0.0	0.0	0.0	0.0	0.0	0.0	1	35
36	0.13377E+03	0.13261E+03	0.13261E+03	0.0	0.0	0.0	0.0	0.0	0.0	2	36
37	0.26247E+02	0.25615E+02	0.25615E+02	0.0	0.0	0.0	0.0	0.0	0.0	2	37
38	0.36602E+02	0.36410E+02	0.36410E+02	0.0	0.0	0.0	0.0	0.0	0.0	2	38
39	0.92792E+02	0.92584E+02	0.92584E+02	0.0	0.0	0.0	0.0	0.0	0.0	2	39
40	0.64063E+03	0.64253E+03	0.64253E+03	0.0	0.0	0.0	0.0	0.0	0.0	2	40
41	0.59795E+04	0.59964E+04	0.59964E+04	0.0	0.0	0.0	0.0	0.0	0.0	2	41
42	0.66436E+02	0.65835E+02	0.57466E+02	0.0	0.0	0.70006E-10	0.0	0.0	0.0	4	42
43	0.10341E+02	0.10112E+02	0.11931E+01	0.37544E-08	0.23195E+01	0.12159E-08	0.0	0.0	0.0	3	43
44	0.13196E+04	0.13130E+04	0.49119E+03	0.81300E+03	0.28733E+01	0.11632E-08	0.0	0.0	0.0	3	44
45	0.94309E+03	0.93506E+03	0.67460E+03	0.16812E+00	0.28698E+01	0.11754E-08	0.0	0.0	0.0	3	45
46	0.98378E+03	0.98283E+03	0.25750E+03	0.71435E+03	0.29323E+01	0.12026E-08	0.0	0.0	0.0	2	46

TABLE C.2: (page 4 of 7)

SCATTERING CROSS-SECTIONS

	GROUP 1					GROUP 2				
I#	G--G	(G-1)--G	(G-2)--G	(G-3)--G		I#	G--G	(G-1)--G	(G-2)--G	(G-3)--G
1.	0.29864E+01	0.0	0.0	0.0	*	1	0.67514E+00	0.16901E+00	0.0	0.0
2	0.26110E+01	0.0	0.0	0.0	*	2	0.45096E+01	0.19399E+00	0.0	0.0
3	0.26110E+01	0.0	0.0	0.0	*	3	0.45096E+01	0.19399E+00	0.0	0.0
4	0.33404E+01	0.0	0.0	0.0	*	4	0.35195E+01	0.13596E+00	0.0	0.0
5	0.33403E+01	0.0	0.0	0.0	*	5	0.35195E+01	0.13596E+00	0.0	0.0
6	0.0	0.0	0.0	0.0	*	6	0.0	0.0	0.0	0.0
7	0.36796E+01	0.0	0.0	0.0	*	7	0.19683E+01	0.22260E+00	0.0	0.0
8	0.0	0.0	0.0	0.0	*	8	0.0	0.0	0.0	0.0
9	0.57402E+01	0.0	0.0	0.0	*	9	0.79089E+01	0.24969E+00	0.0	0.0
10	0.0	0.0	0.0	0.0	*	10	0.0	0.0	0.0	0.0
11	0.59436E+01	0.0	0.0	0.0	*	11	0.77966E+01	0.24982E+00	0.0	0.0
12	0.60133E+01	0.0	0.0	0.0	*	12	0.16104E+02	0.99642E-01	0.0	0.0
13	0.0	0.0	0.0	0.0	*	13	0.0	0.0	0.0	0.0
14	0.0	0.0	0.0	0.0	*	14	0.0	0.0	0.0	0.0
15	0.67552E+01	0.0	0.0	0.0	*	15	0.16886E+02	0.33951E+00	0.0	0.0
16	0.84125E+01	0.0	0.0	0.0	*	16	0.97519E+01	0.38208E+00	0.0	0.0
17	0.67148E+01	0.0	0.0	0.0	*	17	0.12345E+02	0.74951E+00	0.0	0.0
18	0.77997E+01	0.0	0.0	0.0	*	18	0.14797E+02	0.22572E+00	0.0	0.0
19	0.64149E+01	0.0	0.0	0.0	*	19	0.18792E+02	0.11982E+00	0.0	0.0
20	0.66935E+01	0.0	0.0	0.0	*	20	0.10658E+02	0.59237E+00	0.0	0.0
21	0.0	0.0	0.0	0.0	*	21	0.0	0.0	0.0	0.0
22	0.0	0.0	0.0	0.0	*	22	0.0	0.0	0.0	0.0
23	0.73950E+01	0.0	0.0	0.0	*	23	0.13767E+02	0.21494E+00	0.0	0.0
24	0.53410E+01	0.0	0.0	0.0	*	24	0.10011E+02	0.15199E+00	0.0	0.0
25	0.65964E+01	0.0	0.0	0.0	*	25	0.11228E+02	0.17025E+00	0.0	0.0
26	0.62202E+01	0.0	0.0	0.0	*	26	0.10819E+02	0.16109E+00	0.0	0.0
27	0.64554E+01	0.0	0.0	0.0	*	27	0.10735E+02	0.43467E+00	0.0	0.0
28	0.35909E+01	0.0	0.0	0.0	*	28	0.35025E+01	0.11784E+00	0.0	0.0
29	0.0	0.0	0.0	0.0	*	29	0.0	0.0	0.0	0.0
30	0.55512E+01	0.0	0.0	0.0	*	30	0.67560E+01	0.82915E-01	0.0	0.0
31	0.62154E+01	0.0	0.0	0.0	*	31	0.74898E+01	0.13324E+00	0.0	0.0
32	0.0	0.0	0.0	0.0	*	32	0.0	0.0	0.0	0.0
33	0.58950E+01	0.0	0.0	0.0	*	33	0.58681E+01	0.15886E+00	0.0	0.0
34	0.61209E+01	0.0	0.0	0.0	*	34	0.56665E+01	0.12519E+00	0.0	0.0
35	0.0	0.0	0.0	0.0	*	35	0.0	0.0	0.0	0.0
36	0.63066E+01	0.0	0.0	0.0	*	36	0.56493E+01	0.68467E-01	0.0	0.0
37	0.62050E+01	0.0	0.0	0.0	*	37	0.20057E+02	0.89066E-01	0.0	0.0
38	0.63352E+01	0.0	0.0	0.0	*	38	0.11862E+02	0.19640E+00	0.0	0.0
39	0.64350E+01	0.0	0.0	0.0	*	39	0.11863E+02	0.19639E+00	0.0	0.0
40	0.66147E+01	0.0	0.0	0.0	*	40	0.59592E+01	0.21947E+00	0.0	0.0
41	0.67824E+01	0.0	0.0	0.0	*	41	0.69846E+01	0.20832E+00	0.0	0.0
42	0.62600E+01	0.0	0.0	0.0	*	42	0.13846E+02	0.93298E+00	0.0	0.0
43	0.77866E+01	0.0	0.0	0.0	*	43	0.15028E+02	0.20511E+00	0.0	0.0
44	0.61027E+01	0.0	0.0	0.0	*	44	0.11475E+02	0.14701E+00	0.0	0.0
45	0.67150E+01	0.0	0.0	0.0	*	45	0.14877E+02	0.14154E+00	0.0	0.0
46	0.66603E+01	0.0	0.0	0.0	*	46	0.11529E+02	0.27813E+00	0.0	0.0

TABLE C.2: (page 5 of 7)

SCATTERING CROSS-SECTIONS

	GROUP 3					GROUP 4				
I#	G--G	(G-1)--G	(G-2)--G	(G-3)--G		I#	G--G	(G-1)--G	(G-2)--G	(G-3)--G
1	0.67913E+00	0.50043E-01	0.0	0.0	*	1	0.78742E+00	0.44876E-01	0.0	0.0
2	0.46458E+01	0.12309E+00	0.25138E-06	0.0	*	2	0.47586E+01	0.10813E+00	0.0	0.62356E-09
3	0.46458E+01	0.12309E+00	0.25138E-06	0.0	*	3	0.47584E+01	0.10813E+00	0.0	0.62356E-09
4	0.38451E+01	0.72330E-01	0.77666E-07	0.0	*	4	0.38495E+01	0.64912E-01	0.0	0.69002E-10
5	0.38451E+01	0.72330E-01	0.77666E-07	0.0	*	5	0.38945E+01	0.64912E-01	0.0	0.69002E-10
6	0.0	0.0	0.0	0.0	*	6	0.0	0.0	0.0	0.0
7	0.22448E+01	0.27230E-01	0.94332E-06	0.0	*	7	0.17217E+01	0.22549E-01	0.0	0.0
8	0.0	0.0	0.0	0.0	*	8	0.0	0.0	0.0	0.0
9	0.14319E+02	0.25355E-01	0.37641E-05	0.0	*	9	0.0	0.16349E-01	0.0	0.0
10	0.0	0.0	0.0	0.0	*	10	0.0	0.0	0.0	0.0
11	0.81783E+01	0.21304E-01	0.37641E-05	0.0	*	11	0.0	0.15917E-01	0.0	0.0
12	0.11234E+03	0.27177E-01	0.10587E-05	0.0	*	12	0.0	0.10521E-01	0.0	0.0
13	0.0	0.0	0.0	0.0	*	13	0.0	0.0	0.0	0.0
14	0.0	0.0	0.0	0.0	*	14	0.0	0.0	0.0	0.0
15	0.72969E+02	0.81986E-01	0.36596E-04	0.0	*	15	0.19930E+03	0.21802E-01	0.96201E-08	0.0
16	0.18144E+02	0.18637E-01	0.71017E-05	0.0	*	16	0.71494E+01	0.81215E-02	0.0	0.0
17	0.17563E+02	0.38290E-01	0.53958E-04	0.0	*	17	0.44102E+01	0.35373E-02	0.10923E-06	0.0
18	0.25389E+02	0.45703E-01	0.66451E-07	0.0	*	18	0.93746E+01	0.10758E-01	0.0	0.0
19	0.35132E+02	0.48468E-01	0.63703E-06	0.0	*	19	0.90189E+01	0.33698E-02	0.83475E-09	0.0
20	0.12524E+02	0.16959E-01	0.11017E-04	0.0	*	20	0.73636E+01	0.20824E-01	0.0	0.0
21	0.0	0.0	0.0	0.0	*	21	0.0	0.0	0.0	0.0
22	0.0	0.0	0.0	0.0	*	22	0.0	0.0	0.0	0.0
23	0.19164E+02	0.37554E-01	0.54724E-05	0.0	*	23	0.12521E+02	0.15019E-01	0.0	0.0
24	0.11879E+02	0.16738E-01	0.34841E-05	0.0	*	24	0.12525E+02	0.15176E-01	0.0	0.0
25	0.16224E+02	0.19009E-01	0.26823E-05	0.0	*	25	0.90152E+01	0.12559E-01	0.0	0.0
26	0.11759E+02	0.16945E-01	0.30158E-04	0.0	*	26	0.12521E+02	0.16378E-01	0.11974E-07	0.19658E-06
27	0.16262E+02	0.19845E-01	0.68238E-05	0.0	*	27	0.10019E+02	0.12612E-01	0.0	0.0
28	0.36371E+01	0.72361E-01	0.0	0.0	*	28	0.36605E+01	0.63384E-01	0.0	0.0
29	0.0	0.0	0.0	0.0	*	29	0.0	0.0	0.0	0.0
30	0.14276E+02	0.26822E-01	0.43603E-06	0.0	*	30	0.0	0.21418E-01	0.0	0.0
31	0.62431E+01	0.19648E-01	0.12230E-05	0.0	*	31	0.0	0.19705E-01	0.0	0.0
32	0.0	0.0	0.0	0.0	*	32	0.0	0.0	0.0	0.0
33	0.25629E+02	0.27006E-01	0.17962E-05	0.0	*	33	0.0	0.15765E-01	0.0	0.0
34	0.35821E+03	0.12006E-01	0.14342E-05	0.0	*	34	0.0	0.24953E-01	0.0	0.0
35	0.0	0.0	0.0	0.0	*	35	0.0	0.0	0.0	0.0
36	0.11133E+02	0.12548E-01	0.87616E-06	0.0	*	36	0.0	0.71782E-01	0.0	0.0
37	0.48360E+02	0.36329E-01	0.87615E-06	0.0	*	37	0.0	0.31625E-01	0.0	0.0
38	0.41801E+02	0.10266E+00	0.26922E-05	0.0	*	38	0.0	0.13386E-01	0.0	0.0
39	0.44394E+03	0.10266E+00	0.26922E-05	0.0	*	39	0.0	0.19810E-01	0.0	0.0
40	0.52803E+01	0.12106E-01	0.32194E-05	0.0	*	40	0.0	0.93082E-02	0.0	0.0
41	0.76934E+01	0.15462E-01	0.29184E-05	0.0	*	41	0.0	0.14797E-01	0.0	0.0
42	0.11222E+02	0.15020E-01	0.23865E-04	0.0	*	42	0.83687E+01	0.16129E-01	0.17876E-08	0.40431E-10
43	0.34994E+02	0.14630E-01	0.16027E-05	0.0	*	43	0.89187E+01	0.10457E-01	0.31288E-08	0.0
44	0.12907E+02	0.28863E-01	0.22555E-05	0.0	*	44	0.88508E+01	0.11695E-01	0.15757E-08	0.0
45	0.28240E+02	0.13396E-01	0.71412E-06	0.0	*	45	0.60209E+02	0.34161E-01	0.22984E-09	0.0
46	0.12237E+02	0.17643E-01	0.15443E-05	0.0	*	46	0.10980E+02	0.10272E-01	0.0	0.0

TABLE C.2: (page 6 of 7)

CALCULATED CROSS-SECTIONS

REMOVAL

I#	GROUP 1	GROUP 2	GROUP 3	GROUP 4
1	0.16901E+00	0.50843E-01	0.44376E-01	0.0
2	0.19399E+00	0.12309E+00	0.10813E+00	0.0
3	0.19399E+00	0.12309E+00	0.10813E+00	0.0
4	0.13596E+00	0.72330E-01	0.64912E-01	0.0
5	0.13596E+00	0.72330E-01	0.64912E-01	0.0
6	0.0	0.0	0.0	0.0
7	0.22260E+00	0.27230E-01	0.22549E-01	0.0
8	0.0	0.0	0.0	0.0
9	0.24969E+00	0.25355E-01	0.16349E-01	0.0
10	0.0	0.0	0.0	0.0
11	0.24962E+00	0.21384E-01	0.15917E-01	0.0
12	0.59642E-01	0.27177E-01	0.10521E-01	0.0
13	0.0	0.0	0.0	0.0
14	0.0	0.0	0.0	0.0
15	0.33951E+00	0.61986E-01	0.21802E-01	0.0
16	0.38430E+00	0.18637E-01	0.81215E-02	0.0
17	0.74451E+00	0.38240E-01	0.35373E-02	0.0
18	0.22572E+00	0.45703E-01	0.10756E-01	0.0
19	0.11982E+00	0.48406E-01	0.33698E-02	0.0
20	0.59237E+00	0.16959E-01	0.26024E-01	0.0
21	0.0	0.0	0.0	0.0
22	0.0	0.0	0.0	0.0
23	0.21894E+00	0.37554E-01	0.15019E-01	0.0
24	0.15199E+00	0.16738E-01	0.15176E-01	0.0
25	0.17025E+00	0.19009E-01	0.12559E-01	0.0
26	0.16133E+00	0.16945E-01	0.16376E-01	0.0
27	0.48467E+00	0.19845E-01	0.12612E-01	0.0
28	0.11784E+00	0.72361E-01	0.63384E-01	0.0
29	0.0	0.0	0.0	0.0
30	0.82915E-01	0.26822E-01	0.21416E-01	0.0
31	0.13324E+00	0.19648E-01	0.19705E-01	0.0
32	0.0	0.0	0.0	0.0
33	0.15886E+00	0.27006E-01	0.15765E-01	0.0
34	0.12519E+00	0.12000E-01	0.24953E-01	0.0
35	0.0	0.0	0.0	0.0
36	0.68467E-01	0.12548E-01	0.71782E-01	0.0
37	0.49066E-01	0.36329E-01	0.81625E-01	0.0
38	0.19640E+00	0.16236E+00	0.11386E-01	0.0
39	0.19639E+00	0.16236E+00	0.19816E-01	0.0
40	0.21947E+00	0.12106E-01	0.93082E-02	0.0
41	0.20832E+00	0.15462E-01	0.14797E-01	0.0
42	0.93258E+00	0.15820E-01	0.16129E-01	0.0
43	0.20511E+00	0.14830E-01	0.10457E-01	0.0
44	0.14731E+00	0.28861E-01	0.11695E-01	0.0
45	0.14154E+00	0.13396E-01	0.34161E-01	0.0
46	0.27813E+00	0.17843E-01	0.10272E-01	0.0

ABSORPTION

I#	GROUP 1	GROUP 2	GROUP 3	GROUP 4
1	-0.11935E-05	-0.13306E-04	-0.18643E-03	0.29701E-02
2	0.15036E-03	0.83826E-05	0.13959E-03	0.17134E-02
3	0.15036E-03	0.83825E-05	0.13959E-03	0.17134E-02
4	0.23103E-02	0.18412E-06	0.93906E-05	0.77555E-04
5	0.23103E-02	0.18412E-06	0.93906E-05	0.77556E-04
6	0.19274E-03	0.20957E-02	0.34901E-01	0.42835E+00
7	-0.22911E-02	0.79846E-03	0.54183E-02	0.60536E-01
8	0.0	0.15603E-04	0.34798E+02	0.11024E+07
9	0.53372E-01	0.14200E+01	0.56683E+02	0.12602E+02
10	0.0	0.21934E+00	0.46762E+01	0.57399E+02
11	0.30909E-01	0.53922E+00	0.55496E+01	0.37267E+01
12	0.26471E+00	0.63170E+01	0.33780E+03	0.10115E+03
13	0.52015E+01	0.43306E+03	0.45819E+04	0.11565E+05
14	0.13485E+00	0.79956E+03	0.75747E+04	0.64252E+03
15	0.20670E+00	0.47064E+01	0.14671E+03	0.34835E+05
16	0.62769E+00	0.87074E+01	0.25121E+03	0.32448E+04
17	0.20377E+00	0.76459E+01	0.21331E+03	0.16455E+03
18	0.57067E+00	0.16176E+01	0.47183E+02	0.26729E+01
19	0.91708E+00	0.11995E+01	0.16093E+03	0.14259E+02
20	0.79752E+00	0.27151E+01	0.47747E+02	0.12307E+03
21	0.19688E-01	0.24292E+00	0.10236E+01	0.47590E+00
22	0.68585E-01	0.70689E+00	0.11319E+02	0.61550E+01
23	0.17415E+00	0.11138E+01	0.94637E+01	0.30164E+01
24	0.20947E+01	0.65928E+01	0.81354E+02	0.26845E+03
25	0.10309E+01	0.14089E+01	0.85576E+02	0.35613E+02
26	0.13725E+01	0.59804E+01	0.51240E+02	0.25897E+03
27	0.11619E+01	0.40322E+01	0.71622E+02	0.23131E+02
28	0.30835E-02	0.0	0.0	0.76246E-04
29	0.99340E-02	0.10846E+00	0.33452E+02	0.19276E+02
30	0.69312E-01	0.11212E+01	0.26703E+02	0.84844E+02
31	0.16090E+00	0.13468E+01	0.50104E+01	0.15829E+03
32	0.27947E+01	0.30451E+02	0.50762E+03	0.64253E+04
33	0.35252E+00	0.27374E+01	0.21098E+03	0.39897E+02
34	0.74213E-01	0.10422E+01	0.12257E+03	0.51026E+02
35	0.0	0.30785E+00	0.65610E+01	0.81386E+02
36	0.46413E-01	0.97903E+00	0.10744E+02	0.13261E+03
37	0.42534E-01	0.90667E+00	0.46177E+02	0.25615E+02
38	0.48167E-01	0.69471E+00	0.45699E+02	0.36410E+02
39	0.49103E-01	0.68425E+00	0.33529E+03	0.92504E+02
40	0.47468E+00	0.75667E+01	0.97665E+02	0.64253E+03
41	0.16817E+00	0.38695E+01	0.49285E+03	0.59969E+04
42	0.47107E+00	0.34714E+01	0.60012E+02	0.57466E+02
43	0.24916E+00	0.96536E+00	0.25069E+02	0.11931E+01
44	0.17734E+01	0.44668E+01	0.60366E+02	0.13042E+04
45	0.10974E+01	0.17685E+01	0.25839E+02	0.87477E+03
46	0.17649E+01	0.64399E+01	0.97366E+02	0.97185E+03

TABLE C.2: (page 7 of 7)

MICROSCOPIC CROSS-SECTIONS FOR GROUP 1

I#	TRANSPORT	TOTAL	N-GAMMA	FISSION	NU	CHI	N-ALPHA	N-2N	N-D	#SCT	I#
1	0.27510E+01	0.31581E+01	0.0	0.0	0.0	0.0	0.0	0.11934E-05	0.0	1	1
2	0.22512E+01	0.28043E+01	0.77059E-06	0.0	0.0	0.0	0.14949E-03	0.0	0.0	1	2
3	0.22512E+01	0.28043E+01	0.77059E-06	0.0	0.0	0.0	0.14949E-03	0.0	0.0	1	3
4	0.28150E+01	0.35777E+01	-0.12231E-09	0.0	0.0	0.0	0.23150E-02	0.38220E-05	0.0	1	4
5	0.28150E+01	0.35777E+01	-0.12231E-09	0.0	0.0	0.0	0.23150E-02	0.38220E-05	0.0	1	5
6	0.17070E-03	0.19266E-03	0.19266E-03	0.0	0.0	0.0	0.0	0.0	0.0	1	6
7	0.27578E+01	0.35041E+01	0.34474E-03	0.0	0.0	0.0	0.0	0.26362E-02	0.0	1	7
8	0.0	0.0	0.0	0.0	0.0	0.0	0.0	0.0	0.0	1	8
9	0.42689E+01	0.62430E+01	0.53008E-01	0.0	0.0	0.0	0.0	0.0	0.32706E-03	1	9
10	0.0	0.0	0.0	0.0	0.0	0.0	0.0	0.0	0.0	1	10
11	0.60810E+01	0.62241E+01	0.30563E-01	0.0	0.0	0.0	0.0	0.0	0.32706E-03	1	11
12	0.63843E+01	0.63746E+01	0.26435E+00	0.0	0.0	0.0	0.0	0.0	0.28798E-03	1	12
13	0.46052E+01	0.51993E+01	0.51993E+01	0.0	0.0	0.0	0.0	0.0	0.0	1	13
14	0.11939E+00	0.13479E+00	0.13479E+00	0.0	0.0	0.0	0.0	0.0	0.0	1	14
15	0.56617E+01	0.72962E+01	0.20379E+00	0.0	0.0	0.0	0.40136E-04	0.40136E-04	0.27321E-02	1	15
16	0.49328E+01	0.73941E+01	0.62734E+00	0.0	0.0	0.0	0.0	0.0	0.0	1	16
17	0.58414E+01	0.76668E+01	0.20315E+00	0.0	0.0	0.0	0.16454E-04	0.16454E-04	0.46813E-03	1	17
18	0.60077E+01	0.85918E+01	0.23334E+00	0.33580E+00	0.26704E+01	0.96749E+00	0.0	0.0	0.18222E-02	1	18
19	0.51447E+01	0.78525E+01	0.79713E-01	0.83658E+00	0.30694E+01	0.96903E+00	0.0	0.0	0.14026E-02	1	19
20	0.57884E+01	0.80435E+01	0.11190E+00	0.64614E+00	0.33029E+01	0.96903E+00	0.0	0.0	0.0	1	20
21	0.16817E-01	0.19677E-01	0.19677E-01	0.0	0.0	0.0	0.0	0.0	0.0	1	21
22	0.58453E-01	0.68548E-01	0.68548E-01	0.0	0.0	0.0	0.0	0.0	0.0	1	22
23	0.63307E+01	0.77777E+01	0.13288E+00	0.36529E-01	0.23855E+01	0.96673E+00	0.0	0.0	0.47198E-02	1	23
24	0.54618E+01	0.75820E+01	0.99696E-01	0.19926E+01	0.26038E+01	0.96673E+00	0.0	0.0	0.21304E-02	1	24
25	0.51844E+01	0.77951E+01	0.14490E+00	0.88500E+00	0.26078E+01	0.96749E+00	0.0	0.0	0.68069E-03	1	25
26	0.54176E+01	0.77479E+01	0.13386E+00	0.12359E+01	0.25714E+01	0.96749E+00	0.0	0.0	0.26142E-02	1	26
27	0.58661E+01	0.80464E+01	0.17650E+00	0.98313E+00	0.26862E+01	0.96756E+00	0.0	0.0	0.28806E-02	1	27
28	0.26936E+01	0.37169E+01	0.46902E-08	0.0	0.0	0.0	0.30887E-02	0.41268E-05	0.0	1	28
29	0.87916E-02	0.99299E-02	0.99299E-02	0.0	0.0	0.0	0.0	0.0	0.0	1	29
30	0.54404E+01	0.57032E+01	0.69256E-01	0.0	0.0	0.0	0.0	0.0	0.17114E-04	1	30
31	0.61249E+01	0.65088E+01	0.16067E+00	0.0	0.0	0.0	0.0	0.0	0.14703E-03	1	31
32	0.24731E+01	0.27935E+01	0.27935E+01	0.0	0.0	0.0	0.0	0.0	0.0	1	32
33	0.60394E+01	0.64056E+01	0.35217E+00	0.0	0.0	0.0	0.0	0.0	0.20525E-03	1	33
34	0.61944E+01	0.63263E+01	0.73819E-01	0.0	0.0	0.0	0.0	0.0	0.35828E-03	1	34
35	0.0	0.0	0.0	0.0	0.0	0.0	0.0	0.0	0.0	1	35
36	0.64102E+01	0.64401E+01	0.45412E-01	0.0	0.0	0.0	0.0	0.0	0.97478E-03	1	36
37	0.64137E+01	0.64157E+01	0.41534E-01	0.0	0.0	0.0	0.0	0.0	0.97478E-03	1	37
38	0.50917E+01	0.71743E+01	0.45482E-01	0.0	0.0	0.0	0.0	0.0	0.26634E-02	1	38
39	0.50926E+01	0.71752E+01	0.46416E-01	0.0	0.0	0.0	0.0	0.0	0.26633E-02	1	39
40	0.71701E+01	0.73083E+01	0.47416E+00	0.0	0.0	0.0	0.0	0.0	0.41331E-03	1	40
41	0.70048E+01	0.71584E+01	0.16771E+00	0.0	0.0	0.0	0.0	0.0	0.40463E-03	1	41
42	0.55089E+01	0.76619E+01	0.23698E+00	0.23333E+00	0.25955E+01	0.96456E+00	0.0	0.0	0.94481E-03	1	42
43	0.55220E+01	0.82329E+01	0.95338E-01	0.15014E+00	0.27330E+01	0.96535E+00	0.0	0.0	0.38004E-02	1	43
44	0.55933E+01	0.80210E+01	0.73895E-01	0.16988E+01	0.10520E+01	0.96677E+00	0.0	0.0	0.79931E-03	1	44
45	0.55242E+01	0.79530E+01	0.11665E+00	0.98112E+00	0.31175E+01	0.96645E+00	0.0	0.0	0.31823E-03	1	45
46	0.56456E+01	0.86908E+01	0.13250E+00	0.16265E+01	0.31026E+01	0.96570E+00	0.0	0.0	0.56885E-02	1	46

TABLE C.3: FOUR-GROUP CROSS-SECTIONS FOR C/HM = 325 (page 1 of 7)

MICROSCOPIC CROSS-SECTIONS FOR GROUP 2

I#	TRANSPORT	TOTAL	N-GAMMA	FISSION	NU	CHI	N-ALPHA	N-2N	N-D	#SCT	I#
1	0.68[illegible]E+00	0.72599E+00	0.0	0.0	0.0	0.0	0.0	0.13329E-04	0.0	2	1
2	0.43521E+01	0.46329E+01	0.83963E-05	0.0	0.0	0.0	0.0	0.0	0.0	2	2
3	0.43521E+01	0.46329E+01	0.83963E-05	0.0	0.0	0.0	0.0	0.0	0.0	2	3
4	0.34977E+01	0.35919E+01	0.19506E-06	0.0	0.0	0.0	0.0	0.0	0.0	2	4
5	0.34977E+01	0.35919E+01	0.19506E-06	0.0	0.0	0.0	0.0	0.0	0.0	2	5
6	0.20539E-02	0.20992E-02	0.20992E-02	0.0	0.0	0.0	0.0	0.0	0.0	1	6
7	0.19867E+01	0.20172E+01	0.79947E-03	0.0	0.0	0.0	0.0	0.0	0.0	2	7
8	0.15123E-04	0.15681E-04	0.15681E-04	0.0	0.0	0.0	0.0	0.0	0.0	1	8
9	0.92578E+01	0.93591E+01	0.14232E+01	0.0	0.0	0.0	0.0	0.0	0.0	2	9
10	0.21831E+00	0.21989E+00	0.21989E+00	0.0	0.0	0.0	0.0	0.0	0.0	1	10
11	0.82075E+01	0.83545E+01	0.54047E+00	0.0	0.0	0.0	0.0	0.0	0.0	2	11
12	0.21766E+02	0.22479E+02	0.63321E+01	0.0	0.0	0.0	0.0	0.0	0.0	2	12
13	0.42137E+03	0.43445E+03	0.43445E+03	0.0	0.0	0.0	0.0	0.0	0.0	1	13
14	0.77654E+03	0.80222E+03	0.80222E+03	0.0	0.0	0.0	0.0	0.0	0.0	1	14
15	0.21803E+02	0.21701E+02	0.47165E+01	0.0	0.0	0.0	0.0	0.0	0.0	2	15
16	0.17853E+02	0.18479E+02	0.87237E+01	0.0	0.0	0.0	0.0	0.0	0.0	2	16
17	0.19787E+02	0.20050E+02	0.76867E+01	0.0	0.0	0.0	0.0	0.0	0.0	2	17
18	0.16027E+02	0.16473E+02	0.16224E+01	0.0	0.0	0.32508E-01	0.0	0.0	0.0	2	18
19	0.19281E+02	0.20057E+02	0.11795E+01	0.22440E-01	0.28152E+01	0.30966E-01	0.0	0.0	0.0	2	19
20	0.13242E+02	0.13567E+02	0.27195E+01	0.10215E-02	0.30480E+01	0.30966E-01	0.0	0.0	0.0	2	20
21	0.23814E+00	0.24331E+00	0.24331E+00	0.0	0.0	0.0	0.0	0.0	0.0	1	21
22	0.69361E+00	0.70798E+00	0.70798E+00	0.0	0.0	0.0	0.0	0.0	0.0	1	22
23	0.14695E+02	0.14932E+02	0.11221E+01	0.0	0.0	0.33273E-01	0.0	0.0	0.0	2	23
24	0.15987E+02	0.16630E+02	0.72549E+00	0.58753E+01	0.25030E+01	0.33273E-01	0.0	0.0	0.0	2	24
25	0.12288E+02	0.12750E+02	0.14976E+01	0.62564E-02	0.25120E+01	0.32508E-01	0.0	0.0	0.0	2	25
26	0.16143E+02	0.16627E+02	0.18495E+01	0.41398E+01	0.24436E+01	0.32508E-01	0.0	0.0	0.0	2	26
27	0.14909E+02	0.15600E+02	0.48400E+01	0.95759E-03	0.25140E+01	0.32436E-01	0.0	0.0	0.0	2	27
28	0.33946E+01	0.35751E+01	0.0	0.0	0.0	0.0	0.0	0.0	0.0	2	28
29	0.13029E+00	0.13064E+00	0.10364E+00	0.0	0.0	0.0	0.0	0.0	0.0	1	29
30	0.76287E+01	0.79063E+01	0.11239E+01	0.0	0.0	0.0	0.0	0.0	0.0	2	30
31	0.87970E+01	0.88572E+01	0.13487E+01	0.0	0.0	0.0	0.0	0.0	0.0	2	31
32	0.27342E+02	0.30591E+02	0.30591E+02	0.0	0.0	0.0	0.0	0.0	0.0	1	32
33	0.85765E+01	0.86359E+01	0.27398E+01	0.0	0.0	0.0	0.0	0.0	0.0	2	33
34	0.66770E+01	0.67223E+01	0.10447E+01	0.0	0.0	0.0	0.0	0.0	0.0	2	34
35	0.29938E+00	0.30861E+00	0.30861E+00	0.0	0.0	0.0	0.0	0.0	0.0	1	35
36	0.64013E+01	0.66431E+01	0.98154E+00	0.0	0.0	0.0	0.0	0.0	0.0	2	36
37	0.21121E+02	0.21628E+02	0.90931E+00	0.0	0.0	0.0	0.0	0.0	0.0	2	37
38	0.12370E+02	0.12671E+02	0.70057E+00	0.0	0.0	0.0	0.0	0.0	0.0	2	38
39	0.12356E+02	0.12658E+02	0.68605E+00	0.0	0.0	0.0	0.0	0.0	0.0	2	39
40	0.13345E+02	0.13554E+02	0.75426E+01	0.0	0.0	0.0	0.0	0.0	0.0	2	40
41	0.10746E+02	0.10875E+02	0.38787E+01	0.0	0.0	0.0	0.0	0.0	0.0	2	41
42	0.14021E+02	0.14341E+02	0.38778E+01	0.0	0.0	0.35436E-01	0.0	0.0	0.0	2	42
43	0.15533E+02	0.16015E+02	0.96702E+00	0.12054E-03	0.23217E+01	0.34654E-01	0.0	0.0	0.0	2	43
44	0.15483E+02	0.15960E+02	0.17903E+01	0.26031E+01	0.28763E+01	0.33231E-01	0.0	0.0	0.0	2	44
45	0.15944E+02	0.16606E+02	0.16365E+01	0.13517E+00	0.28727E+01	0.33558E-01	0.0	0.0	0.0	2	45
46	0.17182E+02	0.17958E+02	0.13268E+01	0.51226E+01	0.29346E+01	0.34297E-01	0.0	0.0	0.0	2	46

TABLE C.3: (page 2 of 7)

MICROSCOPIC CROSS-SECTIONS FOR GROUP 3

I#	TRANSPORT	TOTAL	N-GAMMA	FISSION	NU	CHI	N-ALPHA	N-2N	N-D	#SCT	I#
1	0.60640E+00	0.72426E+00	0.27732E-04	0.0	0.0	0.0	0.0	0.21603E-03	0.0	2	1
2	0.45007E+01	0.47541E+01	0.14169E-03	0.0	0.0	0.0	0.0	0.0	0.0	3	2
3	0.45007E+01	0.47541E+01	0.14169E-03	0.0	0.0	0.0	0.0	0.0	0.0	3	3
4	0.35627E+01	0.37105E+01	0.94480E-05	0.0	0.0	0.0	0.0	0.0	0.0	3	4
5	0.35620E+01	0.37105E+01	0.94480E-05	0.0	0.0	0.0	0.0	0.0	0.0	3	5
6	0.35470E-01	0.35427E-01	0.35427E-01	0.0	0.0	0.0	0.0	0.0	0.0	1	6
7	0.22223E+01	0.22726E+01	0.55044E-02	0.0	0.0	0.0	0.0	0.0	0.0	3	7
8	0.35904E+02	0.35823E+02	0.35823E+02	0.0	0.0	0.0	0.0	0.0	0.0	1	8
9	0.71598E+02	0.71901E+02	0.57679E+02	0.0	0.0	0.0	0.0	0.0	0.0	3	9
10	0.47524E+01	0.47466E+01	0.47466E+01	0.0	0.0	0.0	0.0	0.0	0.0	1	10
11	0.13631E+02	0.13680E+02	0.54924E+01	0.0	0.0	0.0	0.0	0.0	0.0	3	11
12	0.45065E+03	0.45478E+03	0.34407E+03	0.0	0.0	0.0	0.0	0.0	0.0	3	12
13	0.45597E+04	0.45373E+04	0.45373E+04	0.0	0.0	0.0	0.0	0.0	0.0	1	13
14	0.74971E+04	0.74536E+04	0.74536E+04	0.0	0.0	0.0	0.0	0.0	0.0	1	14
15	0.21953E+03	0.22051E+03	0.14809E+03	0.0	0.0	0.0	0.0	0.0	0.0	3	15
16	0.27410E+03	0.27440E+03	0.25595E+03	0.0	0.0	0.0	0.0	0.0	0.0	3	16
17	0.23480E+04	0.23846E+03	0.21695E+03	0.0	0.0	0.0	0.0	0.0	0.0	3	17
18	0.73175E+02	0.73701E+02	0.48482E+02	0.0	0.0	0.0	0.0	0.0	0.0	3	18
19	0.20106E+03	0.20047E+03	0.16513E+03	0.0	0.0	0.0	0.0	0.0	0.0	3	19
20	0.60764E+02	0.60784E+02	0.48252E+02	0.0	0.0	0.0	0.0	0.0	0.0	3	20
21	0.10112E+01	0.10147E+01	0.10147E+01	0.0	0.0	0.0	0.0	0.0	0.0	1	21
22	0.11380E+02	0.11385E+02	0.11385E+02	0.0	0.0	0.0	0.0	0.0	0.0	1	22
23	0.28719E+02	0.29103E+02	0.10011E+02	0.0	0.0	0.0	0.0	0.0	0.0	3	23
24	0.94536E+02	0.94582E+02	0.15421E+02	0.67256E+02	0.25029E+01	0.0	0.0	0.0	0.0	3	24
25	0.13502E+03	0.13560E+03	0.99145E+02	0.0	0.0	0.0	0.0	0.0	0.0	3	25
26	0.63253E+02	0.63257E+02	0.20566E+02	0.30984E+02	0.24420E+01	0.0	0.0	0.0	0.0	3	26
27	0.98559E+02	0.98576E+02	0.72327E+02	0.0	0.0	0.0	0.0	0.0	0.0	3	27
28	0.35548E+01	0.37006E+01	0.0	0.0	0.0	0.0	0.0	0.0	0.0	2	28
29	0.33639E+02	0.33346E+02	0.33346E+02	0.0	0.0	0.0	0.0	0.0	0.0	1	29
30	0.40370E+02	0.41185E+02	0.26867E+02	0.0	0.0	0.0	0.0	0.0	0.0	3	30
31	0.11278E+02	0.11294E+02	0.50131E+01	0.0	0.0	0.0	0.0	0.0	0.0	3	31
32	0.51597E+03	0.51531E+03	0.51531E+03	0.0	0.0	0.0	0.0	0.0	0.0	1	32
33	0.24075E+03	0.24169E+03	0.21567E+03	0.0	0.0	0.0	0.0	0.0	0.0	3	33
34	0.44390E+03	0.44917E+03	0.12463E+03	0.0	0.0	0.0	0.0	0.0	0.0	3	34
35	0.66690E+01	0.66598E+01	0.66598E+01	0.0	0.0	0.0	0.0	0.0	0.0	1	35
36	0.22047E+02	0.22062E+02	0.10743E+02	0.0	0.0	0.0	0.0	0.0	0.0	3	36
37	0.92745E+02	0.92294E+02	0.49018E+02	0.0	0.0	0.0	0.0	0.0	0.0	3	37
38	0.87225E+02	0.88393E+02	0.46298E+02	0.0	0.0	0.0	0.0	0.0	0.0	3	38
39	0.79773E+03	0.79580E+03	0.34256E+03	0.0	0.0	0.0	0.0	0.0	0.0	3	39
40	0.10325E+03	0.10321E+03	0.97523E+02	0.0	0.0	0.0	0.0	0.0	0.0	3	40
41	0.50784E+03	0.50724E+03	0.50013E+03	0.0	0.0	0.0	0.0	0.0	0.0	3	41
42	0.72134E+02	0.72119E+02	0.60482E+02	0.0	0.0	0.68975E-05	0.0	0.0	0.0	3	42
43	0.60497E+02	0.60190E+02	0.25331E+02	0.22813E-07	0.23195E+01	0.67444E-05	0.0	0.0	0.0	3	43
44	0.73540E+02	0.73551E+02	0.26074E+02	0.34612E+02	0.28733E+01	0.64523E-05	0.0	0.0	0.0	3	44
45	0.52430E+02	0.53895E+02	0.25573E+02	0.19397E+00	0.20698E+01	0.65194E-05	0.0	0.0	0.0	3	45
46	0.11089E+03	0.11061E+03	0.17434E+02	0.81152E+02	0.29325E+01	0.66708E-05	0.0	0.0	0.0	3	46

TABLE C.3: (page 3 of 7)

MICROSCOPIC CROSS-SECTIONS FOR GROUP 4

I#	TRANSPORT	TOTAL	N-GAMMA	FISSION	NU	CHI	N-ALPHA	N-2N	N-D	#SCT	I#
1	0.8447[illegible]E+00	0.79310E+00	0.30409E-02	0.0	0.0	0.0	0.0	0.0	0.0	2	1
2	0.52818E+01	0.47630E+01	0.17542E-02	0.0	0.0	0.0	0.0	0.0	0.0	4	2
3	0.52818E+01	0.47630E+01	0.17542E-02	0.0	0.0	0.0	0.0	0.0	0.0	4	3
4	0.42968E+01	0.38533E+01	0.79399E-04	0.0	0.0	0.0	0.0	0.0	0.0	4	4
5	0.43333E+01	0.38697E+01	0.79399E-04	0.0	0.0	0.0	0.0	0.0	0.0	4	5
6	0.43761E+00	0.43850E+00	0.43850E+00	0.0	0.0	0.0	0.0	0.0	0.0	1	6
7	0.20239E+01	0.17929E+01	0.70169E-01	0.0	0.0	0.0	0.0	0.0	0.0	2	7
8	0.11374E+07	0.11513E+07	0.11513E+07	0.0	0.0	0.0	0.0	0.0	0.0	1	8
9	0.13225E+02	0.12887E+02	0.12887E+02	0.0	0.0	0.0	0.0	0.0	0.0	2	9
10	0.58639E+02	0.58767E+02	0.58767E+02	0.0	0.0	0.0	0.0	0.0	0.0	1	10
11	0.41603E+01	0.38154E+01	0.38154E+01	0.0	0.0	0.0	0.0	0.0	0.0	2	11
12	0.10341E+03	0.10339E+03	0.10339E+03	0.0	0.0	0.0	0.0	0.0	0.0	2	12
13	0.11615E+05	0.11841E+05	0.11841E+05	0.0	0.0	0.0	0.0	0.0	0.0	1	13
14	0.65641E+03	0.65783E+03	0.65783E+03	0.0	0.0	0.0	0.0	0.0	0.0	1	14
15	0.36643E+05	0.36443E+05	0.36244E+05	0.0	0.0	0.0	0.0	0.0	0.0	3	15
16	0.33593E+04	0.33651E+04	0.33579E+04	0.0	0.0	0.0	0.0	0.0	0.0	2	16
17	0.17214E+03	0.17185E+03	0.16748E+03	0.0	0.0	0.0	0.0	0.0	0.0	3	17
18	0.12336E+02	0.12107E+02	0.27317E+01	0.0	0.0	0.0	0.0	0.0	0.0	2	18
19	0.23581E+02	0.23492E+02	0.14472E+02	0.0	0.0	0.0	0.0	0.0	0.0	3	19
20	0.12093E+03	0.11866E+03	0.11129E+03	0.0	0.0	0.0	0.0	0.0	0.0	3	20
21	0.46618E+00	0.48724E+01	0.48724E+00	0.0	0.0	0.0	0.0	0.0	0.0	1	21
22	0.62701E+01	0.62819E+01	0.62819E+01	0.0	0.0	0.0	0.0	0.0	0.0	1	22
23	0.15944E+02	0.15623E+02	0.31000E+01	0.0	0.0	0.0	0.0	0.0	0.0	2	23
24	0.28378E+03	0.28379E+03	0.24934E+02	0.24624E+03	0.25030E+01	0.0	0.0	0.0	0.0	2	24
25	0.45872E+02	0.45702E+02	0.30686E+02	0.0	0.0	0.0	0.0	0.0	0.0	2	25
26	0.27930E+03	0.27935E+03	0.42073E+02	0.22476E+03	0.24301E+01	0.0	0.0	0.0	0.0	4	26
27	0.33931E+02	0.33702E+02	0.23082E+02	0.0	0.0	0.0	0.0	0.0	0.0	2	27
28	0.46590E+01	0.36640E+01	0.76013E-04	0.0	0.0	0.0	0.0	0.0	0.0	2	28
29	0.19692E+02	0.19735E+02	0.19735E+02	0.0	0.0	0.0	0.0	0.0	0.0	1	29
30	0.87301E+02	0.87041E+02	0.87041E+02	0.0	0.0	0.0	0.0	0.0	0.0	2	30
31	0.14939E+03	0.14797E+03	0.14757E+03	0.0	0.0	0.0	0.0	0.0	0.0	2	31
32	0.65641E+04	0.65784E+04	0.65784E+04	0.0	0.0	0.0	0.0	0.0	0.0	1	32
33	0.40934E+02	0.40650E+02	0.40650E+02	0.0	0.0	0.0	0.0	0.0	0.0	2	33
34	0.52594E+02	0.52256E+02	0.52256E+02	0.0	0.0	0.0	0.0	0.0	0.0	2	34
35	0.83145E+02	0.83326E+02	0.83326E+02	0.0	0.0	0.0	0.0	0.0	0.0	1	35
36	0.13737E+03	0.13612E+03	0.13612E+03	0.0	0.0	0.0	0.0	0.0	0.0	2	36
37	0.26072E+02	0.26226E+02	0.26226E+02	0.0	0.0	0.0	0.0	0.0	0.0	2	37
38	0.37494E+02	0.37277E+02	0.37277E+02	0.0	0.0	0.0	0.0	0.0	0.0	2	38
39	0.94790E+02	0.94531E+02	0.94531E+02	0.0	0.0	0.0	0.0	0.0	0.0	2	39
40	0.65661E+03	0.65784E+03	0.65784E+03	0.0	0.0	0.0	0.0	0.0	0.0	2	40
41	0.61264E+04	0.61394E+04	0.61394E+04	0.0	0.0	0.0	0.0	0.0	0.0	2	41
42	0.60768E+02	0.60090E+02	0.51753E+02	0.0	0.0	0.73006E-10	0.0	0.0	0.0	4	42
43	0.10368E+02	0.10140E+02	0.12191E+01	0.31888E-08	0.23195E+01	0.12159E-08	0.0	0.0	0.0	3	43
44	0.13301E+04	0.13232E+04	0.49394E+03	0.82056E+03	0.28733E+01	0.11632E-08	0.0	0.0	0.0	3	44
45	0.83509E+03	0.82390E+03	0.77197E+03	0.14853E+00	0.26698E+01	0.11754E-08	0.0	0.0	0.0	3	45
46	0.10058E+04	0.10043E+04	0.26266E+03	0.73069E+03	0.29323E+01	0.12026E-08	0.0	0.0	0.0	2	46

TABLE C.3: (page 4 of 7)

SCATTERING CROSS-SECTIONS

	GROUP 1					GROUP 2				
I#	G--G	(G-1)--G	(G-2)--G	(G-3)--G		I#	G--G	(G-1)--G	(G-2)--G	(G-3)--G
1	0.29852E+01	0.0	0.0	0.0	*	1	0.67490E+00	0.16877E+00	0.0	0.0
2	0.26105E+01	0.0	0.0	0.0	*	2	0.45091E+01	0.19367E+00	0.0	0.0
3	0.26105E+01	0.0	0.0	0.0	*	3	0.45091E+01	0.19367E+00	0.0	0.0
4	0.34397E+01	0.0	0.0	0.0	*	4	0.35192E+01	0.13574E+00	0.0	0.0
5	0.34396E+01	0.0	0.0	0.0	*	5	0.35192E+01	0.13573E+00	0.0	0.0
6	0.0	0.0	0.0	0.0	*	6	0.0	0.0	0.0	0.0
7	0.36787E+01	0.0	0.0	0.0	*	7	0.19690E+01	0.22223E+00	0.0	0.0
8	0.0	0.0	0.0	0.0	*	8	0.0	0.0	0.0	0.0
9	0.59402E+01	0.0	0.0	0.0	*	9	0.79103E+01	0.24964E+00	0.0	0.0
10	0.0	0.0	0.0	0.0	*	10	0.0	0.0	0.0	0.0
11	0.59430E+01	0.0	0.0	0.0	*	11	0.77974E+01	0.24977E+00	0.0	0.0
12	0.60107E+01	0.0	0.0	0.0	*	12	0.16119E+02	0.99678E-01	0.0	0.0
13	0.0	0.0	0.0	0.0	*	13	0.0	0.0	0.0	0.0
14	0.0	0.0	0.0	0.0	*	14	0.0	0.0	0.0	0.0
15	0.67554E+01	0.0	0.0	0.0	*	15	0.16902E+02	0.33919E+00	0.0	0.0
16	0.84142E+01	0.0	0.0	0.0	*	16	0.97507E+01	0.38199E+00	0.0	0.0
17	0.67153E+01	0.0	0.0	0.0	*	17	0.12351E+02	0.74888E+00	0.0	0.0
18	0.77901E+01	0.0	0.0	0.0	*	18	0.14805E+02	0.22565E+00	0.0	0.0
19	0.68174E+01	0.0	0.0	0.0	*	19	0.14806E+02	0.11972E+00	0.0	0.0
20	0.66928E+01	0.0	0.0	0.0	*	20	0.10859E+02	0.59210E+00	0.0	0.0
21	0.0	0.0	0.0	0.0	*	21	0.0	0.0	0.0	0.0
22	0.0	0.0	0.0	0.0	*	22	0.0	0.0	0.0	0.0
23	0.73934E+01	0.0	0.0	0.0	*	23	0.13773E+02	0.21882E+00	0.0	0.0
24	0.53401E+01	0.0	0.0	0.0	*	24	0.10013E+02	0.15190E+00	0.0	0.0
25	0.65947E+01	0.0	0.0	0.0	*	25	0.11226E+02	0.17026E+00	0.0	0.0
26	0.62193E+01	0.0	0.0	0.0	*	26	0.10820E+02	0.16094E+00	0.0	0.0
27	0.64544E+01	0.0	0.0	0.0	*	27	0.10739E+02	0.43456E+00	0.0	0.0
28	0.35982E+01	0.0	0.0	0.0	*	28	0.35023E+01	0.11764E+00	0.0	0.0
29	0.0	0.0	0.0	0.0	*	29	0.0	0.0	0.0	0.0
30	0.55537E+01	0.0	0.0	0.0	*	30	0.67559E+01	0.82871E-01	0.0	0.0
31	0.62144E+01	0.0	0.0	0.0	*	31	0.74886E+01	0.13323E+00	0.0	0.0
32	0.0	0.0	0.0	0.0	*	32	0.0	0.0	0.0	0.0
33	0.58942E+01	0.0	0.0	0.0	*	33	0.90680E+01	0.15885E+00	0.0	0.0
34	0.61269E+01	0.0	0.0	0.0	*	34	0.56654E+01	0.12521E+00	0.0	0.0
35	0.0	0.0	0.0	0.0	*	35	0.0	0.0	0.0	0.0
36	0.63069E+01	0.0	0.0	0.0	*	36	0.50489E+01	0.88485E-01	0.0	0.0
37	0.62853E+01	0.0	0.0	0.0	*	37	0.20679E+02	0.89083E-01	0.0	0.0
38	0.69349E+01	0.0	0.0	0.0	*	38	0.11870E+02	0.19643E+00	0.0	0.0
39	0.69346E+01	0.0	0.0	0.0	*	39	0.11870E+02	0.19642E+00	0.0	0.0
40	0.66140E+01	0.0	0.0	0.0	*	40	0.59587E+01	0.21940E+00	0.0	0.0
41	0.67823E+01	0.0	0.0	0.0	*	41	0.69846E+01	0.20834E+00	0.0	0.0
42	0.62593E+01	0.0	0.0	0.0	*	42	0.16846E+02	0.93221E+00	0.0	0.0
43	0.77854E+01	0.0	0.0	0.0	*	43	0.15033E+02	0.20503E+00	0.0	0.0
44	0.61016E+01	0.0	0.0	0.0	*	44	0.11477E+02	0.14693E+00	0.0	0.0
45	0.67135E+01	0.0	0.0	0.0	*	45	0.14883E+02	0.14139E+00	0.0	0.0
46	0.68591E+01	0.0	0.0	0.0	*	46	0.11530E+02	0.27780E+00	0.0	0.0

TABLE C.3: (page 5 of 7)

SCATTERING CROSS-SECTIONS

	GROUP 3					GROUP 4				
I#	G--G	(G-1)--G	(G-2)--G	(G-3)--G	I#	G--G	(G-1)--G	(G-2)--G	(G-3)--G
1	0.677796+00	0.51076E-01	0.0	0.0	1	0.78999E+00	0.46223E-01	0.0	0.0
2	0.46423E+01	0.12375E+00	0.25152E-06	0.0	2	0.47612E+01	0.11167E+00	0.0	0.62390E-09
3	0.46423E+01	0.12375E+00	0.25152E-06	0.0	3	0.47610E+01	0.11167E+00	0.0	0.62390E-09
4	0.38415E+01	0.72728E-01	0.77703E-07	0.0	4	0.38531E+01	0.67058E-01	0.0	0.68996E-10
5	0.38434E+01	0.72728E-01	0.77703E-07	0.0	5	0.38495E+01	0.67058E-01	0.0	0.68996E-10
6	0.0	0.0	0.0	0.0	6	0.0	0.0	0.0	0.0
7	0.22918E+01	0.27303E-01	0.94399E-08	0.0	7	0.17227E+01	0.23295E-01	0.0	0.0
8	0.0	0.0	0.0	0.0	8	0.0	0.0	0.0	0.0
9	0.14206E+02	0.25494E-01	0.37632E-05	0.0	9	0.0	0.16890E-01	0.0	0.0
10	0.0	0.0	0.0	0.0	10	0.0	0.0	0.0	0.0
11	0.81713E+01	0.21502E-01	0.37612E-05	0.0	11	0.0	0.16443E-01	0.0	0.0
12	0.11470E+03	0.27326E-01	0.10594E-05	0.0	12	0.0	0.10869E-01	0.0	0.0
13	0.0	0.0	0.0	0.0	13	0.0	0.0	0.0	0.0
14	0.0	0.0	0.0	0.0	14	0.0	0.0	0.0	0.0
15	0.72403E+02	0.82437E-01	0.36554E-04	0.0	15	0.19931E+03	0.22522E-01	0.96078E-08	0.0
16	0.18344E+02	0.18740E-01	0.70986E-05	0.0	16	0.71310E+01	0.83900E-02	0.0	0.0
17	0.17501E+02	0.38500E-01	0.53931E-04	0.0	17	0.44107E+01	0.36542E-02	0.10903E-06	0.0
18	0.25203E+02	0.45954E-01	0.66524E-07	0.0	18	0.93748E+01	0.11113E-01	0.0	0.0
19	0.35272E+02	0.44747E-01	0.63738E-08	0.0	19	0.90197E+01	0.35018E-02	0.83337E-09	0.0
20	0.12510E+02	0.17052E-01	0.11065E-04	0.0	20	0.73637E+01	0.21513E-01	0.0	0.0
21	0.0	0.0	0.0	0.0	21	0.0	0.0	0.0	0.0
22	0.0	0.0	0.0	0.0	22	0.0	0.0	0.0	0.0
23	0.19075E+02	0.37761E-01	0.34740E-05	0.0	23	0.12522E+02	0.15515E-01	0.0	0.0
24	0.11899E+02	0.16830E-01	0.34826E-05	0.0	24	0.12526E+02	0.15678E-01	0.0	0.0
25	0.36445E+02	0.19114E-01	0.26859E-05	0.0	25	0.90150E+01	0.12974E-01	0.0	0.0
26	0.11750E+02	0.17038E-01	0.30116E-04	0.0	26	0.12522E+02	0.16920E-01	0.11952E-07	0.19627E-06
27	0.16236E+02	0.19594E-01	0.88199E-05	0.0	27	0.10020E+02	0.13029E-01	0.0	0.0
28	0.36351E+01	0.72759E-01	0.0	0.0	28	0.36638E+01	0.65479E-01	0.0	0.0
29	0.0	0.0	0.0	0.0	29	0.0	0.0	0.0	0.0
30	0.14296E+02	0.26970E-01	0.43649E-06	0.0	30	0.0	0.22126E-01	0.0	0.0
31	0.62607E+01	0.19757E-01	0.12238E-05	0.0	31	0.0	0.20356E-01	0.0	0.0
32	0.0	0.0	0.0	0.0	32	0.0	0.0	0.0	0.0
33	0.25999E+02	0.27155E-01	0.17967E-05	0.0	33	0.0	0.16287E-01	0.0	0.0
34	0.36455E+03	0.12066E-01	0.14150E-05	0.0	34	0.0	0.25778E-01	0.0	0.0
35	0.0	0.0	0.0	0.0	35	0.0	0.0	0.0	0.0
36	0.11265E+02	0.12617E-01	0.87701E-06	0.0	36	0.0	0.74155E-01	0.0	0.0
37	0.43243E+02	0.36529E-01	0.87701E-06	0.0	37	0.0	0.32671E-01	0.0	0.0
38	0.42041E+02	0.10262E+00	0.26931E-05	0.0	38	0.0	0.13829E-01	0.0	0.0
39	0.45322E+03	0.10262E+00	0.26930E-05	0.0	39	0.0	0.20471E-01	0.0	0.0
40	0.52754E+01	0.12172E-01	0.32197E-05	0.0	40	0.0	0.96159E-02	0.0	0.0
41	0.70961E+01	0.15547E-01	0.29190E-05	0.0	41	0.0	0.15286E-01	0.0	0.0
42	0.11241E+02	0.15906E-01	0.23860E-04	0.0	42	0.83371E+01	0.16683E-01	0.17856E-08	0.40363E-10
43	0.34686E+02	0.14911E-01	0.16037E-05	0.0	43	0.89213E+01	0.10803E-01	0.31236E-08	0.0
44	0.12852E+02	0.29021E-01	0.22545E-05	0.0	44	0.87549E+01	0.12082E-01	0.15750E-08	0.0
45	0.28093E+02	0.13470E-01	0.71404E-06	0.0	45	0.51785E+02	0.35290E-01	0.22946E-09	0.0
46	0.12210E+02	0.17941E-01	0.15434E-05	0.0	46	0.10957E+02	0.10611E-01	0.0	0.0

TABLE C.3: (page 6 of 7)

CALCULATED CROSS-SECTIONS

	REMOVAL					ABSORPTION				
I#	GROUP 1	GROUP 2	GROUP 3	GROUP 4		I#	GROUP 1	GROUP 2	GROUP 3	GROUP 4
1	0.168772E+00	0.51076E-01	0.46223E-01	0.0	*	1	-0.11934E-05	-0.13329E-04	-0.18830E-03	0.30409E-02
2	0.193672E+00	0.12375E+00	0.11167E+00	0.0	*	2	0.15026E-03	0.83963E-05	0.14169E-03	0.17542E-02
3	0.193672E+00	0.12375E+00	0.11167E+00	0.0	*	3	0.15026E-03	0.83963E-05	0.14169E-03	0.17542E-02
4	0.135743E+00	0.72728E-01	0.67056E-01	0.0	*	4	0.23112E-02	0.18506E-06	0.94480E-05	0.79399E-04
5	0.135731E+00	0.72728E-01	0.67056E-01	0.0	*	5	0.23112E-02	0.18506E-06	0.94480E-05	0.79399E-04
6	0.0	0.0	0.0	0.0	*	6	0.19266E-03	0.20992E-02	0.35427E-01	0.43856E+00
7	0.222234E+00	0.27380E-01	0.23295E-01	0.0	*	7	-0.22914E-02	0.79849E-03	0.55044E-02	0.70169E-01
8	0.0	0.0	0.0	0.0	*	8	0.0	0.15681E-04	0.35823E+02	0.11513E+07
9	0.249648E+00	0.25494E-01	0.16896E-01	0.0	*	9	0.53335E-01	0.14232E+01	0.57679E+02	0.12987E+02
10	0.0	0.0	0.0	0.0	*	10	0.0	0.21989E+00	0.47466E+01	0.50767E+02
11	0.249778E+00	0.21502E-01	0.16443E-01	0.0	*	11	0.30890E-01	0.54047E+00	0.54934E+01	0.38154E+01
12	0.996786E-01	0.27320E-01	0.16869E-01	0.0	*	12	0.26464E+00	0.63323E+01	0.34[illegible]7E+03	0.10339E+03
13	0.0	0.0	0.0	0.0	*	13	0.51993E+01	0.43445E+03	0.45373E+04	0.11841E+05
14	0.0	0.0	0.0	0.0	*	14	0.13479E+00	0.80228E+03	0.74530E+04	0.65783E+03
15	0.339198E+00	0.82437E-01	0.22522E-01	0.0	*	15	0.20652E+00	0.47165E+01	0.14809E+03	0.36244E+05
16	0.381992E+00	0.10740E-01	0.83906E-02	0.0	*	16	0.62734E+00	0.87207E+01	0.25545E+03	0.33579E+04
17	0.748886E+00	0.39560E-01	0.36542E-02	0.0	*	17	0.20361E+00	0.76607E+01	0.21695E+03	0.16748E+03
18	0.225656E+00	0.45954E-01	0.11113E-01	0.0	*	18	0.57096E+00	0.16228E+01	0.48482E+02	0.27317E+01
19	0.119722E+00	0.48747E-01	0.35918E-02	0.0	*	19	0.91769E+00	0.12020E+01	0.16513E+03	0.14472E+02
20	0.592102E+00	0.17052E-01	0.21513E-01	0.0	*	20	0.75805E+00	0.27205E+01	0.48252E+02	0.11129E+03
21	0.0	0.0	0.0	0.0	*	21	0.19677E-01	0.24331E+00	0.10147E+01	0.48724E+00
22	0.0	0.0	0.0	0.0	*	22	0.68548E-01	0.70798E+00	0.11385E+02	0.62819E+01
23	0.218826E+00	0.37761E-01	0.15515E-01	0.0	*	23	0.17413E+00	0.11221E+01	0.10013E+02	0.31000E+01
24	0.151992E+00	0.16830E-01	0.15678E-01	0.0	*	24	0.20945E+01	0.66008E+01	0.82677E+02	0.27117E+03
25	0.170268E+00	0.19114E-01	0.14[illegible]74E-01	0.0	*	25	0.10314E+01	0.15039E+01	0.99145E+02	0.36686E+02
26	0.160994E+00	0.17038E-01	0.16926E-01	0.0	*	26	0.13724E+01	0.59893E+01	0.51491E+02	0.26683E+03
27	0.434562E+00	0.19954E-01	0.13029E-01	0.0	*	27	0.11625E+01	0.48409E+01	0.72325E+02	0.23682E+02
28	0.117648E+00	0.72759E-01	0.65479E-01	0.0	*	28	0.30946E-02	0.0	0.0	0.78063E-04
29	0.0	0.0	0.0	0.0	*	29	0.99299E-02	0.10864E+00	0.33346E+02	0.19735E+02
30	0.482871E-01	0.26970E-01	0.22126E-01	0.0	*	30	0.69273E-01	0.11234E+01	0.26867E+02	0.87041E+02
31	0.133235E+00	0.19757E-01	0.20356E-01	0.0	*	31	0.16082E+00	0.13487E+01	0.50131E+01	0.14797E+03
32	0.0	0.0	0.0	0.0	*	32	0.27935E+01	0.30501E+02	0.51531E+03	0.65784E+04
33	0.158652E+00	0.27155E-01	0.16287E-01	0.0	*	33	0.35237E+00	0.27398E+01	0.21567E+03	0.40650E+02
34	0.125218E+00	0.12066E-01	0.25778E-01	0.0	*	34	0.74177E-01	0.10447E+01	0.12460E+03	0.52256E+02
35	0.0	0.0	0.0	0.0	*	35	0.0	0.30861E+00	0.66598E+01	0.83326E+02
36	0.884852E-01	0.12617E-01	0.74155E-01	0.0	*	36	0.46387E-01	0.98154E+00	0.10723E+02	0.13612E+03
37	0.890431E-01	0.36529E-01	0.32671E-01	0.0	*	37	0.42509E-01	0.90901E+00	0.49018E+02	0.26228E+02
38	0.196431E+00	0.10262E+00	0.13625E-01	0.0	*	38	0.48145E-01	0.70057E+00	0.46298E+02	0.37277E+02
39	0.196422E+00	0.10262E+00	0.26471E-01	0.0	*	39	0.49308E-01	0.66605E+00	0.34256E+03	0.94531E+02
40	0.219468E+00	0.12172E-01	0.96159E-02	0.0	*	40	0.47458E+00	0.75826E+01	0.97923E+02	0.65784E+03
41	0.208348E+00	0.15547E-01	0.15206E-01	0.0	*	41	0.16812E+00	0.38787E+01	0.50013E+03	0.61398E+04
42	0.932212E+00	0.15906E-01	0.16663E-01	0.0	*	42	0.47125E+00	0.34778E+01	0.60882E+02	0.51753E+02
43	0.205338E+00	0.14911E-01	0.10803E-01	0.0	*	43	0.24928E+00	0.96714E+00	0.25331E+02	0.12191E+01
44	0.146938E+00	0.29021E-01	0.12082E-01	0.0	*	44	0.17735E+01	0.44734E+01	0.60686E+02	0.13144E+04
45	0.141398E+00	0.13470E-01	0.35296E-01	0.0	*	45	0.10981E+01	0.17717E+01	0.25767E+02	0.77212E+03
46	0.277650E+00	0.17941E-01	0.10611E-01	0.0	*	46	0.17647E+01	0.64494E+01	0.98586E+02	0.99335E+03

TABLE C.3: (page 7 of 7)

MICROSCOPIC CROSS-SECTIONS FOR GROUP 1

I#	TRANSPORT	TOTAL	N-GAMMA	FISSION	NU	CHI	N-ALPHA	N-2N	N-D	#SCT	I#
1	0.27521E+01	0.31601E+01	0.0	0.0	0.0	0.0	0.0	0.11932E-05	0.0	1	1
2	0.22535E+01	0.28035E+01	0.77029E-06	0.0	0.0	0.0	0.14939E-03	0.0	0.0	1	2
3	0.22535E+01	0.28035E+01	0.77029E-06	0.0	0.0	0.0	0.14939E-03	0.0	0.0	1	3
4	0.28139E+01	0.35769E+01	-0.12220E-09	0.0	0.0	0.0	0.23159E-02	0.38176E-05	0.0	1	4
5	0.28139E+01	0.35768E+01	-0.12220E-09	0.0	0.0	0.0	0.23159E-02	0.38176E-05	0.0	1	5
6	0.17062E-03	0.19259E-03	0.19259E-03	0.0	0.0	0.0	0.0	0.0	0.0	1	6
7	0.27566E+01	0.39029E+01	0.34440E-03	0.0	0.0	0.0	0.0	0.26365E-02	0.0	1	7
8	0.0	0.0	0.0	0.0	0.0	0.0	0.0	0.0	0.0	1	8
9	0.49681E+01	0.62429E+01	0.52974E-01	0.0	0.0	0.0	0.0	0.0	0.32678E-03	1	9
10	0.0	0.0	0.0	0.0	0.0	0.0	0.0	0.0	0.0	1	10
11	0.49638E+01	0.62249E+01	0.30545E-01	0.0	0.0	0.0	0.0	0.0	0.32678E-03	1	11
12	0.63846E+01	0.83750E+01	0.26427E+00	0.0	0.0	0.0	0.0	0.0	0.28771E-03	1	12
13	0.46031E+01	0.51973E+01	0.51973E+01	0.0	0.0	0.0	0.0	0.0	0.0	1	13
14	0.11934E+00	0.13474E+00	0.13474E+00	0.0	0.0	0.0	0.0	0.0	0.0	1	14
15	0.56999E+01	0.72959E+01	0.20362E+00	0.0	0.0	0.0	0.40143E-04	0.40143E-04	0.27311E-02	1	15
16	0.49320E+01	0.73937E+01	0.62701E+00	0.0	0.0	0.0	0.0	0.0	0.0	1	16
17	0.58393E+01	0.76663E+01	0.20300E+00	0.0	0.0	0.0	0.16457E-04	0.16457E-04	0.46769E-03	1	17
18	0.60061E+01	0.85905E+01	0.23329E+00	0.33612E+00	0.26703E+01	0.96749E+00	0.0	0.0	0.18215E-02	1	18
19	0.51436E+01	0.78517E+01	0.79670E-01	0.83719E+00	0.30694E+01	0.96903E+00	0.0	0.0	0.14022E-02	1	19
20	0.57880E+01	0.80430E+01	0.11180E+00	0.64074E+00	0.33029E+01	0.96903E+00	0.0	0.0	0.0	1	20
21	0.16867E-01	0.19667E-01	0.19667E-01	0.0	0.0	0.0	0.0	0.0	0.0	1	21
22	0.58417E-01	0.68514E-01	0.68514E-01	0.0	0.0	0.0	0.0	0.0	0.0	1	22
23	0.63253E+01	0.77765E+01	0.13283E+00	0.36502E-01	0.23854E+01	0.96673E+00	0.0	0.0	0.47199E-02	1	23
24	0.54603E+01	0.75017E+01	0.99621E-01	0.19925E+01	0.26039E+01	0.96673E+00	0.0	0.0	0.21303E-02	1	24
25	0.51934E+01	0.77942E+01	0.14483E+00	0.88635E+00	0.26878E+01	0.96749E+00	0.0	0.0	0.68029E-03	1	25
26	0.54166E+01	0.77468E+01	0.13378E+00	0.12359E+01	0.25715E+01	0.96749E+00	0.0	0.0	0.26141E-02	1	26
27	0.58058E+01	0.80459E+01	0.17635E+00	0.98838E+00	0.26862E+01	0.96756E+00	0.0	0.0	0.28800E-02	1	27
28	0.26928E+01	0.37181E+01	0.46859E-08	0.0	0.0	0.0	0.30896E-02	0.41221E-05	0.0	1	28
29	0.87396E-02	0.99260E-02	0.99260E-02	0.0	0.0	0.0	0.0	0.0	0.0	1	29
30	0.54398E+01	0.57026E+01	0.69219E-01	0.0	0.0	0.0	0.0	0.0	0.17090E-04	1	30
31	0.61238E+01	0.65078E+01	0.16063E+00	0.0	0.0	0.0	0.0	0.0	0.14687E-03	1	31
32	0.24720E+01	0.27924E+01	0.27924E+01	0.0	0.0	0.0	0.0	0.0	0.0	1	32
33	0.60324E+01	0.64046E+01	0.35222E+00	0.0	0.0	0.0	0.0	0.0	0.20504E-03	1	33
34	0.61943E+01	0.63263E+01	0.73786E-01	0.0	0.0	0.0	0.0	0.0	0.35798E-03	1	34
35	0.0	0.0	0.0	0.0	0.0	0.0	0.0	0.0	0.0	1	35
36	0.64104E+01	0.64407E+01	0.45367E-01	0.0	0.0	0.0	0.0	0.0	0.97423E-03	1	36
37	0.64141E+01	0.64560E+01	0.41511E-01	0.0	0.0	0.0	0.0	0.0	0.97423E-03	1	37
38	0.50912E+01	0.71140E+01	0.45461E-01	0.0	0.0	0.0	0.0	0.0	0.26625E-02	1	38
39	0.50921E+01	0.71149E+01	0.45396E-01	0.0	0.0	0.0	0.0	0.0	0.26625E-02	1	39
40	0.71700E+01	0.73082E+01	0.47406E+00	0.0	0.0	0.0	0.0	0.0	0.41293E-03	1	40
41	0.70046E+01	0.71583E+01	0.16766E+00	0.0	0.0	0.0	0.0	0.0	0.40425E-03	1	41
42	0.55074E+01	0.76007E+01	0.23694E+00	0.23354E+00	0.25954E+01	0.96456E+00	0.0	0.0	0.94430E-03	1	42
43	0.55207E+01	0.82317E+01	0.95319E-01	0.15020E+00	0.27329E+01	0.96535E+00	0.0	0.0	0.37947E-02	1	43
44	0.55922E+01	0.80200E+01	0.73825E-01	0.16989E+01	0.30521E+01	0.96677E+00	0.0	0.0	0.79928E-03	1	44
45	0.55232E+01	0.79519E+01	0.11661E+00	0.98179E+00	0.31176E+01	0.96645E+00	0.0	0.0	0.31804E-03	1	45
46	0.56442E+01	0.68893E+01	0.13246E+00	0.16266E+01	0.31027E+01	0.96570E+00	0.0	0.0	0.56894E-02	1	46

TALBE C.4: FOUR-GROUP CROSS-SECTIONS FOR C/HM = 450 (page 1 of 7)

MICROSCOPIC CROSS-SECTIONS FOR GROUP 2

I#	TRANSPORT	TOTAL	N-GAMMA	FISSION	NU	CHI	N-ALPHA	N-2N	N-D	#SCT	I#
1	0.6628[illegible]E+00	0.72599E+00	0.0	0.0	0.0	0.0	0.0	0.13352E-04	0.0	2	1
2	0.435202E+01	0.463311E+01	0.840994E-05	0.0	0.0	0.0	0.0	0.0	0.0	2	2
3	0.435290E+01	0.463312E+01	0.840994E-05	0.0	0.0	0.0	0.0	0.0	0.0	2	3
4	0.349795E+01	0.359[illegible]E+01	0.185995E-06	0.0	0.0	0.0	0.0	0.0	0.0	2	4
5	0.349795E+01	0.359208E+01	0.185995E-06	0.0	0.0	0.0	0.0	0.0	0.0	2	5
6	0.[illegible]E-02	0.210425E-02	0.210425E-02	0.0	0.0	0.0	0.0	0.0	0.0	1	6
7	0.[illegible]E+01	0.201802E+01	0.796522E-03	0.0	0.0	0.0	0.0	0.0	0.0	2	7
8	0.[illegible]E-04	0.157555E-04	0.157555E-04	0.0	0.0	0.0	0.0	0.0	0.0	1	8
9	0.926343E+01	0.93837L+01	0.142631E+01	0.0	0.0	0.0	0.0	0.0	0.0	2	9
10	0.21395E+00	0.220[illegible]E+00	0.220436E+00	0.0	0.0	0.0	0.0	0.0	0.0	1	10
11	0.[illegible]E+01	0.[illegible]E+01	0.541[illegible]E+00	0.0	0.0	0.0	0.0	0.0	0.0	2	11
12	0.[illegible]E+02	0.[illegible]E+02	0.[illegible]E+01	0.0	0.0	0.0	0.0	0.0	0.0	2	12
13	0.42276E+03	0.43577E+03	0.43577E+03	0.0	0.0	0.0	0.0	0.0	0.0	1	13
14	0.779863E+03	0.80488E+03	0.80488E+03	0.0	0.0	0.0	0.0	0.0	0.0	1	14
15	0.214122E+02	0.21727E+02	0.472[illegible]E+01	0.0	0.0	0.0	0.0	0.0	0.0	2	15
16	0.176695E+02	0.184[illegible]E+02	0.673[illegible]E+01	0.0	0.0	0.0	0.0	0.0	0.0	2	16
17	0.[illegible]E+02	0.20069E+02	0.767[illegible]E+01	0.0	0.0	0.0	0.0	0.0	0.0	2	17
18	0.160422E+02	0.164[illegible]E+02	0.[illegible]E+01	0.0	0.0	0.325C8E-01	0.0	0.0	0.0	2	18
19	0.[illegible]E+02	0.200[illegible]E+02	0.[illegible]E+01	0.22410E-01	0.28152E+01	0.33966E-01	0.0	0.0	0.0	2	19
20	0.[illegible]E+02	0.136046E+02	0.272[illegible]E+01	0.10198E-02	0.30480E+01	0.30966E-01	0.0	0.0	0.0	2	20
21	0.[illegible]E+00	0.[illegible]E+00	0.[illegible]E+00	0.0	0.0	0.0	0.0	0.0	0.0	1	21
22	0.[illegible]E+00	0.709025E+00	0.709025E+00	0.0	0.0	0.0	0.0	0.0	0.0	1	22
23	0.[illegible]E+02	0.14946E+02	0.[illegible]E+01	0.0	0.0	0.33273E-01	0.0	0.0	0.0	2	23
24	0.[illegible]E+02	0.[illegible]E+02	0.[illegible]E+00	0.58818E+01	0.25030E+01	0.33273E-01	0.0	0.0	0.0	2	24
25	0.[illegible]E+02	0.12752E+02	0.[illegible]E+01	0.62440E-02	0.25120E+01	0.32509E-01	0.0	0.0	0.0	2	25
26	0.[illegible]E+02	0.[illegible]E+02	0.[illegible]E+01	0.[illegible]E+01	0.24436E+01	0.32506E-01	0.0	0.0	0.0	2	26
27	0.[illegible]E+02	0.[illegible]E+02	0.[illegible]E+01	0.95591E-03	0.25140E+01	0.32436E-01	0.0	0.0	0.0	2	27
28	0.339668E+01	0.35752E+01	0.0	0.0	0.0	0.0	0.0	0.0	0.0	2	28
29	0.[illegible]E+03	0.[illegible]E+03	0.[illegible]E+03	0.0	0.0	0.0	0.0	0.0	0.0	1	29
30	0.[illegible]E+01	0.[illegible]E+01	0.[illegible]E+01	0.0	0.0	0.0	0.0	0.0	0.0	2	30
31	0.[illegible]E+01	0.[illegible]E+01	0.[illegible]E+01	0.0	0.0	0.0	0.0	0.0	0.0	2	31
32	0.[illegible]E+02	0.[illegible]E+02	0.[illegible]E+02	0.0	0.0	0.0	0.0	0.0	0.0	1	32
33	0.[illegible]E+01	0.[illegible]E+01	0.[illegible]E+01	0.0	0.0	0.0	0.0	0.0	0.0	2	33
34	0.[illegible]E+01	0.[illegible]E+01	0.[illegible]E+01	0.0	0.0	0.0	0.0	0.0	0.0	2	34
35	0.[illegible]E+00	0.[illegible]E+00	0.[illegible]E+00	0.0	0.0	0.0	0.0	0.0	0.0	1	35
36	0.[illegible]E+01	0.[illegible]E+01	0.[illegible]E+00	0.0	0.0	0.0	0.0	0.0	0.0	2	36
37	0.211468E+02	0.216[illegible]E+02	0.[illegible]E+00	0.0	0.0	0.0	0.0	0.0	0.0	2	37
38	0.[illegible]E+02	0.[illegible]E+02	0.[illegible]E+00	0.0	0.0	0.0	0.0	0.0	0.0	2	38
39	0.[illegible]E+02	0.[illegible]E+02	0.[illegible]E+00	0.0	0.0	0.0	0.0	0.0	0.0	2	39
40	0.[illegible]E+02	0.[illegible]E+02	0.[illegible]E+01	0.0	0.0	0.0	0.0	0.0	0.0	2	40
41	0.[illegible]E+02	0.[illegible]E+02	0.[illegible]E+01	0.0	0.0	0.0	0.0	0.0	0.0	2	41
42	0.140[illegible]E+02	0.[illegible]E+02	0.348[illegible]E+01	0.0	0.0	0.35436E-01	0.0	0.0	0.0	2	42
43	0.155422E+02	0.160[illegible]E+02	0.[illegible]E+00	0.12093E-03	0.23217E+01	0.34654E-01	0.0	0.0	0.0	2	43
44	0.[illegible]E+02	0.[illegible]E+02	0.[illegible]E+01	0.26859E+01	0.28763E+01	0.33231E-01	0.0	0.0	0.0	2	44
45	0.[illegible]E+02	0.[illegible]E+02	0.[illegible]E+01	0.[illegible]E+00	0.28727E+01	0.33558E-01	0.0	0.0	0.0	2	45
46	0.171962E+02	0.180[illegible]E+02	0.[illegible]E+01	0.51295E+01	0.29[illegible]E+01	0.34297E-01	0.0	0.0	0.0	2	46

TABLE C.4: (page 2 of 7)

MICROSCOPIC CROSS-SECTIONS FOR GROUP 3

I#	TRANSPORT	TOTAL	N-GAMMA	FISSION	NU	CHI	N-ALPHA	N-2N	N-D	#SCT	I#
1	0.63569E+00	0.72427E+00	0.28694E-04	0.0	0.0	0.0	0.0	0.21897E-03	0.0	2	1
2	0.44983E+01	0.47542E+01	0.14395E-03	0.0	0.0	0.0	0.0	0.0	0.0	3	2
3	0.44983E+01	0.47542E+01	0.14395E-03	0.0	0.0	0.0	0.0	0.0	0.0	3	3
4	0.35616E+01	0.37111E+01	0.45096E-05	0.0	0.0	0.0	0.0	0.0	0.0	3	4
5	0.35616E+01	0.37111E+01	0.95095E-05	0.0	0.0	0.0	0.0	0.0	0.0	3	5
6	0.35916E-01	0.35991E-01	0.35991E-01	0.0	0.0	0.0	0.0	0.0	0.0	1	6
7	0.21215E+01	0.22724E+01	0.55470E-02	0.0	0.0	0.0	0.0	0.0	0.0	3	7
8	0.36938E+02	0.36939E+02	0.36937E+02	0.0	0.0	0.0	0.0	0.0	0.0	1	8
9	0.72509E+02	0.72873E+02	0.58706E+02	0.0	0.0	0.0	0.0	0.0	0.0	3	9
10	0.48256E+01	0.48222E+01	0.48222E+01	0.0	0.0	0.0	0.0	0.0	0.0	1	10
11	0.13565E+02	0.13611E+02	0.54301E+01	0.0	0.0	0.0	0.0	0.0	0.0	3	11
12	0.46584E+03	0.46819E+03	0.35099E+03	0.0	0.0	0.0	0.0	0.0	0.0	3	12
13	0.45067E+04	0.44892E+04	0.44892E+04	0.0	0.0	0.0	0.0	0.0	0.0	1	13
14	0.73566E+04	0.73219E+04	0.73219E+04	0.0	0.0	0.0	0.0	0.0	0.0	1	14
15	0.22081E+03	0.22133E+03	0.14953E+03	0.0	0.0	0.0	0.0	0.0	0.0	3	15
16	0.27969E+03	0.27969E+03	0.26102E+03	0.0	0.0	0.0	0.0	0.0	0.0	3	16
17	0.23855E+03	0.23832E+03	0.22089E+03	0.0	0.0	0.0	0.0	0.0	0.0	3	17
18	0.73792E+02	0.74304E+02	0.49270E+02	0.0	0.0	0.0	0.0	0.0	0.0	3	18
19	0.20551E+03	0.20516E+03	0.10973E+03	0.0	0.0	0.0	0.0	0.0	0.0	3	19
20	0.61266E+02	0.61300E+02	0.48782E+02	0.0	0.0	0.0	0.0	0.0	0.0	3	20
21	0.10025E+01	0.10059E+01	0.10051E+01	0.0	0.0	0.0	0.0	0.0	0.0	1	21
22	0.11445E+02	0.11455E+02	0.11455E+02	0.0	0.0	0.0	0.0	0.0	0.0	1	22
23	0.29327E+02	0.29635E+02	0.10840E+02	0.0	0.0	0.0	0.0	0.0	0.0	3	23
24	0.95965E+02	0.96905E+02	0.15092E+02	0.68398E+02	0.25029E+01	0.0	0.0	0.0	0.0	3	24
25	0.13780E+03	0.13844E+03	0.10173E+03	0.0	0.0	0.0	0.0	0.0	0.0	3	25
26	0.61487E+02	0.63514E+02	0.20659E+02	0.11098E+02	0.24420E+01	0.0	0.0	0.0	0.0	3	26
27	0.87253E+02	0.89287E+02	0.73044E+02	0.0	0.0	0.0	0.0	0.0	0.0	3	27
28	0.35929E+01	0.37006E+01	0.0	0.0	0.0	0.0	0.0	0.0	0.0	2	28
29	0.33422E+02	0.33213E+02	0.33213E+02	0.0	0.0	0.0	0.0	0.0	0.0	1	29
30	0.43712E+02	0.41309E+02	0.27033E+02	0.0	0.0	0.0	0.0	0.0	0.0	3	30
31	0.11255E+02	0.11276E+02	0.50177E+01	0.0	0.0	0.0	0.0	0.0	0.0	3	31
32	0.52395E+03	0.52356E+03	0.52356E+03	0.0	0.0	0.0	0.0	0.0	0.0	1	32
33	0.23615E+03	0.24723E+03	0.22081E+03	0.0	0.0	0.0	0.0	0.0	0.0	3	33
34	0.49665E+03	0.49787E+03	0.12671E+03	0.0	0.0	0.0	0.0	0.0	0.0	3	34
35	0.67766E+01	0.67659E+01	0.67659E+01	0.0	0.0	0.0	0.0	0.0	0.0	1	35
36	0.22135E+02	0.22104E+02	0.19079E+02	0.0	0.0	0.0	0.0	0.0	0.0	3	36
37	0.92796E+02	0.92516E+02	0.49306E+02	0.0	0.0	0.0	0.0	0.0	0.0	3	37
38	0.86483E+02	0.86937E+02	0.46482E+02	0.0	0.0	0.0	0.0	0.0	0.0	3	38
39	0.81354E+03	0.81299E+03	0.35012E+03	0.0	0.0	0.0	0.0	0.0	0.0	3	39
40	0.10350E+03	0.10347E+03	0.98193E+02	0.0	0.0	0.0	0.0	0.0	0.0	3	40
41	0.51539E+03	0.51505E+03	0.50794E+03	0.0	0.0	0.0	0.0	0.0	0.0	3	41
42	0.73046E+02	0.73062E+02	0.61025E+02	0.0	0.0	0.68975E-05	0.0	0.0	0.0	3	42
43	0.60662E+02	0.60290E+02	0.25597E+02	0.42997E-07	0.23175E+01	0.67444E-05	0.0	0.0	0.0	3	43
44	0.73799E+02	0.73610E+02	0.26166E+02	0.34840E+02	0.28733E+01	0.64523E-05	0.0	0.0	0.0	3	44
45	0.52258E+02	0.53643E+02	0.25469E+02	0.19161E+00	0.28698E+01	0.65195E+01	0.0	0.0	0.0	3	45
46	0.11207E+03	0.11205E+03	0.17034E+02	0.82223E+02	0.29325E+01	0.66708E-05	0.0	0.0	0.0	3	46

TABLE C.4: (page 3 of 7)

MICROSCOPIC CROSS-SECTIONS FOR GROUP 4

I#	TRANSPORT	TOTAL	N-GAMMA	FISSION	NU	CHI	N-ALPHA	N-2N	N-D	#SCT	I#
1	0.844e14E+00	0.755d2E+00	0.311248E-02	0.0	0.0	0.0	0.0	0.0	0.0	2	1
2	0.527b5E+01	0.47b56E+01	0.17955E-02	0.0	0.0	0.0	0.0	0.0	0.0	4	2
3	0.527b5E+01	0.47b56E+01	0.1795 E-02	0.0	0.0	0.0	0.0	0.0	0.0	4	3
4	0.42953E+01	0.385e3E+01	0.412b2E-04	0.0	0.0	0.0	0.0	0.0	0.0	4	4
5	0.433b3E+01	0.3b947E+01	0.81262E-04	0.0	0.0	0.0	0.0	0.0	0.0	4	5
6	0.44b26E+00	0.44bd7E+00	0.44bd7E+00	0.0	0.0	0.0	0.0	0.0	0.0	1	6
7	0.2b234E+01	0.17955E+01	0.71819E-01	0.0	0.0	0.0	0.0	0.0	0.0	2	7
8	0.11b77E+07	0.12007E+07	0.12007E+07	0.0	0.0	0.0	0.0	0.0	0.0	1	8
9	0.131173E+02	0.13175E+02	0.13175E+02	0.0	0.0	0.0	0.0	0.0	0.0	2	9
10	0.6e0e7E+02	0.601493E+02	0.601493E+02	0.0	0.0	0.0	0.0	0.0	0.0	1	10
11	0.39492E+01	0.39052E+01	0.39052E+01	0.0	0.0	0.0	0.0	0.0	0.0	2	11
12	0.10574E+03	0.10564E+03	0.10564E+03	0.0	0.0	0.0	0.0	0.0	0.0	2	12
13	0.12133E+05	0.12120E+05	0.12120E+05	0.0	0.0	0.0	0.0	0.0	0.0	1	13
14	0.67239E+03	0.67350E+03	0.67350E+03	0.0	0.0	0.0	0.0	0.0	0.0	1	14
15	0.37777E+05	0.37b61E+05	0.37b62E+05	0.0	0.0	0.0	0.0	0.0	0.0	3	15
16	0.34d19E+04	0.34e09E+04	0.34733E+04	0.0	0.0	0.0	0.0	0.0	0.0	2	16
17	0.17531E+03	0.17e87E+03	0.17e86E+03	0.0	0.0	0.0	0.0	0.0	0.0	3	17
18	0.12397E+02	0.121e6E+02	0.27911E+01	0.0	0.0	0.0	0.0	0.0	0.0	2	18
19	0.23778E+02	0.23710E+02	0.14689E+02	0.0	0.0	0.0	0.0	0.0	0.0	3	19
20	0.10995E+03	0.10713E+03	0.99769E+02	0.0	0.0	0.0	0.0	0.0	0.0	3	20
21	0.49d32E+03	0.49e70E+03	0.49870E+03	0.0	0.0	0.0	0.0	0.0	0.0	1	21
22	0.64d33E+01	0.641c4E+01	0.641094E+01	0.0	0.0	0.0	0.0	0.0	0.0	1	22
23	0.1e633E+02	0.15708E+02	0.31845E+01	0.0	0.0	0.0	0.0	0.0	0.0	2	23
24	0.2e6e1E+03	0.2e653E+03	0.25003E+02	0.24900E+03	0.25030E+01	0.0	0.0	0.0	0.0	2	24
25	0.4e748E+02	0.467e0E+02	0.47769E+02	0.0	0.0	0.0	0.0	0.0	0.0	2	25
26	0.2f64dE+03	0.2e66aE+03	0.43193E+02	0.23096E+03	0.24301E+01	0.0	0.0	0.0	0.0	4	26
27	0.14505E+02	0.34240E+02	0.24239E+02	0.0	0.0	0.0	0.0	0.0	0.0	2	27
28	0.40961E+01	0.3e674E+01	0.79889E-04	0.0	0.0	0.0	0.0	0.0	0.0	2	28
29	0.2317aE+02	0.20199E+02	0.20199E+02	0.0	0.0	0.0	0.0	0.0	0.0	1	29
30	0.e9937E+02	0.69259E+02	0.89259E+02	0.0	0.0	0.0	0.0	0.0	0.0	2	30
31	0.13913E+03	0.137e2E+03	0.137e1E+03	0.0	0.0	0.0	0.0	0.0	0.0	2	31
32	0.67239E+04	0.67331E+04	0.67331E+04	0.0	0.0	0.0	0.0	0.0	0.0	1	32
33	0.41721E+02	0.41413E+02	0.41411E+02	0.0	0.0	0.0	0.0	0.0	0.0	2	33
34	0.53372E+02	0.53499E+02	0.53499E+02	0.0	0.0	0.0	0.0	0.0	0.0	2	34
35	0.85169E+02	0.852e6E+02	0.852e6E+02	0.0	0.0	0.0	0.0	0.0	0.0	1	35
36	0.14132E+03	0.139e8E+03	0.13964E+03	0.0	0.0	0.0	0.0	0.0	0.0	2	36
37	0.27596E+02	0.26849E+02	0.26849E+02	0.0	0.0	0.0	0.0	0.0	0.0	2	37
38	0.38396E+02	0.38154E+02	0.38154E+02	0.0	0.0	0.0	0.0	0.0	0.0	2	38
39	0.96632E+02	0.96501E+02	0.96501E+02	0.0	0.0	0.0	0.0	0.0	0.0	2	39
40	0.67259E+03	0.67331E+03	0.67331E+03	0.0	0.0	0.0	0.0	0.0	0.0	2	40
41	0.62759E+04	0.62842E+04	0.62842E+04	0.0	0.0	0.0	0.0	0.0	0.0	2	41
42	0.55214E+02	0.54471E+02	0.96164E+02	0.0	0.0	0.70006E-10	0.0	0.0	0.0	4	42
43	0.10395E+02	0.10169E+02	0.12453E+01	0.26328E-08	0.23195E+01	0.12159E-08	0.0	0.0	0.0	3	43
44	0.13398E+04	0.13327E+04	0.49640E+03	0.82764E+03	0.28733E+01	0.11632E-08	0.0	0.0	0.0	3	44
45	0.72333E+03	0.71406E+03	0.67057E+03	0.12919E+00	0.22698E+01	0.11754E-08	0.0	0.0	0.0	3	45
46	0.10277E+04	0.10256E+04	0.26777E+03	0.74691E+03	0.29323E+01	0.12026E-08	0.0	0.0	0.0	2	46

TABLE C.4: (page 4 of 7)

SCATTERING CROSS-SECTIONS

	GROUP 1					GROUP 2				
I#	G--G	(G-1)--G	(G-2)--G	(G-3)--G		I#	G--G	(G-1)--G	(G-2)--G	(G-3)--G
1	0.29915E+01	0.0	0.0	0.0	*	1	0.67467E+00	0.16853E+00	0.0	0.0
2	0.20899E+01	0.0	0.0	0.0	*	2	0.45057E+01	0.19336E+00	0.0	0.0
3	0.29190E+01	0.0	0.0	0.0	*	3	0.45087E+01	0.19336E+00	0.0	0.0
4	0.34703E+01	0.0	0.0	0.0	*	4	0.35187E+01	0.13552E+00	0.0	0.0
5	0.34389E+01	0.0	0.0	0.0	*	5	0.35169E+01	0.13552E+00	0.0	0.0
6	0.0	0.0	0.0	0.0	*	6	0.0	0.0	0.0	0.0
7	0.36776E+01	0.0	0.0	0.0	*	7	0.19897E+01	0.22109E+00	0.0	0.0
8	0.0	0.0	0.0	0.0	*	8	0.0	0.0	0.0	0.0
9	0.59401E+01	0.0	0.0	0.0	*	9	0.79117E+01	0.24959E+00	0.0	0.0
10	0.0	0.0	0.0	0.0	*	10	0.0	0.0	0.0	0.0
11	0.59436E+01	0.0	0.0	0.0	*	11	0.77983E+01	0.24972E+00	0.0	0.0
12	0.60111E+01	0.0	0.0	0.0	*	12	0.16133E+02	0.99712E-01	0.0	0.0
13	0.0	0.0	0.0	0.0	*	13	0.0	0.0	0.0	0.0
14	0.0	0.0	0.0	0.0	*	14	0.0	0.0	0.0	0.0
15	0.67556E+01	0.0	0.0	0.0	*	15	0.16918E+02	0.33839E+00	0.0	0.0
16	0.84157E+01	0.0	0.0	0.0	*	16	0.97496E+01	0.38190E+00	0.0	0.0
17	0.87152E+01	0.0	0.0	0.0	*	17	0.12356E+02	0.74828E+00	0.0	0.0
18	0.77969E+01	0.0	0.0	0.0	*	18	0.14812E+02	0.22556E+00	0.0	0.0
19	0.84166E+01	0.0	0.0	0.0	*	19	0.18820E+02	0.11963E+00	0.0	0.0
20	0.86920E+01	0.0	0.0	0.0	*	20	0.10661E+02	0.59185E+00	0.0	0.0
21	0.0	0.0	0.0	0.0	*	21	0.0	0.0	0.0	0.0
22	0.0	0.0	0.0	0.0	*	22	0.0	0.0	0.0	0.0
23	0.78926E+01	0.0	0.0	0.0	*	23	0.13777E+02	0.21870E+00	0.0	0.0
24	0.93363E+01	0.0	0.0	0.0	*	24	0.18014E+02	0.15196E+00	0.0	0.0
25	0.65930E+01	0.0	0.0	0.0	*	25	0.11225E+02	0.17026E+00	0.0	0.0
26	0.82145E+01	0.0	0.0	0.0	*	26	0.10821E+02	0.16079E+00	0.0	0.0
27	0.84516E+01	0.0	0.0	0.0	*	27	0.10742E+02	0.43446E+00	0.0	0.0
28	0.19972E+01	0.0	0.0	0.0	*	28	0.35021E+01	0.11746E+00	0.0	0.0
29	0.0	0.0	0.0	0.0	*	29	0.0	0.0	0.0	0.0
30	0.55532E+01	0.0	0.0	0.0	*	30	0.67558E+01	0.82830E-01	0.0	0.0
31	0.82136E+01	0.0	0.0	0.0	*	31	0.74875E+01	0.13322E+00	0.0	0.0
32	0.0	0.0	0.0	0.0	*	32	0.0	0.0	0.0	0.0
33	0.56934E+01	0.0	0.0	0.0	*	33	0.58696E+01	0.15884E+00	0.0	0.0
34	0.61270E+01	0.0	0.0	0.0	*	34	0.56644E+01	0.12522E+00	0.0	0.0
35	0.0	0.0	0.0	0.0	*	35	0.0	0.0	0.0	0.0
36	0.63073E+01	0.0	0.0	0.0	*	36	0.56486E+01	0.88502E-01	0.0	0.0
37	0.62857E+01	0.0	0.0	0.0	*	37	0.20700E+02	0.89099E-01	0.0	0.0
38	0.67340E+01	0.0	0.0	0.0	*	38	0.11877E+02	0.19646E+00	0.0	0.0
39	0.67340E+01	0.0	0.0	0.0	*	39	0.11877E+02	0.19644E+00	0.0	0.0
40	0.66149E+01	0.0	0.0	0.0	*	40	0.59582E+01	0.21949E+00	0.0	0.0
41	0.67823E+01	0.0	0.0	0.0	*	41	0.69845E+01	0.20836E+00	0.0	0.0
42	0.62594E+01	0.0	0.0	0.0	*	42	0.10346E+02	0.93172E+00	0.0	0.0
43	0.77642E+01	0.0	0.0	0.0	*	43	0.15039E+02	0.20455E+00	0.0	0.0
44	0.81000E+01	0.0	0.0	0.0	*	44	0.11479E+02	0.14686E+00	0.0	0.0
45	0.87119E+01	0.0	0.0	0.0	*	45	0.14089E+02	0.14125E+00	0.0	0.0
46	0.68580E+01	0.0	0.0	0.0	*	46	0.11532E+02	0.27750E+00	0.0	0.0

TABLE C.4: (page 5 of 7)

SCATTERING CROSS-SECTIONS

	GROUP 3					GROUP 4				
I#	G--G	(G-1)--G	(G-2)--G	(G-3)--G		I#	G--G	(G-1)--G	(G-2)--G	(G-3)--G
1	0.67633E+00	0.51300E-01	0.0	0.0	*	1	0.79265E+00	0.47691E-01	0.0	0.0
2	0.46382E+01	0.12440E+00	0.25165E-06	0.0	*	2	0.47634E+01	0.11551E+00	0.0	0.62422E-09
3	0.46382E+01	0.12440E+00	0.25165E-06	0.0	*	3	0.47636E+01	0.11551E+00	0.0	0.62422E-09
4	0.38417E+01	0.73112E-01	0.77735E-07	0.0	*	4	0.38567E+01	0.69384E-01	0.0	0.68988E-10
5	0.38417E+01	0.73112E-01	0.77736E-07	0.0	*	5	0.38946E+01	0.69384E-01	0.0	0.68988E-10
6	0.0	0.0	0.0	0.0	*	6	0.0	0.0	0.0	0.0
7	0.22427E+01	0.27524E-01	0.94462E-08	0.0	*	7	0.17236E+01	0.24103E-01	0.0	0.0
8	0.0	0.0	0.0	0.0	*	8	0.0	0.0	0.0	0.0
9	0.14085E+02	0.25629E-01	0.37025E-05	0.0	*	9	0.0	0.17475E-01	0.0	0.0
10	0.0	0.0	0.0	0.0	*	10	0.0	0.0	0.0	0.0
11	0.81689E+01	0.21615E-01	0.37625E-05	0.0	*	11	0.0	0.17014E-01	0.0	0.0
12	0.11722E+03	0.27470E-01	0.10608E-05	0.0	*	12	0.0	0.11246E-01	0.0	0.0
13	0.0	0.0	0.0	0.0	*	13	0.0	0.0	0.0	0.0
14	0.0	0.0	0.0	0.0	*	14	0.0	0.0	0.0	0.0
15	0.71777E+02	0.82671E-01	0.36514E-04	0.0	*	15	0.19933E+03	0.23304E-01	0.95961E-08	0.0
16	0.14559E+02	0.18038E-01	0.70962E-05	0.0	*	16	0.71289E+01	0.86810E-02	0.0	0.0
17	0.17436E+02	0.38702E-01	0.51906E-04	0.0	*	17	0.48111E+01	0.37810E-02	0.10885E-06	0.0
18	0.25536E+02	0.46197E-01	0.66552E-07	0.0	*	18	0.93750E+01	0.11499E-01	0.0	0.0
19	0.35435E+02	0.49004E-01	0.63768E-04	0.0	*	19	0.90205E+01	0.36233E-02	0.83205E-09	0.0
20	0.12490E+02	0.17142E-01	0.10954E-04	0.0	*	20	0.73639E+01	0.22259E-01	0.0	0.0
21	0.0	0.0	0.0	0.0	*	21	0.0	0.0	0.0	0.0
22	0.0	0.0	0.0	0.0	*	22	0.0	0.0	0.0	0.0
23	0.16977E+02	0.37952E-01	0.34755E-05	0.0	*	23	0.12523E+02	0.16054E-01	0.0	0.0
24	0.11933E+02	0.16514E-01	0.34813E-05	0.0	*	24	0.12527E+02	0.16222E-01	0.0	0.0
25	0.36693E+02	0.19214E-01	0.26035E-05	0.0	*	25	0.90165E+01	0.13424E-01	0.0	0.0
26	0.11743E+02	0.17128E-01	0.30977E-04	0.0	*	26	0.12523E+02	0.17507E-01	0.11931E-07	0.19598E-06
27	0.16219E+02	0.26059E-01	0.48162E-05	0.0	*	27	0.10021E+02	0.11481E-01	0.0	0.0
28	0.36324E+01	0.73142E-01	0.0	0.0	*	28	0.36673E+01	0.67750E-01	0.0	0.0
29	0.0	0.0	0.0	0.0	*	29	0.0	0.0	0.0	0.0
30	0.11313E+02	0.27112E-01	0.43693E-06	0.0	*	30	0.0	0.22893E-01	0.0	0.0
31	0.62378E+01	0.19061E-01	0.12240E-05	0.0	*	31	0.0	0.21063E-01	0.0	0.0
32	0.0	0.0	0.0	0.0	*	32	0.0	0.0	0.0	0.0
33	0.26436E+02	0.27296E-01	0.17372E-05	0.0	*	33	0.0	0.16851E-01	0.0	0.0
34	0.37114E+03	0.12130E-01	0.14358E-05	0.0	*	34	0.0	0.26672E-01	0.0	0.0
35	0.0	0.0	0.0	0.0	*	35	0.0	0.0	0.0	0.0
36	0.11438E+02	0.12684E-01	0.87702E-06	0.0	*	36	0.0	0.76727E-01	0.0	0.0
37	0.43102E+02	0.36721E-01	0.87702E-06	0.0	*	37	0.0	0.33804E-01	0.0	0.0
38	0.42373E+02	0.16316E+00	0.26733E-05	0.0	*	38	0.0	0.14308E-01	0.0	0.0
39	0.66295E+03	0.10316E+00	0.26933E-05	0.0	*	39	0.0	0.21182E-01	0.0	0.0
40	0.52722E+01	0.12236E-01	0.32200E-05	0.0	*	40	0.0	0.99495E-02	0.0	0.0
41	0.79990E+01	0.18629E-01	0.29197E-05	0.0	*	41	0.0	0.15816E-01	0.0	0.0
42	0.11220E+02	0.15980E-01	0.23835E-04	0.0	*	42	0.83063E+01	0.17241E-01	0.17837E-08	0.40300E-10
43	0.34682E+02	0.14990E-01	0.16947E-05	0.0	*	43	0.89239E+01	0.11177E-01	0.31187E-08	0.0
44	0.12792E+02	0.29173E-01	0.22535E-05	0.0	*	44	0.86585E+01	0.12501E-01	0.15742E-08	0.0
45	0.27931E+02	0.13541E-01	0.71396E-06	0.0	*	45	0.43385E+02	0.36514E-01	0.22910E-09	0.0
46	0.12160E+02	0.18036E-01	0.15427E-05	0.0	*	46	0.10925E+02	0.10979E-01	0.0	0.0

TABLE C.4: (page 6 of 7)

CALCULATED CROSS-SECTIONS

I	REMOVAL GROUP 1	REMOVAL GROUP 2	REMOVAL GROUP 3	REMOVAL GROUP 4	I	ABSORPTION GROUP 1	ABSORPTION GROUP 2	ABSORPTION GROUP 3	ABSORPTION GROUP 4
1	0.16853E+00	0.51300E-01	0.47691E-01	0.0	1	-0.11932E-05	-0.13352E-04	-0.19028E-03	0.31124E-02
2	0.19386E+00	0.12440E+00	0.11551E+00	0.0	2	0.15016E-03	0.84094E-05	0.14395E-03	0.17955E-02
3	0.19386E+00	0.12440E+00	0.11551E+00	0.0	3	0.15016E-03	0.84094E-05	0.14395E-03	0.17955E-02
4	0.13552E+00	0.73112E-01	0.69384E-01	0.0	4	0.23120E-02	0.18595E-06	0.95096E-05	0.81262E-04
5	0.13552E+00	0.73112E-01	0.69384E-01	0.0	5	0.23120E-02	0.18595E-06	0.95096E-05	0.81262E-04
6	0.0	0.0	0.0	0.0	6	0.19259E-03	0.21025E-02	0.35991E-01	0.44887E+00
7	0.22183E+00	0.27524E-01	0.24103E-01	0.0	7	-0.22916E-02	0.79852E-03	0.55970E-02	0.71819E-01
8	0.0	0.0	0.0	0.0	8	0.0	0.15755E-04	0.36939E+02	0.12007E+07
9	0.24957E+00	0.25629E-01	0.17475E-01	0.0	9	0.53300E-01	0.14263E+01	0.58764E+02	0.13175E+02
10	0.0	0.0	0.0	0.0	10	0.0	0.22043E+00	0.48222E+01	0.60149E+02
11	0.24972E+00	0.21615E-01	0.17314E-01	0.0	11	0.50471E-01	0.54166E+00	0.54301E+01	0.39052E+01
12	0.97712E-01	0.27470E-01	0.11246E-01	0.0	12	0.26456E+00	0.63470E+01	0.35 [illegible]E+03	0.10564E+03
13	0.0	0.0	0.0	0.0	13	0.51973E+01	0.43577E+03	0.44892E+04	0.12120E+05
14	0.0	0.0	0.0	0.0	14	0.13474E+00	0.80488E+03	0.73219E+04	0.67330E+03
15	0.33889E+00	0.62871E-01	0.23304E-01	0.0	15	0.20635E+00	0.47262E+01	0.14953E+03	0.37662E+05
16	0.36190E+00	0.14818E-01	0.88410E-02	0.0	16	0.62701E+00	0.87334E+01	0.26132E+03	0.34738E+04
17	0.75824E+00	0.38702E-01	0.37810E-02	0.0	17	0.20347E+00	0.76748E+01	0.22089E+03	0.17046E+03
18	0.22568E+00	0.46197E-01	0.11499E-01	0.0	18	0.57124E+00	0.16259E+01	0.49270E+02	0.27911E+01
19	0.11963E+00	0.49004E-01	0.36233E-02	0.0	19	0.91827E+00	0.12042E+01	0.16973E+03	0.14689E+02
20	0.59185E+00	0.17142E-01	0.22259E-01	0.0	20	0.75654E+00	0.27256E+01	0.48782E+02	0.99769E+02
21	0.0	0.0	0.0	0.0	21	0.19667E-01	0.24369E+00	0.10053E+01	0.40870E+00
22	0.0	0.0	0.0	0.0	22	0.68514E-01	0.70902E+00	0.11455E+02	0.64104E+01
23	0.21470E+00	0.37959E-01	0.16354E-01	0.0	23	0.17411E+00	0.11305E+01	0.10640E+02	0.31845E+01
24	0.15196E+00	0.16919E-01	0.16222E-01	0.0	24	0.20942E+01	0.66084E+01	0.84069E+02	0.27400E+03
25	0.17028E+00	0.19214E-01	0.17524E-01	0.0	25	0.10319E+01	0.15073E+01	0.10173E+03	0.37769E+02
26	0.16079E+00	0.17124E-01	0.17507E-01	0.0	26	0.13723E+01	0.59979E+01	0.51747E+02	0.27416E+03
27	0.43546E+00	0.20659E-01	0.13481E-01	0.0	27	0.11631E+01	0.48492E+01	0.73064E+02	0.24239E+02
28	0.11780E+00	0.73142E-01	0.67750E-01	0.0	28	0.30855E-02	0.0	0.0	0.79859E-04
29	0.0	0.0	0.0	0.0	29	0.99260E-02	0.10481E+00	0.33213E+02	0.20199E+02
30	0.82833E-01	0.27112E-01	0.22893E-01	0.0	30	0.69236E-01	0.11265E+01	0.27033E+02	0.89255E+02
31	0.13322E+00	0.19861E-01	0.21063E-01	0.0	31	0.16075E+00	0.13506E+01	0.50177E+01	0.13762E+03
32	0.0	0.0	0.0	0.0	32	0.27924E+01	0.30546E+02	0.52356E+03	0.67331E+04
33	0.15884E+00	0.27298E-01	0.16351E-01	0.0	33	0.35232E+00	0.27421E+01	0.22081E+03	0.41413E+02
34	0.12522E+00	0.12130E-01	0.20672E-01	0.0	34	0.74144E-01	0.10471E+01	0.12671E+03	0.53499E+02
35	0.0	0.0	0.0	0.0	35	0.0	0.30933E+00	0.67659E+01	0.85286E+02
36	0.85503E-01	0.12684E-01	0.76727E-01	0.0	36	0.46362E-01	0.98395E+00	0.10679E+02	0.13968E+03
37	0.87099E-01	0.36721E-01	0.33804E-01	0.0	37	0.42485E-01	0.91124E+00	0.49300E+02	0.26844E+02
38	0.19644E+00	0.10310E+00	0.14808E-01	0.0	38	0.48124E-01	0.70233E+00	0.46982E+02	0.39154E+02
39	0.19644E+00	0.10310E+00	0.21132E-01	0.0	39	0.49058E-01	0.68776E+00	0.35012E+03	0.96501E+02
40	0.21944E+00	0.12230E-01	0.99495E-02	0.0	40	0.47448E+00	0.75979E+01	0.98193E+02	0.67331E+03
41	0.20836E+00	0.15629E-01	0.15816E-01	0.0	41	0.16886E+00	0.38676E+01	0.50794E+03	0.62842E+04
42	0.93172E+00	0.15983E-01	0.17241E-01	0.0	42	0.47142E+00	0.34838E+01	0.61825E+02	0.46164E+02
43	0.20495E+00	0.14960E-01	0.11177E-01	0.0	43	0.24939E+00	0.96884E+00	0.25597E+02	0.12453E+01
44	0.14686E+00	0.29173E-01	0.12501E-01	0.0	44	0.17736E+01	0.44796E+01	0.61006E+02	0.13240E+04
45	0.14125E+00	0.13541E-01	0.36514E-01	0.0	45	0.10987E+01	0.17747E+01	0.25681E+02	0.67070E+03
46	0.27750E+00	0.18036E-01	0.10979E-01	0.0	46	0.17647E+01	0.64565E+01	0.99850E+02	0.10147E+04

TABLE C.4: (page 7 of 7)

APPENDIX D

COMPUTER CODE INPUT PARAMETERS

D.1 Introduction

In this appendix are detailed the parameters used in the PDQ-7 calculations described in Chapter 3. Specific spectrum-dependent parameters and nuclide depletion chain paramters were generated using the AMPX code.

D.2 Nuclide Identification

Table [D.1] lists the 46 nuclides treated by the AMPX code system. Reference numbers are used for identification of nuclides in PDQ-7.

D.3 Number Densities

This section describes the reference ball design used both in cross-section generation in the AMPX code and in modeling the pebble bed breed/burn system for PDQ-7.

TABLE D.1

NUCLIDE IDENTIFICATION

NUCLIDE	REFERENCE NUMBER[4]	I#[5]	NUCLIDE	REFERENCE NUMBER[4]	I#[5]
Am243	24395	20	Pm147	14761	12
Carbon	1206	2	Pm148	14861	14
Cs133	13355	9	Pm148m	14800	13
Cs134	13455	10	Pm149	14461	28
Cs135	13555	11	[3]Pa233	23391	42
Eu153	15363	17	[3]Recvel	1200	6
Eu154	15463	40	Rh103	10345	31
Eu155	15563	41	Rh105	10545	32
[1]FP 1	10001	22	Sm149	14962	15
[2]FP 2	10002	21	Sm150	15062	38
Helium	402	1	Sm151	15162	16
I135	13553	4	Sm152	15262	39
Kr82	8236	29	Silicon	1428	7
Kr83	8336	30	Ag109	10947	33
Nd143	14360	36	Th232	23290	23
Nd145	14560	37	U233	23392	24
Nd147	14760	3	U234	23492	25
Np239	23993	27	U235	23592	26
Oxygen	1608	5	U236	23692	18
Pu239	23994	44	U238	23892	43
Pu240	24094	45	Xe131	13154	34
Pu241	24194	46	Xe133	13354	35
Pu242	24294	19	Xe135	13554	8

[1] Slowly-saturating fission products (lumped)

[2] Non-saturating fission products (lumped)

[3] Reciprocal-velocity correction to account for graphite impurities [W3]

[4] Combined mass number and atomic number for identification in PDQ-7

[5] Identification number for AMPX code and cross-section tables of Appendices [A] and [C]

D.3.1 Nomenclature

C/HM = Ratio of carbon number density to heavy metal number density

ε = Fissile enrichment

$$= \frac{N^{23}}{N^{23} + N^{02}}$$

N_A = Avogadro's number

$$= 0.6022 \frac{cm^2\text{-atoms}}{b\text{-mole}}$$

^1M_x = Atomic mass of indicated nuclide, [gm/mole]

$^1\rho_x$ = Density of indicated nuclide, [gm/cm^3]

P.F. = Packing factor of balls

$$= \frac{\text{Volume of balls}}{\text{Volume of reactor}} = 0.61$$

V_B = Volume of single ball, [cm^3]

V'_B = Effective volume of ball (cell-averaged), [cm^3]

^1V_x = Volume of indicated nuclide in ball, [cm^3]

$^1V'_x$ = Effective volume of nuclide in ball (cell-averaged), [cm^3]

^2N_x = Atom density of indicated nuclide in ball, [$b^{-1}cm^{-1}$]

$^2N'_x$ = Effective atom density of indicated nuclide in ball [$b^{-1}cm^{-1}$]

R_b = Radius of ball, [cm]

[1]Subscript T, C or U indicates $Th^{232}O_2$, graphite or $U^{233}O_2$, respectively.

[2]Subscript T, C, U or O indicates Th232, graphite, U233 or oxygen, respectively.

D.3.2 Material Properties

Calculation of initial number densities, as a function of U233 enrichment, involved considerations of the volume fractions of the particular materials within a fuel cell. Fuel cells were defined as the volume of one fuel ball divided by the packing factor, P.F. Properties of the major substances in the fuel balls are shown in Table [D.2]

The makeup of the fuel balls is illustrated in Figure [D.1], appropriately dimensioned. Packing fractions of fueled grains in the meat are listed in Table [D.3]. Number densities for all materials present at beginning-of-life are given, and all others appearing in the depletion chains are initially zero.

TABLE D.2

BALL MATERIAL PROPERTIES [W3]

Material	ρ_x (gm/cm^3)	M_x (gm/mole)
Heavy metal oxides	9.5	264
Graphite:		
grain coating	1.5	12.0
meat	1.0	12.0
outer shell	1.75	12.0

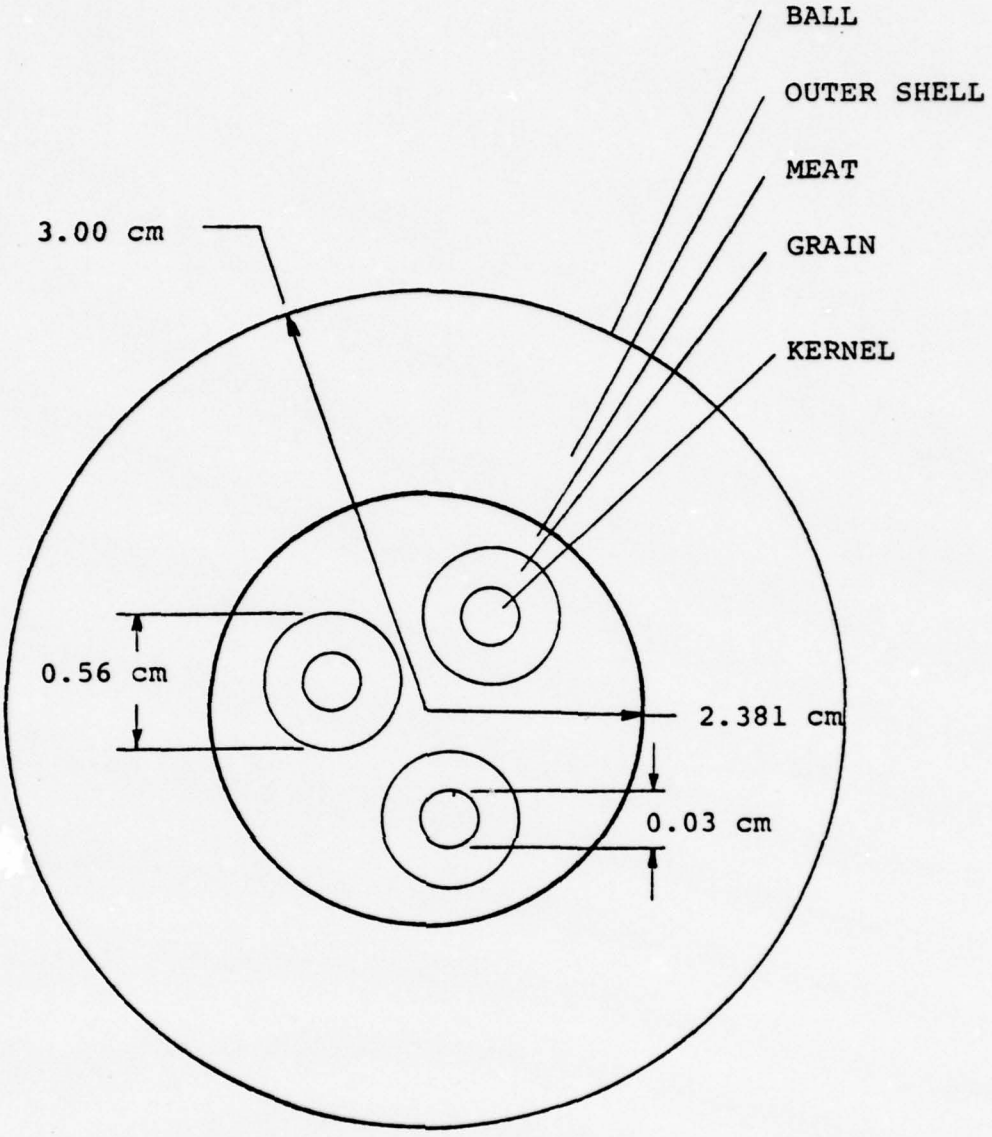

FIGURE D.1: SECTIONAL VIEW OF FUEL BALL
(not to scale)

TABLE D.3

PACKING FRACTIONS OF GRAINS IN MEAT [W3]

C/HM ATOM RATIO	PACKING FRACTION*
110	0.39073
250	0.168
325	0.127
450	0.091987

$$*\text{Packing fraction} = \frac{(\text{Number of grains})(\text{Volume per grain})}{\text{Volume of Meat}}$$

D.3.3 Calculation of Number Densities

The volume of a fuel element is given by:

$$V_B = \frac{4}{3}\pi R^3 = 113.1 \text{ cm}^3, \tag{D.1}$$

so the effective volume (cell-averaged) is:

$$V_B' = \frac{V_B}{P.F.} = 185.4 \text{ cm}^3. \tag{D.2}$$

Number densities for thorium, oxygen, uranium, and carbon were determined using the following relationships:

$$N_{HM} = \frac{\rho_{HM} N_A}{M_{HM}} \tag{D.3}$$

$$N_C = \frac{\rho_C N_A}{M_C} \tag{D.4}$$

$$N_O = \frac{\rho_O N_A}{M_O} \tag{D.5}$$

where the densities, ρ, are "smeared" throughout the ball. In addition,

$$C/HM = \frac{N_C}{N_T + N_U} = \frac{N_C}{N_{HM}} \tag{D.6}$$

and

$$\varepsilon = \frac{N_U}{N_T + N_U} = \frac{N_U}{N_{HM}} \; . \tag{D.7}$$

To find the smeared densities for heavy metal and carbon:

$$\rho_{HM} = \rho_{HMO_2} \left(\frac{M_{HM}}{M_{HMO_2}}\right)\left(\frac{V_{Kernel}}{V_{Grain}}\right)\left(\frac{V_{Grain}}{V_{Meat}}\right)\left(\frac{V_{Meat}}{V_{Ball}}\right) \tag{D.8}$$

$$\rho_C = \rho_{Grain}\left(1 - \frac{V_{Kernel}}{V_{Grain}}\right)\left(\frac{V_{Grain}}{V_{Meat}}\right)\left(\frac{V_{Meat}}{V_{Ball}}\right)$$
$$+ \rho_{Meat}\left(1 - \frac{V_{Grain}}{V_{Meat}}\right)\left(\frac{V_{Meat}}{V_{Ball}}\right)$$
$$+ \rho_{Outer\ Shell}\left(1 - \frac{V_{Meat}}{V_{Ball}}\right) . \qquad (D.9)$$

Since $N_x' = N_x(P.F.)$, the effective number densities (cell-averaged) can be summarized as follows:

$$N_U' = \varepsilon\rho_{HMO_2}\left(\frac{M_{HM}}{M_{HMO_2}}\right)\left(\frac{V_{Kernel}}{V_{Ball}}\right)(P.F.)\frac{N_A}{M_{HM}} \qquad (D.10)$$

$$N_T' = (1 - \varepsilon)\rho_{HMO_2}\left(\frac{M_{HM}}{M_{HMO_2}}\right)\left(\frac{V_{Kernel}}{V_{Ball}}\right)(P.F.)\frac{N_A}{M_{HM}} \qquad (D.11)$$

$$N_C' = \frac{N_A}{N_{HM}}(P.F.)\left[\rho_{Grain}\left(1 - \frac{V_{Kernel}}{V_{Grain}}\right)\left(\frac{V_{Grain}}{V_{Ball}}\right)\right.$$
$$+ \rho_{Meat}\left(1 - \frac{V_{Grain}}{V_{Meat}}\right)\left(\frac{V_{Meat}}{V_{Ball}}\right)$$
$$\left. + \rho_{Outer\ Shell}\left(1 - \frac{V_{Meat}}{V_{Ball}}\right)\right] \qquad (D.12)$$

In addition to the above, initial number densities were used as input for silicon; the recvel correction (reciprocal velocity [W3]) for graphite impurity is used at a concentration of approximately 2 ppb carbon, so that the effective number densities (cell-averaged) become:

$$N'_{recvel} = (2.05E\text{-}9)N_C' \qquad (D.13)$$

$$N'_{helium} = 8.308E\text{-}5 \qquad (D.14)$$

$$N'_{silicon} = (9.14E\text{-}3)\left(\frac{V_{Meat}}{V_{Ball}}\right)\left(\frac{V_{Grain}}{V_{Meat}}\right) \qquad (D.15)$$

Representative values for N_U' and N_{Th}' are given in Table [D.4], while values for N'_{HM}, N'_O, N'_C, N'_{recvel}, $N'_{silicon}$, and N'_{helium} are listed in Table [D.5].

TABLE D.4

INITIAL CELL-AVERAGED HEAVY METAL NUMBER DENSITIES*

C/HM ATOM RATIO	ε(%)	U233	Th232
110	2.0	7.9408E-6	3.8910E-4
110	4.5	1.7867E-5	3.7918E-4
110	7.0	2.7793E-5	3.6925E-4
250	2.0	3.4143E-6	1.6730E-4
250	4.5	7.6821E-6	1.6303E-4
250	7.0	1.1950E-5	1.5876E-4
325	2.0	2.5810E-6	1.2647E-4
325	4.5	5.8073E-6	1.2324E-4
325	7.0	9.0336E-6	1.2002E-4
450	2.0	1.8695E-6	9.1604E-5
450	4.5	4.2063E-6	8.9267E-5
450	7.0	6.5431E-6	8.6930E-5

* In $b^{-1}cm^{-1}$.

TABLE D.5

INITIAL CELL NUMBER DENSITIES*

C/HM ATOM RATIO	HEAVY METAL	OXYGEN	CARBON	RECVEL	SILICON	HELIUM
110	3.9704E-4	7.9409E-4	4.3702E-2	8.9590E-11	1.0892E-3	8.3082E-5
250	1.7071E-4	3.4143E-4	4.2784E-2	8.7707E-11	4.6833E-4	8.3083E-5
325	1.2905E-4	2.5810E-4	4.2615E-2	8.7361E-11	3.5404E-4	8.3083E-5
450	9.3470E-5	1.8695E-4	4.2471E-2	8.7065E-11	2.5647E-4	8.3082E-5

* In $b^{-1}cm^{-1}$.

D.4 Exposure Times

This section describes the calculation of exposure times (hours) used in PDQ-7 depletion calculations for fuel burnups up to 120,000 MWD/MTHM. Calculated exposure times are tabulated as a function of the carbon-to-heavy metal atom ratio in Table [D.6].

D.4.1 Nomenclature

$\bar{q}'''$ = Average core power density
= 5.0 watts/cm^3

N'_{HM} = Cell-averaged heavy metal atom density, [$b^{-1}cm^{-1}$]

t = Exposure time at full power, [hours]

N_A = Avogadro's number
= 0.6022 cm^2-atoms/b-mole

M_{HM} = Atomic mass of heavy metal nuclides
≈ 232 gm/mole

B = Fuel burnup, [MWD/MTHM]

V_R = Volume of relevant reactor portion, [cm^3]

D.4.2 Calculation of Exposure Times

Exposure times, t[hours], were calculated to correspond to specific values of fuel burnup, B [MWD/MTHM]. As a function of the cell-averaged heavy metal number density, N'_{HM} [$b^{-1}cm^{-1}$], the fuel burnup is given by:

$$B = (2.4E\text{-}23)\frac{\bar{q}'''N_A t}{N'_{HM}M_{HM}} \text{ MWD/MTHM} \qquad (D.16)$$

so that the exposure time, t [hours], can be expressed as

$$t\ [\text{hours}] = (1.8492E+3)B[\text{MWD/MTHM}]N'_{HM}[b^{-1}cm^{-1}] \qquad (D.17)$$

where N'_{HM} can be found by summing Equations (D.10) and (D.11). Representative values for the exposure times are given in Table [D.6] as a function of C/HM atom ratio.

TABLE D.6

EXPOSURE TIMES*

	C/HM ATOM RATIO			
B(MWD/MTHM)	110	250	325	450
100	7.3421E+1	3.1568E+1	2.3864E+1	1.7285E+1
1000	7.3421E+2	3.1568E+2	2.3864E+2	1.7285E+2
2000	1.4684E+3	6.3136E+2	4.7728E+2	3.4570E+2
3000	2.2026E+3	9.4704E+2	7.1592E+2	5.1855E+2
6000	4.4053E+e	1.8941E+4	1.4318E+3	1.0371E+3
10,000	7.3421E+3	3.1568E+3	2.3864E+3	1.7285E+3
15,000	1.1013E+4	4.7352E+3	3.5796E+3	2.5927E+3
20,000	1.4684E+4	6.3136E+3	4.7728E+3	3.4570E+3
25,000	1.8355E+4	7.8920E+3	5.9660E+3	4.3212E+3
30,000	2.2026E+4	9.4704E+3	7.1592E+3	5.1855E+3
45,000	3.3040E+4	1.4206E+4	1.0739E+4	7.7783E+3
60,000	4.4053E+4	1.8941E+4	1.4318E+4	1.0370E+4
75,000	5.5966E+4	2.3676E+4	1.7898E+4	1.2964E+4
90,000	6.6079E+4	2.8411E+4	2.1478E+4	1.5556E+4
100,000	7.3421E+4	3.1568E+4	2.3864E+4	1.7285E+4
120,000	8.8106E+4	3.7882E+4	2.8637E+4	2.0742E+4

*Times in hours.

For comparison, note that 8766 hours = 1 year.

D.5 Depletion Treatment

D.5.1 Depletion Chains

Depletion chains for the 46 nuclides considered are shown in Table[D.7]. PDQ-7 solves the sequence of chains in order, Chain 1 through Chain 19, for each pass through the depletion mesh. In Table [D.7] Chains 1 through 14 are depleting. Underscoring indicates the existence of a fission yield, given in Table [D.9], for the indicated nuclide. Reactions are indicated as follows:

(1) : (β^-)

(2) : (n,γ)

(3) : (n,γ) plus (β^-)

D.5.2 Nuclide Decay Constants

In Table [D.8] are tabulated all nuclide decay constants used in the subject PDQ-7 calculations.

D.5.3 Fission Product Yields

Table [D.9] lists the yields of each fission product treated for six fertile and fissile nuclides.

D.5.4 Energy Release per Fission

The energy release per fission for all heavy metals treated by the AMPX code are given in Table [D.10].

D.5.5 Chi (Neutron Yield) Spectra

As a function of the carbon-to-heavy metal atom ratio, the groupwise distributions for fission neutrons, χ, are given in Table [D.11].

TABLE D.7 (page 1 of 4)

DEPLETION CHAINS

CHAIN 1: U233 Chain

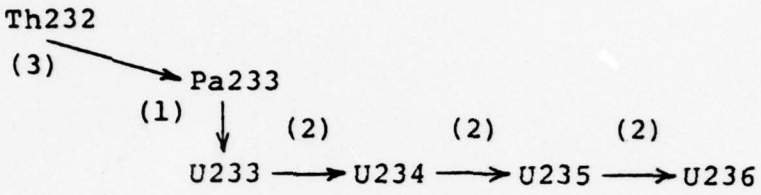

CHAIN 2: Xe135 Chain

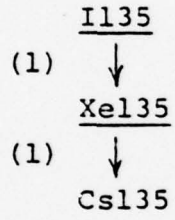

CHAIN 3: Sm149 Chain 1

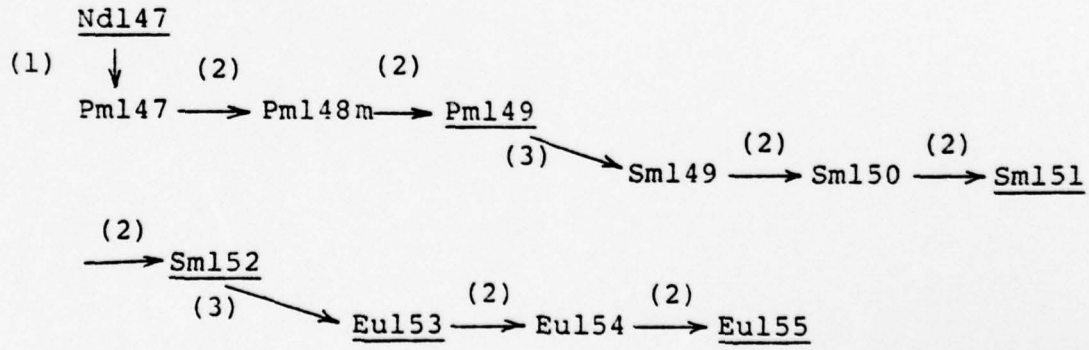

TABLE D.7 (page 2 of 4)

CHAIN 4: Sm149 Chain 2

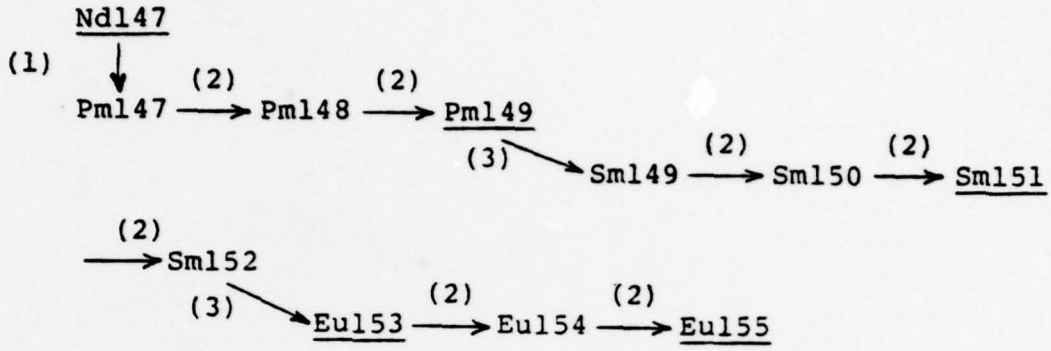

CHAIN 5: Kr83 Chain

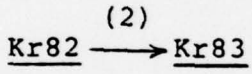

CHAIN 6: Rh103 Chain

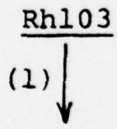

CHAIN 7: Rh105 Chain

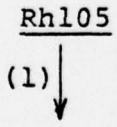

CHAIN 8: Ag109 Chain

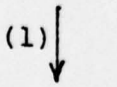

TABLE D.7 (page 3 of 4)

CHAIN 9: Xe131 Chain

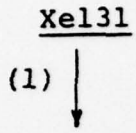

CHAIN 10: Fission Product Chain (lumped)

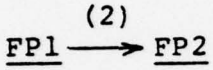

CHAIN 11: Nd143 Chain

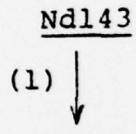

CHAIN 12: Xe133 Chain

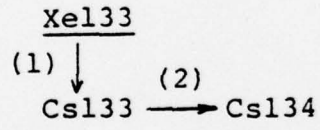

CHAIN 13: Nd145 Chain

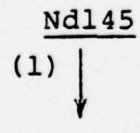

CHAIN 14: Pu239 Chain

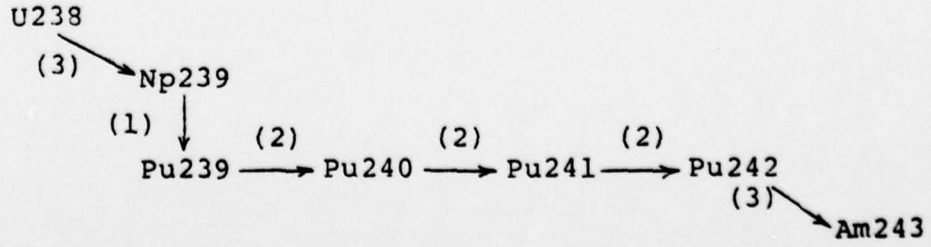

TABLE D.7 (page 4 of 4)

CHAIN 15: Helium Chain (non-depleting)

Helium

CHAIN 16: Carbon Chain (non-depleting)

Carbon

CHAIN 17: Oxygen Chain (non-depleting)

Oxygen

CHAIN 18: Recvel Chain (non-depleting)

Recvel

CHAIN 19: Silicon Chain (non-depleting)

Silicon

TABLE D.8 (page 1 of 2)

NUCLIDE DECAY CONSTANTS

CHAIN #	I#	REFERENCE NUMBER	NUCLIDE	*λ,[sec^{-1}]
1	23	23290	Th232	1.58E-18
1	42	23391	Pa233	2.93E-7
1	24	23392	U233	1.358E-13
1	25	23492	U234	8.856E-14
1	25	23592	U235	3.08E-17
1	18	23692	U236	9.189E-16
2	4	13553	I135	2.87E-5
2	8	13554	Xe135	2.09E-5
2	11	13555	Cs135	1.098E-14
3,4	3	14760	Nd147	7.32E-7
3,4	12	14761	Pm147	8.29E-9
3	13	14800	Pm148m	1.98E-7
4	14	14861	Pm148	1.49E-6
3,4	28	14961	Pm149	3.63E-6
3,4	15	14962	Sm149	5.491E-23
3,4	38	15062	Sm150	Stable
3,4	16	15162	Sm151	2.75E-10
3,4	39	15262	Sm152	Stable
3,4	17	15363	Eu153	Stable
3,4	40	15463	Eu154	1.37E-9
3,4	41	15563	Eu155	1.16E-8
5	29	8236	Kr82	Stable
5	30	8336	Kr83	Stable
6	31	10345	Rh103	Stable
7	32	10545	Rh105	5.36E-5
8	33	10947	Ag109	Stable

TABLE D.8 (page 2 of 2)

9	34	13154	Xe131	Stable
10	22	10001	FP1	Stable
10	21	10002	FP2	Stable
11	36	14360	Nd143	Stable
12	35	13354	Xe133	1.52E-6
12	9	13355	Cs133	Stable
12	10	13455	Cs134	9.55E-9
13	37	14560	Nd145	Stable
14	43	23892	U238	4.87E-18
14	27	23993	Np239	3.41E-6
14	44	23994	Pu249	9.016E-13
14	45	24094	Pu240	3.249E-12
14	46	24194	Pu241	1.68E-9
14	19	24294	Pu242	5.795E-14
14	20	24395	Am243	2.871E-12
15	1	402	Helium	Stable
16	2	1206	Carbon	Stable
17	5	1608	Oxygen	Stable
18	6	1200	Recvel	Stable
19	7	1428	Silicon	Stable

* For stable nuclides, λ = 0.1E-20 sec^{-1} was used.

TABLE D.9

FISSION PRODUCT YIELDS

FISSION PRODUCT	I#	FISSION SOURCE					
		Th232	U233	U235	U238	Pu239	Pu241
I135	4	0.0539	0.0562	0.0617	0.0578	0.0693	0.0626
Xe135	8	0.0021	0.0022	0.0024	0.0022	0.0027	0.0024
Pm149	28	0.00945	0.0077	0.0113	0.021	0.013	0.012
Nd143	36	0.08	0.0591	0.0603	0.48	0.046	0.056
FP1	22	0.301	0.309	0.298	0.273	0.324	0.324
FP2	21	1.137	1.119	1.26	1.426	1.456	1.456
Kr82	29	0.01	0.0069	0.0028	0.0005	0.0017	0.0007
Kr83	30	0.0199	0.0114	0.00544	0.0009	0.0029	0.001
Rh103	31	0.0016	0.016	0.03	0.062	0.056	0.062
Rh105	32	0.0005	0.005	0.009	0.037	0.055	0.058
Ag109	33	0.00055	0.0004	0.0003	0.003	0.0155	0.031
Xe131	34	0.017	0.0341	0.0293	0.023	0.038	0.034
Xe133	35	0.037	0.0588	0.659	0.052	0.069	0.06
Nd145	37	0.066	0.0338	0.0398	0.039	0.031	0.036
Eu153	17	0.00038	0.0015	0.00169	0.0038	0.0034	0.002
Eu155	41	0.00009	0.0003	0.00033	0.0013	0.0016	0.001
Nd147	3	0.038	0.0193	0.0236	0.028	0.0205	0.022
Sm151	16	0.002	0.0035	0.0044	0.009	0.008	0.005
Sm152	39	0.00085	0.0022	0.00281	0.006	0.006	0.003

TABLE D.10

ENERGY RELEASE PER FISSION

FISSIONABLE NUCLIDE	κ [watt-sec/fission]
Th232	3.18×10^{-11}
Pa233	3.19×10^{-11}
U233	3.19×10^{-11}
U234	3.19×10^{-11}
U235	3.21×10^{-11}
U236	3.26×10^{-11}
U238	3.31×10^{-11}
Np239	3.27×10^{-11}
Pu239	3.34×10^{-11}
Pu240	3.36×10^{-11}
Pu241	3.37×10^{-11}
Pu242	3.37×10^{-11}
Am243	3.39×10^{-11}

TABLE D.11

CHI (NEUTRON YIELD) SPECTRA

	C/HM ATOM RATIO			
	110	250	325	450
χ_1	9.66727E-1	9.66727E-1	9.66727E-1	9.66727E-1
χ_2	3.32743E-2	3.32745E-2	3.32746E-2	3.32743E-2
χ_3	4.90742E-9	5.67340E-9	5.91979E-9	5.17704E-9
χ_4	4.98079E-14	5.75821E-14	6.00830E-14	5.25449E-14

D.5.6 Neutron Flux

Table [D.12] tabulates the groupwise relative neutron flux generated for each carbon-to-heavy metal atom ratio by the AMPX code. Group parameters are given in Table [D.13]. These flux values were used to collapse the four-group constants given in Appendix C to one-group, for use in the analysis of Chapter 2.

TABLE D.12

GROUPWISE RELATIVE NEUTRON FLUX*

	C/HM ATOM RATIO			
FLUX	110	250	325	450
ϕ_1	1.000	1.000	1.000	1.000
ϕ_2	1.534	1.533	1.533	1.534
ϕ_3	1.025	1.194	1.236	1.282
ϕ_4	0.920	2.305	2.939	3.874

* Normalized by using ϕ_g/ϕ_1 for each C/HM atom ratio.

TABLE D.13

ENERGY GROUPS

	Group 1	Group 2	Group 3	Group 4
Upper Energy (eV)	1.4918E+7	1.8316E+5	5.8295E+2	1.8554E+0
Lower Energy (eV)	1.8316E+5	5.8295E+2	1.8554E+0	5.00E-3
Lethargy width, Δu	4.400	5.750	5.750	5.916

APPENDIX E

REFERENCES

[A1] Atefi, Bahman, "Specific Inventory and Ore Usage Correlations for Pressurized Water Reactors," N.E. Thesis, Department of Nuclear Engineering, M.I.T. (May, 1977).

[B1] Baxter, A. M., M. H. Merrill and R. C. Dahlberg, "The Use of Nonproliferation Fuel Cycles in the HTGR," TANSAO 28 (1978).

[B2] Breen, R. J., O. J. Marlowe and C. J. Pfeiffer, "HARMONY: System for Nuclear Reactor Depletion Computation," WAPD-TM-478 (January, 1965).

[C1] Cadwell, W. R., "PDQ-7 Reference Manual," WAPD-TM-678 (January, 1967).

[D1] Dahlberg, R. C. et al, "Physics Developments in the Design of Alternate Fuel Systems," TANSAO 28, (1978).

[D2] Dahlberg, R. C., "Benefits of HTGR Fuel Cycle Compilation and Summary," GA-A14398 (March, 1977).

[F1] Fischer, G. J., H. J. C. Kouts and C. Durston, "Reactor Concept with Fuel Resource Utilization and Anti-Proliferation Advantages," TANSAO 27 (1977).

[F2] Fujita, E. K., M. J. Driscoll and D. D. Lanning, "Design and Fuel Management of PWR Cores to Optimize the Once-Through Fuel Cycle," MITNE-215 (August, 1978).

[G1] Garel, K. C. and M. J. Driscoll, "Fuel Cycle Optimization of Thorium and Uranium Fueled PWR Systems," MITNE-204 (October, 1977).

[G2] Greene, N. M. et al, "AMPX: A Modular Code System to Generate Coupled Multigroup Neutron Gamma Cross-Sections from ENDF/B," ORNL-TM-3706 (1976).

[H1] Henry, Allan F., Nuclear Reactor Theory, M.I.T. Press, Cambridge, MA (1975).

[K1] Karam, R. A., "The ^{233}U-^{232}Th Fuel Cycle as an Alternative to LMFBRs," TANSAO 27 (1977).

[K2] Kasten, P. R. et al, "Assessment of the Thorium Fuel Cycle in Power Reactors," ORNL/TM-5565 (January, 1977).

[L1] Lamarsh, J. R., Introduction to Nuclear Engineering, Addison-Wesley Publishing Co., Inc., Reading, MA (1975).

[L2] Lamarsh, J. R., Introduction to Nuclear Reactor Theory, Addison-Wesley Publishing Co., Inc., Reading, MA (1966).

[L3] Lane, J. A., "Economic Incentives for Thorium Reactor Developments," Utilization of Thorium in Power Reactors," Technical Report Series, No. 52, IAEA (June, 1965).

[L4] Lee, Clarence E., "Resource Conservation of the Pebble Bed Prebreeder," TANSAO 28 (1978).

[N1] "Nuclear Proliferation and Safeguards," OTA-E-48 (June, 1977).

[P1] "Proliferation in Perspective," Water Reactors Division, Westinghouse Electric Corporation, Pittsburgh, PA (March, 1977).

[R1] Reactor Physics Constants, ANL-5800, USAEC (July, 1963).

[R2] Reutten, H. J., E. Teuchert and R. Schulten, "The Pebble Bed HTR as a Thermal Breeder," TANSAO 27, (1977).

[S1] Sheaffer, M. K., M. J. Driscoll and I. Kaplan, "A One-Group Method for Fast Reactor Calculations," MITNE-108 (September, 1970).

[S2] Shin, J. I. and M. J. Driscoll, "Evaluation of Advanced Fast Reactor Blanket Designs," MITNE-199 (March, 1977).

[S3] Shirley, G. W. and R. H. Broglie, "HTGR Near Breeder Cycles," TANSAO 28 (1978).

[S4] Silvennoinen, P., Reactor Core Fuel Management, Pergammon Press, Oxford, U.K. (1976).

[S5] Simnad, M. T. and L. R. Zumwalt, Materials and Fuels for High-Temperature Nuclear Applications, M.I.T. Press, Cambridge, MA (1964).

[T1] Teuchert, E., "'Once-Through' Cycles in the Pebble Bed HTR," JüL-1470 (December, 1977).

[V1] Vondy, D. R., "Interim Report on Core Physics and Fuel Cycle Analysis of the Pebble Bed Reactor Power Plant Concept," ORNL/TM-6142 (December, 1977).

[W1] Weissert, L. R. and G. Schileo, Fabrication of Thorium Fuel Elements, American Nuclear Society (1968).

[W2] Wirtz, Karl, Lectures on Fast Reactors, Kernforschungszentrum Karlsruhe (1973).

[W3] Worley, Brian A., Personal Communication, Oak Ridge National Laboratory (July-August, 1978).